2012

Cometabolic Degradation of Halogenated Aliphatic Hydrocarbons by Aerobic Microorganisms Naturally Associated with Wetland Plant Roots

Madelyn M. Smith
Wright State University

COMETABOLIC DEGRADATION OF HALOGENATED ALIPHATIC HYDROCARBONS BY AEROBIC MICROORGANISMS NATURALLY ASSOCIATED WITH WETLAND PLANT ROOTS

A thesis submitted in partial fulfillment of the
requirements for the degree of
Master of Science

By

MADELYN M SMITH
B.S., University of Toledo, 2010

2012
Wright State University

WRIGHT STATE UNIVERSITY

GRADUATE SCHOOL

June 9, 2012

I HEREBY RECOMMEND THAT THE THESIS PREPARED UNDER MY SUPERVISION BY Madelyn M Smith ENTITLED Cometabolic Degradation of Halogenated Aliphatic Hydrocarbons by Aerobic Microorganisms Naturally Associated with Wetland Plant Roots BE ACCEPTED IN PARTIAL FULFILLMENT OF THE REQUIREMENTS FOR THE DEGREE OF Master of Science

Abinash Agrawal, Ph. D.
Thesis Director

David Dominic, Ph. D.
Chair, Department of Earth and Environmental Sciences

Committee on
Final Examination

Abinash Agrawal, Ph. D.

James Amon, Ph. D

Garrett Struckhoff, Ph. D.

Christina Powell, Ph. D.

Andrews Hsu, Ph. D.
Dean, Wright State University Graduate School

ABSTRACT

Smith, Madelyn M. M.S. Department of Earth and Environmental Sciences, Wright State University, 2012. Cometabolic Degradation of Halogenated Aliphatic Hydrocarbons by Aerobic Microorganisms Naturally Associated with Wetland Plant Roots.

Wetland systems provide both anaerobic (reducing) and aerobic (oxidizing) zones for the biodegradation of chlorinated aliphatic hydrocarbons (CAH). In particular, wetland plant roots provide micro-oxidizing environments for methanotrophic bacteria from the presence of methane, which is produced in anaerobic zones, and oxygen, which is brought to the subsurface by roots of wetland plants; this shows the potential for cometabolic degradation of common organic pollutants.

This study explored the natural attenuation of CAHs by methanotrophic bacteria naturally associated with roots of the common wetland plant, *Carex comosa*. Root microcosms were amended with varying concentrations of methane; trichloroethene; *cis* 1,2-dichloroethene; 1,2-dichloroethane; or dichloromethane. Transformation Yield (T_y) increased with increasing CAH concentration. T_y and pseudo first-order degradation rate constants were often at least one order of magnitude lower than published values.

A suite of halogenated aliphatic hydrocarbons (HAH) were studied in bench scale root microcosms for their potential to be cometabolically degraded by methanotrophic bacteria naturally associated with the roots of *Carex comosa*. Among the HAHs

investigated, 1,1,2-trichloroethane, 1,2-dichloropropane, and 1,3-dichloropropene did not cometabolically degrade in the aerobic microcosm systems. However, four trihalomethanes (chloroform, bromodichloromethane, dibromochloromethane, and bromoform) as well as 1,1-dichloroethene; 1,2-dichloroethane, and 1,2-dibromoethane were found to cometabolically degrade in the systems. T_y as well as pseudo first-order degradation rate constants normalized to biomass ($k_{1\text{-CAH}}$) were calculated for compounds that did degrade.

Past studies have explored the possibility of plant-microbe interactions for the bioremediation of harmful pollutants in soil. In this study, numerous chlorinated aliphatic hydrocarbons were examined for their potential to cometabolically degrade by aerobic bacteria naturally associated with *Carex comosa*. The bacteria present along with the roots were able to degrade trichloroethene and *cis* 1,2-dichloroethene as well as low amounts of 1,1-dichloroethene; *trans* 1,2-dichloroethene; and 1,2-dichloroethane without the need for added growth substrate or an incubation period. Carbon tetrachloride and chloroform did not degrade in the systems. T_y was determined for compounds that did degrade but were often one to two orders of magnitude lower than published values. The growth substrate naturally present in the microcosm systems was unclear. Immediate degradation of chlorinated ethenes and removal of low levels of other types of CAHs indicates that cometabolic microorganisms are naturally present in and around the roots of wetland plants – even if the wetland system has not been previously exposed to chemical pollutants.

Results of this study help to fill in key data for cometabolism of emerging pollutants by methanotrophic bacteria naturally associated with wetland plant roots.

Results provide support for the use of wetland systems as means of natural attenuation of contaminated groundwater and provide more realistic degradation rate constants for natural attenuation.

TABLE OF CONTENTS

Page

LIST OF FIGURES

LIST OF TABLES

ACKNOWLEDGEMENTS

Generous technical assistance was kindly provided by Drs. Garrett Struckhoff, James Amon, and Christina Powell. Amanda Stine assisted in experimental sampling. Research funding was provided from the United States Air Force through Dr. Michael Shelley, Air Force Institute of Technology, Wright-Patterson Air Force Base, Ohio.

1. SUBSTRATE CONCENTRATION EFFECTS ON COMETABOLISM OF CHLORINATED ALIPHATIC HYDROCARBONS BY METHANOTROPHIC BACTERIA NATURALLY ASSOCIATED WITH WETLAND PLANT ROOTS

I.1 BACKGROUND

Treatment wetlands and biodegradation

Chlorinated aliphatic hydrocarbons (CAH) are a major source of groundwater pollution in the United States (Zogorski *et al.* 2006; ATSDR 1997). These chemicals consist of carbon and hydrogen chains with substituted chlorine atoms, and can be removed from the environment through chemical, physical, and biological methods. Bioremediation is the application of microorganisms or plants for the decomposition and removal of harmful pollutants (Amon *et al*. 2007; Kuiper *et al.* 2004).

Wetlands are areas of water saturated soil and can be used for bioremediation because they provide the ideal environment for degradation of numerous pollutants (Amon *et al*. 2007). Within the saturated anaerobic soils in wetlands, methane (CH_4) is produced by methanogenic bacteria due to the degradation of organic matter; CH_4 can then be consumed within the aerobic root zone of wetland plants through oxidation by methanotrophic bacteria (King 1996).

Cometabolism is a process that occurs biologically and involves fortuitous transformation of a non-growth substrate by bacteria without the production of energy for

cell growth. There is a variety of microorganisms that are capable of cometabolism; these organisms produce enzymes that have demonstrated oxidation of CAHs and can often utilize numerous substrates. Methanotrophic bacteria have been found to produce a non-specific enzyme, methane monooxygenase (MMO), that can metabolize CH_4 and also fortuitously catalyze the breakdown of numerous, harmful CAHs (Jiang *et al.* 2010). There are two forms of MMO: a particulate, membrane-associated form (pMMO), and a soluble, cytoplasmic form (sMMO).

Cometabolic degradation of CAHs in plant roots

The degradation of a common groundwater contaminant, trichloroethene (TCE), was examined in the roots of live wetland plants at bench scale with cattail (*Typha latifolia*) and eastern cottonwood (*Populus deltoides*) species (Bankston *et al*. 2002). TCE and CH_4 were found to degrade over time in microcosms: (a) with sandy soil and cottonwood species, and (b) with organic soil and cattail species. The results revealed that the indigenous microbial communities present in two soil types and in association with roots of two plant species were able to oxidize/mineralize TCE (Bankston *et al*. 2002).

Cometabolic degradation of TCE was also investigated by the CH_4- and ammonia- utilizing bacteria naturally associated with roots of the wetland plant, *Carex comosa* (*C. comosa*). Results showed that the indigenous methanotrophic bacteria were able to colonize the microcosms within a short period: The microbial culture demonstrated their ability to degrade 150 µg of TCE liter^{-1} (Powell *et al*. 2011).

Effect of growth substrate and CAH concentration on cometabolism

Past studies have examined effects of toxicity, aeration, and reductant supply on TCE transformation by aerobic cometabolism, specifically by mixed methanotrophic cultures in suspension (Alvarez-Cohen and McCarty 1991). There are three common factors that may adversely affect the cometabolic degradation of CAHs: i) Competitive Inhibition may occur when the primary growth substrate and cometabolic substrate complete for the same oxygenase enzyme binding site. This will result in decreased CAH transformation rates and an apparent decrease in enzyme affinity for each substrate (Alvarez-Cohen and Speitel 2001). ii) The oxidation of growth substrate generates energy that will further metabolism, whereas microorganisms cannot use the intermediates of CAH oxidation. Therefore, oxidation potential of CAHs by cometabolism is often limited by the availability of growth substrate because without growth substrate there is not enough energy for the continued production of cometabolic oxidation enzymes (Alvarez-Cohen and Speitel 2001; Arp *et al.* 2001). iii) Oftentimes, the byproducts of CAH degradation poison and/or kill the bacteria; in this way, CAHs can further inhibit cometabolism (Alvarez-Cohen and Speitel 2001).

Research objectives

This study examined the natural attenuation potential of specific CAHs by methanotrophic microorganisms collected from wetland plant roots. The main objective was to investigate the effects of growth substrate (CH_4) and CAH concentration on the transformation of CAHs by methanotrophic bacteria naturally associated with the roots of a common wetland plant, *C. comosa*. The focus of this research was to expand on the recent studies of CAH biodegradation by methanotrophs associated *C. comosa* roots; results from past research suggest that, similar to other published studies, the methane

oxidizing activity resulted in cometabolic dechlorination of CAHs (Powell and Agrawal 2011; Powell *et al.* 2011). Results of this study may have implications for pollutant mitigation and site management by constructed or restored wetlands: i) degradation of CAHs shows the potential that wetlands have for complete mineralization of harmful pollutants; ii) results from microcosm studies provide further insight into root-microbial relations; and iii) literature review shows the need for more realistic experiments in which batch cultures more closely resemble natural settings.

II.1 MATERIALS AND METHOD

Experimental design

Five sets of six microcosms were created to investigate the effect of CH_4 and CAH concentration on cometabolism (Table 1.1). The experiments were conducted in multiple phases; in Phase I, the effect of CH_4 on TCE cometabolism was investigated in microcosms with 1.0-g of *C. comosa* roots. These experiments were amended with varying CH_4 concentrations, while TCE concentration was held constant. In Phases II through V, concentration effects of CAHs were investigated in similar microcosm setups with 1.0- or 0.5-g *C. comosa* roots. In these experiments, the level of CH_4 was held constant while the concentration of CAH was varied.

Growth media

Growth media "A" was prepared for addition to live microcosms as described in Fogel *et al.* (1986). Growth media "A" consisted of the following salts dissolved in one liter of deionized water (DIW) 98 mg $MgSO_4$, 20 mg $CaCl_2$•$2H_2O$, 1000 mg $NaNO_3$, 40 mg KCl, 160 mg KH_2PO_4, 180 mg NaH_2PO_4•H_2O, 20 µg $MnCl_2$•$4H_2O$, 20 µg H_3BO_4, 100 µg $CoCl_2$•$6H_2O$, 10 µg $CuCl_2$, 20 µg $NiCl_2$•$6H_2O$, 700 µg $ZnSO_4$•$7H_2O$, 3000 µg

$FeSO_4 \cdot 7H_2O$. In some instances, 180 mg $NaH_2PO_4 \cdot H_2O$ was substituted with 184 mg Na_2HPO_4 and with NaOH added for pH adjustment. Control microcosms received mineral media "B", which was prepared similar to media "A", but with 100 mg sodium azide (NaN_3) liter^{-1}. NaN_3 is a known microbicide for gram-negative bacteria. Both solutions had a final pH of 6.80.

Microcosm set-up

C. comosa plants were harvested periodically from a natural wetland located in Beavercreek, OH (USA). The plants were maintained in a greenhouse at Wright State University, Dayton, OH (USA) until use, if necessary. For microcosm set-up, the roots from *C. comosa* plants were removed/clipped from the plant, washed with DIW to remove all soil, and patted dry with paper towel prior to weighing for microcosm set up. Equal amounts of washed wetland plant roots (typically 1.0-g) were added to six, 160 mL borosilicate glass serum bottles (Wheaton, Millville, NJ). Three bottles were prepared as 'live' microcosms with 100 mL of growth media "A", and the remaining three bottles prepared as 'control' microcosms with 100 mL of media "B". After these additions, a headspace of 60 mL remained in each microcosm. Prior to sealing the microcosms with Teflon-lined butyl rubber stoppers and aluminum crimps, all microcosms were bubbled with air for ~15 minutes to start the experiment with an aerated headspace and dissolved oxygen (DO) concentration of ~8 mg liter^{-1}. All bottles were wrapped in aluminum foil to simulate light-free conditions, and placed upside down on a rotary shaker (Glas-Col, Terre Haute, IN) at 30 revolutions per minute (rpm) for gentle horizontal mixing. All experiments were conducted at bench-scale at a temperature of 22 ± 1 ^{o}C.

Enrichment cycles with CH_4

In Phase I, there were four cycles of microbial enrichment with CH_4 as a substrate (cycles 1 through 4, with no TCE added; Figure 1.1), where each cycle corresponded to a period during which CH_4 degraded nearly completely in the microcosms and needed to be replenished. During enrichment cycles, pure gaseous CH_4 was added to each live and control microcosm using a gas-tight glass syringe (Hamilton, Reno NV). Before CH_4 addition, an equal amount of microcosm headspace was withdrawn. During enrichment cycles, CH_4, oxygen (O_2), and carbon dioxide (CO_2) levels were monitored until all CH_4 degraded to aqueous concentrations o 0.05 to 0.001 mg liter^{-1} (Figure 1.1). The enrichment cycles were also completed with fresh *C. comosa* roots prior to CAH degradation experiments in Phases II through V, as described in tables 1.2 through 1.5.

Phase I – Effect of [CH_4] on TCE degradation

Following enrichment cycles, five-day experiments were conducted in Phase I to investigate TCE degradation in the presence of variable CH_4 for 22 weekly cycles (Table 1.2). In this study, the initial aqueous phase TCE concentrations remained constant at approximately 156 μg liter^{-1}, while aqueous CH_4 concentrations (mg liter^{-1}) were varied: 0.36; 1.1; 2.2; and 3.3 (Table 1.2). Each CH_4 concentration was evaluated for at least two, weekly cycles. Experimental procedure was identical as in enrichment cycles, but with added TCE. After each TCE cycle, there were short inter-cycle periods where the microcosms were reset by bubbling with air for ~15 minutes to remove any remaining volatiles and to oxygenate the system. After bubbling, the microcosms were sealed, amended with CH_4 only, and incubated on the rotator for two days.

Phase II through V – Effect of CAH concentration on degradation

TCE, *cis* 1,2-DCE, 1,2-dichloroethane (1,2-DCA), and dichloromethane (DCM) degradation was investigated following microbial enrichment; five- or seven-day (weekly) experimental cycles followed in which initial aqueous CH_4 concentration was ~1.1 mg liter^{-1}. More CH_4 was added throughout the cycle as needed (typically on day three and day five). Each CAH concentration was examined for at least two cycles. Here as well, the experimental procedures were identical as in enrichment cycles, but with added CAH. Again, microcosms were reset by bubbling with air after each CAH cycle, to remove volatiles and to oxygenate the system. The microcosms were then sealed, amended with CH_4 only, and incubated on the rotator for two days.

Chemicals and analysis

CAH stock solutions were prepared by adding 20 μL of the organic compound to a 160 mL borosilicate glass serum bottle containing organic-free Milli-Q water, and sealed with a Teflon-lined rubber stopper and aluminum crimp without headspace. The bottle was then placed on a rotary shaker for 48 h to allow CAH compounds to dissolve completely (see APPENDIX A for complete calculations).

Headspace samples from the microcosms were analyzed daily in each cycle by gas chromatography to estimate the aqueous phase concentration and total amount of CH_4, O_2, inorganic carbon, and CAH in each microcosm. In Phases I, II, and III, CH_4 and CAHs were analyzed by an HP 6890 gas chromatograph (GC) system, while in Phases IV and V, CH_4 and CAHs were analyzed by an Agilent 7890A GC system, both equipped with flame ionization (FID) and electron capture (ECD) detectors. CH_4 was separated on a capillary column (GS GasPro, 30 m × 0.32 mm; J&W Scientific) connected to the FID, and CAHs were separated on a capillary column (HP-624, 30 m ×

0.32 mm; Agilent Technologies) connected to the ECD. O_2 and CO_2 were analyzed by an HP 5890 series GC system with a thermal conductivity detector and a packed column (Shin Carbon 100/120, 2 m× 1 mm; Restek, Bellefonte, PA).

The peak area values for CAHs from GC analysis were transformed into their respective aqueous concentrations at equilibrium and total CAH amount in the microcosms using laboratory calibration curves and a published method (Burris et al. 1996) and its dimensionless Henry's constant (K'_H for CAHs at 25°C given in SI section VIII.3; after USEPA 2012; Sander 1999; Gossett 1987). The aqueous CH_4 concentrations at equilibrium and total CH_4 amount in the microcosms were calculated by the application of Gas Law and Henry's Law (Burris *et al.* 1996) and its dimensionless Henry's constant (K'_H for CH_4 at 25°C = 28.5; Gossett 1987).

Based on measured partial pressures of O_2 in the microcosm headspace, the dissolved oxygen (DO) concentration and total oxygen amount (TO) were calculated using Henry's Law (K'_H for O_2 gas at 25°C = 3.8×10^{-2}; Lide and Frederikse 1995). Similarly, the dissolved inorganic carbon (DIC) concentration and total inorganic carbon (TIC) amount were calculated using Henry's Law (K'_H for CO_2 gas at 25°C = 0.83) and carbonate system equilibrium relationships at measured pH (Pankow 1991). The pH measurements were made using a handheld meter (model AP10 pH/mV/temp, Denver Instrument, Bohemia, NY) by collecting 2.5 mL aqueous samples from each microcosm after gas sampling (see APPENDIX A for calculation procedure). All concentrations for CH_4, DIC, DO, and CAH were determined from standard calibration curves that encompassed the concentration(s) of interest.

Data treatment

The amount of volatile compounds lost in control microcosms was subtracted from the live microcosms to account for amount loss by factors other than microbial degradation due to methanotrophic activity; such loss may have occurred from sorption of CAH to root surfaces and escape of volatiles through septa. Average loss of TO, CH_4, and CAH compounds (mmol) in live and control microcosms was calculated by taking the difference between the average measure amount on day one and the average measure amount on day five, i.e., at the beginning and end of any given cycle. Similarly, average TIC production was determined by subtracting the average measure amount of TIC on day give from the average initial amount on day one.

In Phases II through V, all experimental (weekly) cycles were subdivided into sub-cycles, each about two days long; in this approach, CH_4 was added on day one and allowed to degrade for 48 hours, until day 3; then, after sampling on the third day, microcosms were amended with additional CH_4, that was allowed to degrade for two more days. Such CH_4 amendments twice during a cycle divided each into two sub-cycles. In Phases II through V, initial CH_4 was held constant for sub-cycles at aqueous concentrations of 1.1 mg liter^{-1} (CH_4 amount ~0.12 mmoles); in other words, total aqueous CH_4 added to the microcosms in each cycle was 2.2 mg liter^{-1} (~0.25 mmol). When appropriate, TO consumption and TIC production was also determined for each sub-cycle. CH_4 consumption for whole cycles was determined by adding the difference in initial and final masses of all sub-cycles.

CAH degradation (μmol) in live and control microcosms was determined for the whole cycles similar to calculations for CH_4 consumption described above. Chlorinated compounds were not analyzed on the day that they were injected into the microcosms to

allow for a 24-hour equilibration period between the headspace and liquid. When CAH was added to the microcosms more than once in a cycle (i.e., without microcosm reset), DO and CH_4 consumption, CAH degradation, and TIC production were computed by sub-cycles.

Transformation Yield (T_y) was determined by dividing average net CAH degradation (mol) by average net CH_4 consumption (mol).

The microbial biomass in each whole cycle of Phase I microcosms and in sub-cycles and whole cycles for Phase II through V was estimated using the stoichiometry of O_2 and CH_4 consumption, as outlined in Jenal-Wanner and McCarty (1997) and Powell *et al.* (in review). Similar to Powell *et al.* (in review), biomass may be assumed to reach a steady state after the enrichment period due to the balance between biomass growth and decay (Arvin 1991) (see APPENDIX A for complete calculations).

The pseudo first-order degradation rate constants ($k_{obs\text{-}CAH}$; d^{-1}) were determined from the slope of ln[CAH amount (μmol)] versus time (day) scatter plots for the first three days of each CAH whole cycle and CH_4 sub-cycle. $k_{obs\text{-}CAH}$ was then normalized with respect to steady-state biomass concentration (X_{ss}; mg cell $liter^{-1}$), now termed "biomass-normalized rate constant", $k_{1\text{-}CAH}$, expressed as liter mg $cell^{-1}$ d^{-1}. A similar approach was used to obtain degradation rate constants for CH_4 consumption ($k_{obs\text{-}CH4}$), and then normalized with respect to steady-state biomass concentration to obtain $k_{1\text{-}CH4}$ (liter mg^{-1} cell d^{-1}).

III.1 RESULTS AND DISCUSSION

Phase I - Effect of [CH_4] on TCE degradation

C. comosa plant roots were harvested and monitored for the promotion of methanotrophic bacterial growth in Phase I microcosms. After four enrichment cycles, each with approximately 0.36 mg liter^{-1} of initial aqueous CH_4, there was significant CH_4 consumption in the live microcosms, which indicates that, to begin with, there was an active microbial population associated with the *C. comosa* roots (Figure 1.1). CH_4 consumption for the first three days of each enrichment cycle followed pseudo first-order kinetics, with initial CH_4 degradation rate constants (k_{obs}) that exhibited coefficient of determination values (r^2) from 0.95–1.0 (Figure S1.1); r^2 values around 1.0 indicate that the data can realistically be described as first-order decay. Biomass normalized rate constants ($k_{1\text{-}CH4,}$ liter mg^{-1} cell d^{-1}) were determined for enrichment cycles two, three, and four: 2) 0.16; 3) 0.19; and 4) 0.13.

Initial incubation of *C. comosa* roots resulted in the selective enrichment of a methanotrophic population that was originally present with the roots. To prove that methanotrophic microorganisms came from roots, three microcosms were set up similarly to experimental root microcosms, but with no roots and 100 mL of non-sterilized mineral media "A". CH_4 loss did eventually occur within the microcosms; however, CH_4 consumption within these rootless systems did not occur until the microcosms had been rotating for eight days. In live microcosms with *C. comosa* roots, significant CH_4 loss was seen by day three (Figure 1.1).

Following enrichment cycles, 21 experimental cycles were carried out to determine the effect of CH4 concentration on TCE degradation in methane oxidizing systems; CH_4 concentration was increased periodically while aqueous TCE concentration was held constant at 160 µg liter^{-1}. The concentration of growth substrate did have a

reproducible effect on TCE transformation (Figure 1.2). Results show that, as CH_4 mass was increased, the T_y decreased, which suggests that T_y is dependent upon growth substrate concentration. Decrease in T_y with increasing CH_4 concentration was most likely from competitive inhibition. It is apparent that at higher CH_4 concentrations, TCE competes less effectively than CH_4 for binding sites on the cometabolic MMO enzyme. Toxicity from the presence of TCE and its intermediates was not seen: Comparable T_y (Figure 1.2) and $k_{1\text{-CAH}}$ (Table 1.2) from experiments that were separated by time but had a corresponding CH_4 concentration suggest that toxicity from the breakdown of TCE did not build up in the systems.

Increasing CH_4 concentration showed an increase in the total amount of TCE degraded up to aqueous CH_4 concentrations of 2.2 mg liter^{-1}; TCE degradation was lower at the highest growth substrate concentration examined (Figure 1.3). This further suggests that at aqueous CH_4 concentrations of 3.3 mg liter^{-1}, CH_4 inhibits TCE from oxidizing by MMO.

Optimal growth substrate concentrations were determined by increasing CH_4 concentrations periodically. Steady state biomass concentration (X_{ss}, mg cell liter^{-1}) was not determinable at the lowest CH_4 concentration analyzed. X_{ss} did not vary largely across increasing aqueous CH_4 additions of 1.1, 2.2 and 3.3 mg liter^{-1}: average X_{ss} was 8.2 ± 2.8 (n=14) (Table 1.2). The low variation in biomass with increasing CH_4 indicates that the microcosm systems were at a steady state of microbial growth and that increasing CH_4 was not toxic to the bacteria. A lowering of biomass with increasing CH_4 would have suggested toxicity from TCE degradation or CH_4 level.

In general, CH_4 consumption normalized biomass rate constants ($k_{1\text{-}CH4}$) and TCE degradation normalized biomass rate constants ($k_{1\text{-}TCE}$) decreased with increasing CH_4 concentration (Table 1.2). Decrease in $k_{1\text{-}CH4}$ with increasing CH_4 concentration is to be expected because first-order decay rates are the product of substrate concentration and rate constant. $k_{1\text{-}TCE}$ decreased with increasing CH_4 concentration most likely from competitive inhibition by high CH_4 levels; as more CH_4 was added, relatively less TCE was degraded and as a result $k_{1\text{-}TCE}$ appeared to decrease.

Effect of [CAH] on cometabolism

Phase II – Trichloroethene

In Phase II microcosms, TCE was added in increasing aqueous concentration from 30–250 μg liter^{-1}, while CH_4 was held constant. There does not appear to be a significant effect of CAH concentration on T_y and substrate consumption rates with increasing TCE within the concentration range sampled (Figure 1.4). T_y was not increasing or decreasing significantly at aqueous TCE concentrations of 60, 125, 155, and 200 μg liter^{-1}. Competitive inhibition of CH_4 may have hindered TCE oxidation, or the maximum removal of TCE may have been reached within the concentration range sampled.

Initial TCE degradation in live Phase II microcosms followed pseudo first-order degradation rate kinetics (Table 1.3); rate constants were not determined for control microcosms because there was limited to no removal of CH_4 or TCE within the microcosms. $k_{1\text{-}TCE}$ values were significantly different only when the highest and lowest TCE concentrations had a wide range (namely, $k_{1\text{-}TCE}$ for 30 and 60 aqueous μg liter^{-1} versus 200 and 250 aqueous μg liter^{-1}). This also indicates that the maximum removal of

TCE may have been reached within the concentration range sampled. Results indicate the limitations of root associated bacteria to degrade TCE and indicate that wetlands may be more suited for remediation of low levels of TCE contamination.

Phase III – cis 1,2-Dichloroethene

cis 1,2-DCE was added to Phase III microcosms in increasing aqueous concentration from 360–1090 μg liter^{-1}, and then in decreasing aqueous concentration from 910–730 μg liter$^{-1.}$ *cis* 1,2-DCE has been shown to be toxic in the literature, specifically to methanotrophic bacteria (Chang and Alvarez-Cohen 1996); toxicity is likely to have occurred after aqueous *cis* 1,2-DCE additions of 1090 μg liter^{-1}. Later cycles of aqueous 910 and 730 μg liter^{-1} additions had diminished T_y when compared to previous experiments at lower *cis* 1,2-DCE concentrations (Figure 1.5). Toxicity at 1090 μg liter^{-1} shows the limitations for root associated bacteria to degrade *cis* 1,2-DCE.

$k_{1\text{-cDCE}}$ decreased with increasing *cis* 1,2-DCE, though toxicity may have caused values obtained for aqueous *cis* 1,2-DCE concentrations of 910 and 730 μg liter^{-1} to be lower than expected (Table 1.4). Toxicity may account for $k_{1\text{-cDCE}}$ at varying *cis* 1,2-DCE concentrations that had no significant trend (Table 1.4).

Phase IV – 1,2-Dichloroethane

In Phase IV microcosms, 1,2-DCA was added in increasing aqueous concentration from 108–4005 μg liter^{-1}, while CH_4 concentration was held constant. T_y values were calculated for 1,2-DCA degradation (Figure 1.6): The observed trend between T_y and 1,2-DCA concentration was linear, as seen by an r^2 value of 0.98 for live data analysis and 0.90 for net T_y. The strong linear fit between 1,2-DCA concentration and T_y indicates that, within the concentration range sampled, 1,2-DCA concentration

linearly affects T_y. Continued complete mineralization of 1,2-DCA shows that aerobic microbial systems are suitable for mitigation of 1,2-DCA contamination.

Phase V – Dichloromethane

Rapid removal of DCM occurred in Phase V microcosms up to aqueous concentrations of at least 2530 μg liter^{-1}. As a result of the quick degradation, kinetic parameters for DCM loss were unattainable; similarly X_{ss} values were undeterminable, save for the first experimental cycle (Table 1.5). T_y values were calculated for DCM degradation (Figure 1.7): As DCM concentration increased, T_y increased fairly linearly ($r^2 = 0.92$). Similar to 1,2-DCA results, within the concentration range sampled, DCM concentration linearly affects T_y.

Toxicity

$k_{1\text{-}CH4}$ consumption followed similar trends in all microcosm sets. Though normalized biomass rates were not significantly different, there was a slight drop in $k_{1\text{-}CH4}$ during "b" sub-cycles. This apparent decrease in consumption rates may result from toxicity and recovery of the methanotrophic population. During experiments when CAH was present, toxic intermediates of CAH cometabolism may build up in the system and adversely affect the microbial population. Between each experimental cycle, the microcosms were rotated for at least two days in the presence of CH_4 to allow for recuperation of the bacterial population after CAH addition. This recovery period may have succeeded in rebuilding the methanotrophic population, as seen by increased CH_4 consumption rates for the first part of the weekly experimental cycles. As the added CAH was degraded throughout the cycle, toxic intermediates may have built up in the system and caused harm to the methanotrophic bacteria present – this may account for

slower $k_{1\text{-}CH4}$ and $k_{1\text{-}CAH}$ in "b" sub-cycles. If this is the case, the generated toxicity must have been reversible as by the next experimental cycle, $k_{1\text{-}CH4}$ had recovered.

One other possible explanation for this apparent slowing in consumption is the dependence of CH_4 consumption on O_2 concentration. It has been suggested that methanotrophy is most affected by the concentration of O_2, rather than the concentration of CH_4 (King 1996). O_2 levels fell throughout the experimental cycle and lower O_2 in the second half of the experiments may have caused the apparent slowing in CH_4 consumption.

As DCM was degraded in Phase III systems, $k_{obs\text{-}CH4}$ declined. After DCM additions, the nutrient solution in both the control and live Phase V microcosms was replaced with fresh media, the bottles were bubbled with air for ~15 minutes, and 1.1 mg liter^{-1} gaseous CH_4 was added. The microcosms were run for eight days to explore the potential of reviving the methanotrophic population. $k_{obs\text{-}CH4}$ values increased slightly from previous experiments: rates dropped from 1.7 to 0.23 throughout DCM experiments, then rose slightly during regeneration cycles to 0.65. The increase in CH_4 consumption rate constants further suggests that, in general, the toxic effects of CAH cometabolism are reversible.

Transformation and kinetics with respect to published work

Past studies have shown that the presence of CH_4, even aqueous concentrations as low as ~0.40 mg liter^{-1}, greatly reduced the amount of CAH transformed and subsequently slowed the rate of CAH degradation (Speitel *et al.* 1993; Hanson *et al.* 1989; Palumbo *et al.* 1990). Data from Phase I experiments follows this trend and indicates that when CH_4 and CAH are present together, the potential for competitive

inhibition is great; this applies directly to wetland systems as a means of remediation because, within natural wetland settings, growth substrates will be constantly present.

Transformation capacity (T_c) can only be determined when there is a shut down in growth substrate consumption; for purposes of this study, only the T_y was calculated. Similarly, zero-order degradation rate constants (k, d^{-1}) have been reported by the literature; however, initial pseudo first-order degradation rate constants are reported in this work because they are most commonly reported in the literature and aid in direct comparison of root-microbial systems to pure and mixed cultures (Arp *et al.* 2001).

TCE, *cis* 1,2-DCE, 1,2-DCA and DCM have all been found to degrade cometabolically by methanotrophic bacteria, though to different degrees based upon the experimental system (Alvarez-Cohen and Speitel 2001; Anderson and McCarty 1997; Dolan and McCarty 1997; Smith *et al.* 1997; Chang and Alvarez-Cohen 1996; van Hylckama Vlieg *et al.* 1996; Chang and Alvarez-Cohen 1995; Speitel *et al.* 1993; Alvarez-Cohen and McCarty 1991(a); Alvarez-Cohen and McCarty 1991(b); Alvarez-Cohen and McCarty 1991(c); Oldenhuis *et al.* 1991; Phelps *et al.* 1990). Historically within the literature, large deviations in rates most often resulted from methanotrophic populations expressing sMMO rather than pMMO cometabolic enzymes and/or addition of the secondary growth substrate, formate. In particular, pure cultures expressing sMMO in the presence of formate have yielded the fastest transformation rates (Anderson and McCarty 1994; Speitel *et al.* 1993; Oldenhuis *et al.* 1991).

TCE and *cis* 1,2-DCE degradation within the root microcosms yielded T_y values that were one order of magnitude lower than those reported by other studies. T_y has not been reported for 1,2-DCA or DCM by methanotrophic bacteria, nor have there been

reports of $k_{1\text{-}CH4}$ in the presence of CAH. $k_{1\text{-}CAH}$ examined were at least one order of magnitude lower than those reported in the literature.

Lower T_y and slower degradation rate constants may result from limitations of movement across a biofilm in these CH_4 systems (Anderson and McCarty 1994). Also, it is not known what type of MMO enzyme was expressed in the mixed culture CH_4 systems, though it is most likely pMMO. sMMO is only produced by select methanotrophic bacteria and expressed only in environments with copper limitation; within the methane oxidizing systems, copper was added to the mineral solution, which was replaced every five days to account for depletion of nutrients. Because copper was present within the nutrient solution, it is highly unlikely that sMMO was expressed.

Many of the literature values summarized here are from pure, suspended methanotrophic cultures, expressing sMMO, and grown in the presence of a secondary growth substrate, typically formate. Suspended cultures typically produce faster rates of substrate removal because there is more surface area and less opportunity for mass transfer limitations that biofilms typically produce (Anderson and McCarty 1994; Oldenhuis *et al.* 1991). Studies clearly state that sMMO is less specific than pMMO and produces faster rates of CAH degradation (Alvarez-Cohen and Speitel 2001; Anderson and McCarty 1997; Speitel *et al.* 1993; Tsien *et al.* 1989). Secondary growth substrates are added to systems to limit the effect of competitive inhibition because these compounds are oxidized by different enzymes and thus do not compete with the CAH for cometabolic enzyme binding sites (Anderson and McCarty 1997; Speitel *et al.* 1993). The absence of mass transfer limitations, the presence of the non-specific sMMO enzyme, and lack of competitive inhibition with continued production of energy by

secondary growth substrates can account for the difference in literature values and values reported in this work.

Biofilm processes

During enrichment cycles in Phase II microcosms, two types of mixing regimes were used to determine the optimal environment for methanotrophic microorganisms. Mixing regimes included end-over-end and gentle horizontal both at 30 rpm on a rotary shaker. End-over-end mixing caused CH_4 consumption to occur rapidly within the microcosms, while gentle horizontal mixing allowed for longer cycle lengths and slower daily consumption rates. There was significant difference in daily rate of TIC production and TO and CH_4 consumption in live microcosms between the two types of mixing (Figure 1.8).

Consumption and production rates were most likely greater in systems rotated end-over-end because this type of movement promoted homogenous mixing and continuously exposed all areas of the roots to liquid and dissolved gasses. In addition, enhanced mixing allows the gasses to dissolve from the headspace faster. Increased exposure to dissolved gases may have promoted fast removal rates.

Gentle, horizontal mixing resulted in relatively slower $k_{1\text{-}CH4}$. This difference in rates may suggest that chemical reactions within the microcosms are taking place mainly across a biofilm, which is generated by the methanotrophic microorganisms. End-over-end mixing may yield higher consumption rates as this type of mixing allows more movement and flow of dissolved gases across the root area and subsequently across the methanotrophic biofilm. In addition, the continued movement of liquid, gas, and roots in the microcosms from end-over-end mixing, may have dislodged bacteria otherwise

attached to the root and microcosm surfaces and created a suspended culture. Cultures in suspension would produce more surface area for diffusion of gasses across membranes.

Reasons for the difference in T_y and kinetics of reported values and values given in this work may stem from diffusion limitations of substrates across the biofilm in the CH_4 microcosm systems(Anderson and McCarty 1994), as literature values compiled in this work come mostly from suspended cultures,

IV.1 CONCULSIONS

This work explored the effect of concentration on the biodegradation of CAHs by methanotrophic microorganisms. Though methanotrophic microorganisms have been studied extensively for their ability to degrade chemical pollutants, few studies have explored these microorganisms from their native habitat. In this way, when compared to literature experiments of methanotrophic cometabolism, the root-microcosm approach used here is more appropriate in exploring the role of the aerobic microenvironment in vegetated wetlands, and more accurately depicts processes that would occur in a natural setting.

Results from CAH concentration effect experiments aid in understanding the applicability of wetland systems as a means of remediation. Experimental results indicate that the concentration and type of CAH in question can affect the biological removal of the CAH. Wetland processes can also affect the cometabolic removal of CAHs: Growth substrates that require cometabolic oxygenase enzymes for oxidation will be continually present within the wetland setting and may affect the amount of CAH removed. Diffusion limitations, which arise from the movement of liquid and gas across microbial biofilms in the rhizosphere can also affect the amount of CAH removed.

V.1 REFERENCES

Alvarez-Cohen, L.; McCarty, P. L (a). A cometabolic biotransformation model for halogenated aliphatic compounds exhibiting product toxicity. *Environmental Science and Technology* **1991**, *25* (8), 1381–1387.

Alvarez-Cohen, L.; McCarty, P. L (b). Effects of toxicity, aeration, and reductant supply on trichloroethylene transformation by a mixed methanotrophic culture. *Applied and Environmental Microbiology* **1991**, *57* (1), 228–235.

Alvarez-Cohen, L.; McCarty, P. L (c). Product toxicity and cometabolic competitive inhibition modeling of chloroform and trichloroethylene transformation by methanotrophic resting cells. *Applied and Environmental Microbiology* **1991**, *57* (4), 1031–1037.

Alvarez- Cohen, L.; Speitel, G. E., Jr. Kinetics of aerobic cometabolism of chlorinated solvents. *Biodegradation* **2001**, *12*, 105–126.

Anderson, J. E.; McCarty, P. L. Model for treatment of trichloroethylene by methanotrophic biofilms. *Journal of Environmental Engineering-ASCE* **1994**, *120* (2), 379–400.

Anderson, J. E.; McCarty, P. L. Transformation yields of chlorinated ethenes by a methanotrophic mixed culture expressing particulate methane monooxygenase. *Applied and Environmental Microbiology* **1997**, *63* (2), 687–693.

Arp, D. J.; Yeager, C. M.; Hyman, M. R. Molecular and cellular fundamentals of aerobic

cometabolism of trichloroethylene. *Biodegradation* **2001**, *12*, 81–103.

Arvin, E. Biodegradation kinetics of chlorinated aliphatic hydrocarbons with methane oxidizing bacteria in an aerobic fixed biofilm reactor. *Water Resources* **1991**, *25* (7), 873–881.

Bankston, J. L.; Sola, D. L.; Komor, A. T.; Dwyer, D. F. Degradation of trichloroethylene in wetland microcosms containing broad-leaved cattail and eastern cottonwood. *Water Research* **2002**, *36*, 1539–1546.

Chang, H.; Alvarez-Cohen, L. Biodegradation of individual and multiple chlorinated aliphatic hydrocarbons by methane-oxidizing cultures. *Applied and Environmental Microbiology* **1996**, *62* (9), 3371–3377.

Chang H.; Alvarez-Cohen, L. Transformation capacities of chlorinated organics by mixed cultures enriched on methane, propane, toluene, or phenol. *Biotechnology and Bioengineering* **1995**, *45* (5), 440–449.

Dolan, M. E.; McCarty, P. L. Methanotrophic chloroethene transformation capacities and 1,1-dichloroethene transformation product toxicity. *Environmental Science and Technology* **1997**, *29* (11), 2741–2747.

Fogel, M. M.; Taddeo, A. R.; Fogel, S. Biodegradation of chlorinated ethenes by a methane-utilizing mixed culture. *Applied and Environmental Microbiology* **1986**, *51* (4), 720–724.

Hanson R. S.; Brusseau, G. A.; Wackett, L. P. Development of methanotrophs for the biodegradation of trichloroethylene and other chlorinated olefins. *Abstracts of Papers of the American Chemical Society* **1989**, *29*, 365–367.

Jiang, H.; Chen, Y.; Jiang, P.; Zhang, C.; Smith, T. J.; Murrell, C.; Xing, X. Methanotrophs: Multifunctional bacteria with promising applications in environmental bioengineering. *Biochemical Engineering Journal* **2010**, *49*, 277–288.

Jenal-Wanner, U.; McCarty, P. L. Development and evaluation of semicontinuous slurry microcosms to stimulate *in situ* biodegradation of trichloroethylene in contaminated aquifers. *Environmental Science and Technology* **1997**, *31* (10), 2915–2922.

King, G. M. In situ analyses of methane oxidation associated with the roots and rhizomes of a bur reed, *Sparganium eurycarpum*, in a Maine wetland. *Applied and Environmental Microbiology* **1996**, *62* (12), 4548–4555.

Lide, D. R.; Frederikse, H. P. R. *CRC Handbook of Chemistry and Physics, 76th Edition*. 76th Edition, ed.; CRC Press, Inc.: Boca Raton, FL, 1995.

Oldenhuis, R.; Oedzes, J. Y.; van der Waarde, J. J.; Janssen D. B. Kinetics of chlorinated hydrocarbon degradation by *Mythylosinus tichosporium* OB3b and toxicity of trichloroethylene. *Applied and Environmental Microbiology* **1991**, *57* (1), 7–14.

Palumbo A. V.; Eng W.; Standberg, G. W. The effects of groundwater chemistry on co-metabolism of chlorinated solvents by methanotrophic bacteria. *Abstracts of Papers of the American Chemical Society* **1990**, *199* (1), 140-ENVR.

Phelps, T. J.; Niedzielski, J. J.; Schram, R. M.; Herbes, S. E.; White, D. C. Biodegradation of trichloroethylene in continuous-recycle expanded-bed bioreactors. *Applied and Environmental Microbiology* **1990**, *56* (6), 1702–1709.

Powell, C. L.; Agrawal, A. Biodegradation of trichloroethene by methane oxidizers naturally associated with wetland plant roots. *Wetlands* **2011**, *31* (1), 45–52.

Powell, C. L.; Goltz, M. N.; Agrawal, A. Degradation kinetics of chlorinated aliphatic hydrocarbons by cometabolizing methane oxidizers naturally-associated with wetland plant roots. In review.

Powell, C. L.; Nogaro, G.; Agrawal, A. Aerobic cometabolic degradation of trichloroethene by methane and ammonia oxidizing microorganisms naturally associated with *Carex comosa* roots. *Biodegradation* **2011**, *22* (3), 527–538; DOI: 10.1007/s10532-010-9425-1

Smith, L. H.; Kitanidis, P. K.; McCarty, P. L. Numerical modeling and uncertainties in rate coefficients for methane utilization and TCE cometabolism by a methane-oxidizing mixed culture. *Biotechnology and Bioengineering* **1997**, *53* (3), 320–331.

Speitel, G. E. Jr.; Thompson, R. C.; Weissman, D. Biodegradation kinetics of *Methylosinus trichosporium* OB3b at low concentrations of chloroform in the presence and absence of enzyme competition by methane. *Water Resources* **1993**, *27* (1), 15–24.

Tsien, H.; Brusseau G. A.; Hanson, R. S.; Waclett, L. P. Biodegradation of trichloroethylene by *Methylosinus trichosporium* OB3b. *Applied and Environmental Microbiology* **1989**, *55* (12), 3155–3161.

USEPA. EPA On-line Tools for Site Assessment Calculation. Ecosystems Research, Athens GA, 05 Jan. 2012. Web. 20 Mar. 2012. <http://www.epa.gov/athens/learn2model/part-two/onsite/esthenry.html>

van Hylckama Vlieg, J. E.; de Koning, W.; Janssen, D. B. Transformation kinetics of chlorinated ethenes by *Methylosinus trichosporium* OB3b and detection of unstable epoxides by on-line gas chromatography. *Applied Environmental Microbiology* **1996**, *62* (9), 3304–3312.

Zogorski, J. S.; Carter, J. M.; Ivahnenko, T.; Lapham, W. W.; Moran, M. J.; Rowe, B. L.; Squillace, P. J.; Toccalino, P. L. **2006**. The quality of our Nation's waters–Volatile organic compounds in the nation's ground water and drinking-water supply wells: U.S. Geological Survey Circular 1292, 101 p.

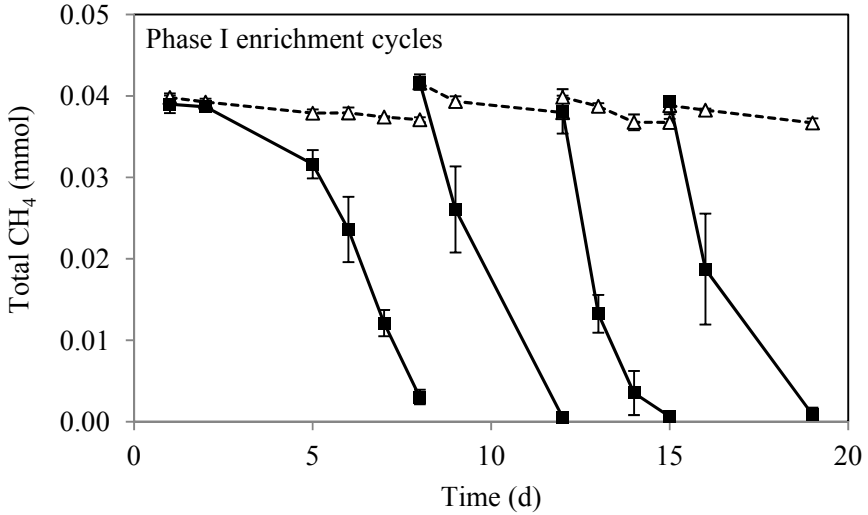

Figure 1.1 Methane enrichment cycles in Phase I. The results show average methane (CH_4) consumption in control (open triangles) and live (closed squares) microcosms in enrichment cycles 1 through 4. Initial aqueous CH_4 was 0.36 mg liter^{-1}; initial CH_4 amount in the bottle equaled 0.041 mmol. Error bars show standard deviation in triplicate microcosms.

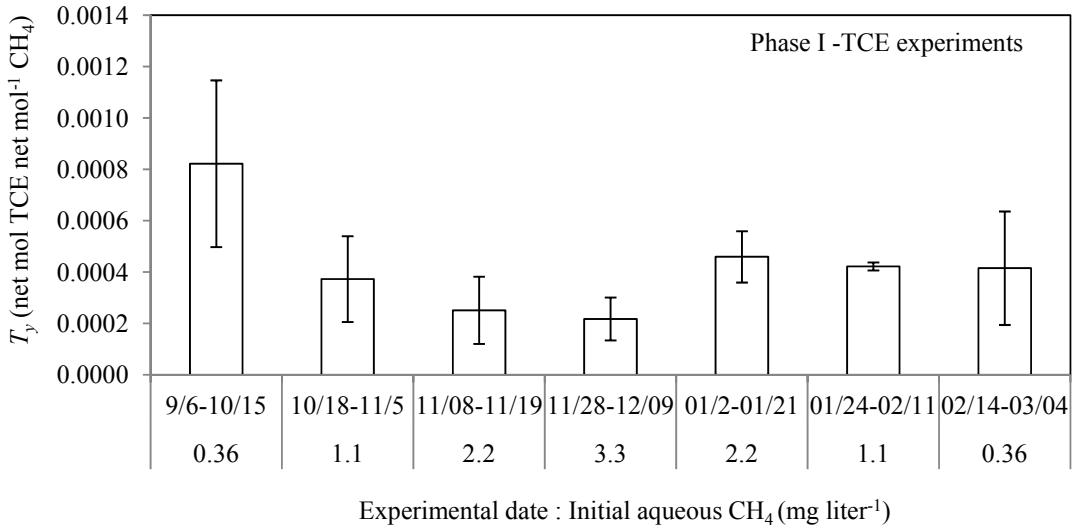

Figure 1.2 Average Transformation Yield (T_y), in mol trichloroethene (TCE) degraded mol^{-1} methane (CH_4) consumed, in Phase I experiments one through seven. Initial aqueous added TCE was the same for all experiments and their respective five-day whole cycles – ~156 µg liter^{-1} (0.14 µmol). Error bars represent one standard deviation.

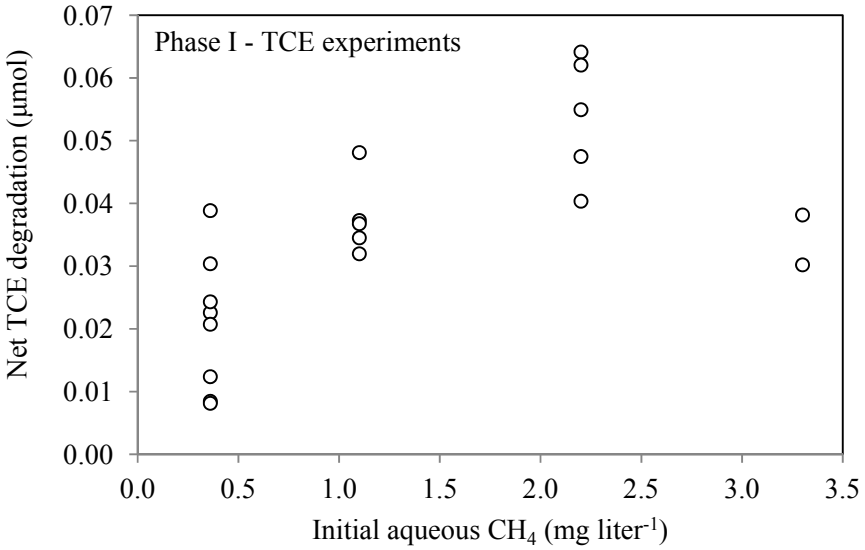

Figure 1.3 Net trichloroethene (TCE) degraded (µmol) with increasing aqueous methane (CH_4) concentration (mg $liter^{-1}$) in Phase I, experiments one through seven and their respective five-day whole cycles.

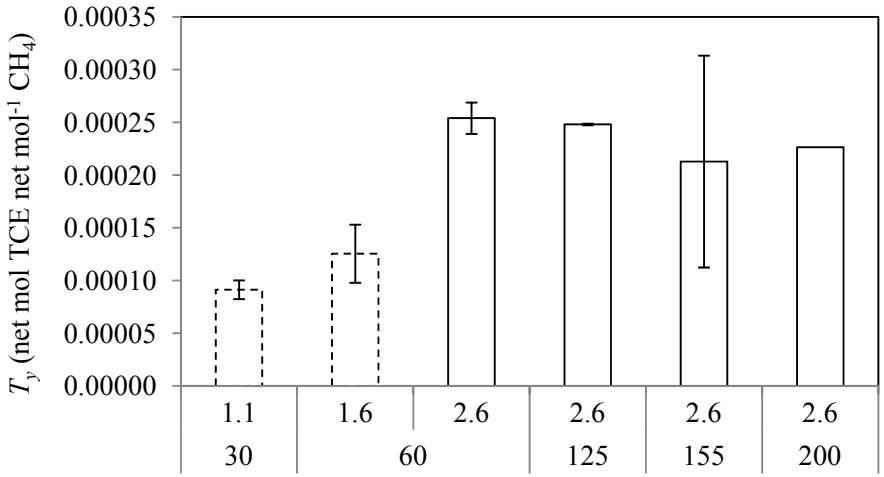

Figure 1.4 Average Transformation Yield (T_y), net mol trichloroethene (TCE) degraded net mol^{-1} methane (CH_4) consumed, for whole cycles of experiments one through six in Phase II microcosms. Dashed lines indicate a deviation in total CH_4 amount added. Error bars represent one standard deviation (no error bar was attainable for experiments with aqueous TCE of 200 µg liter^{-1}).

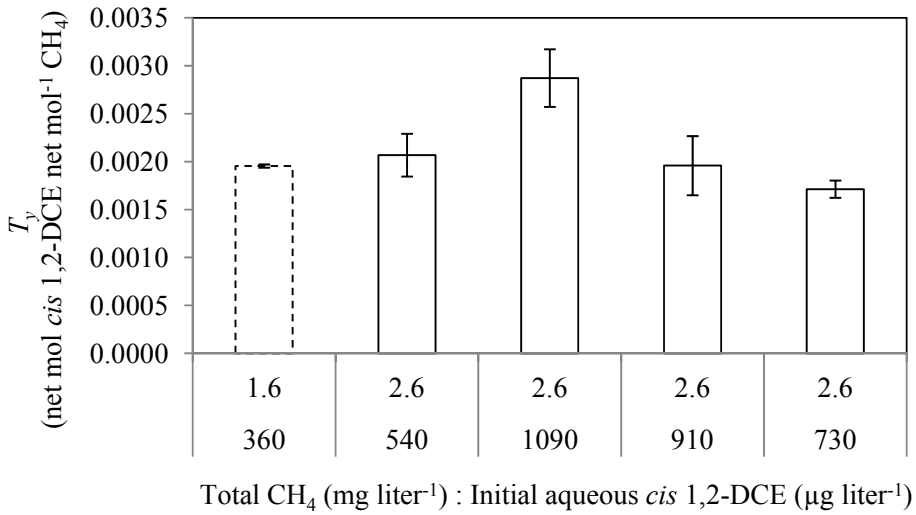

Figure 1.5 Average Transformation Yield (T_y), net mol *cis* 1,2-dichloroethene (*cis* 1,2-DCE) degraded net mol^{-1} methane (CH_4) consumed, for whole cycles of experiments one through five in Phase III. Dashed lines indicate deviation in total CH_4 amount added. Error bars give one standard deviation.

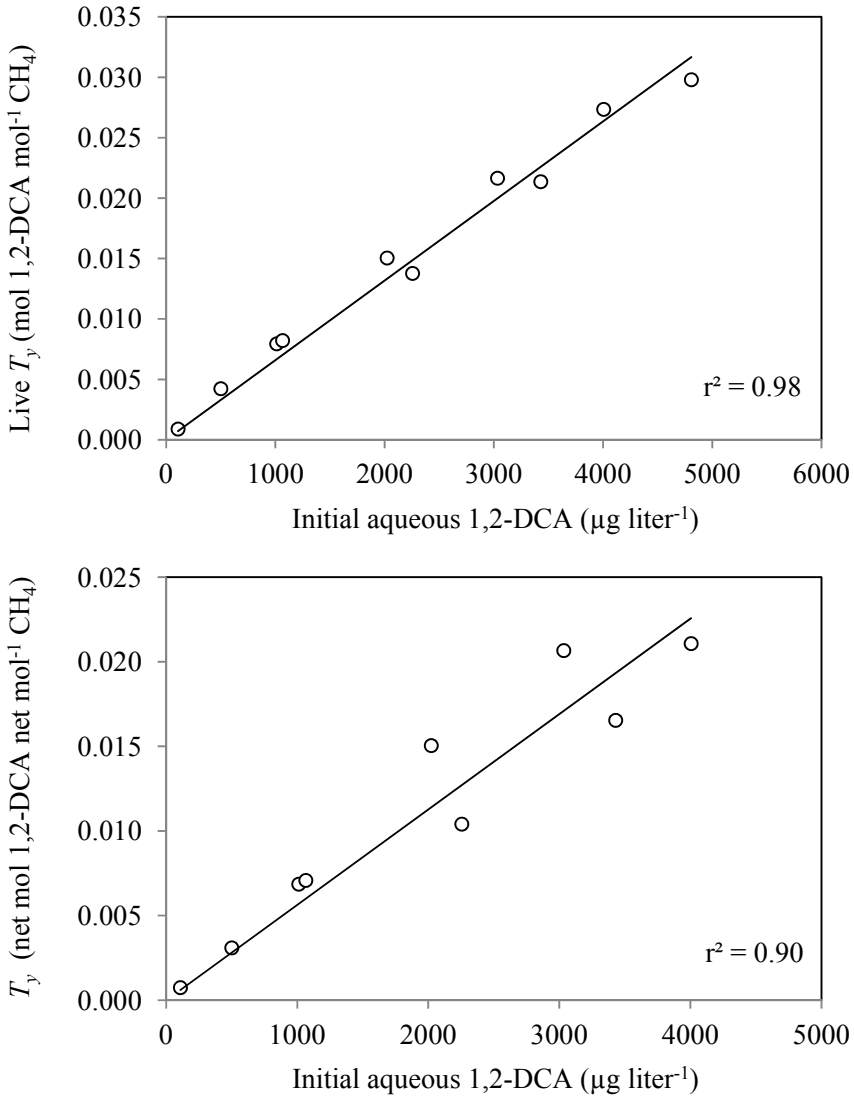

Figure 1.6 Live and net Transformation Yield (T_y), in mol 1,2-dichloroethane (1,2-DCA) degraded mol^{-1} methane (CH_4) consumed, for sub-cycles of experiments two and three in Phase IV. Initial aqueous CH_4 for sub-cycles was 1.1 mg liter^{-1} (0.12 mmol). Aqueous 1,2-DCA concentrations given are calculated values for "a" sub-cycles and observed values for "b" sub-cycles.

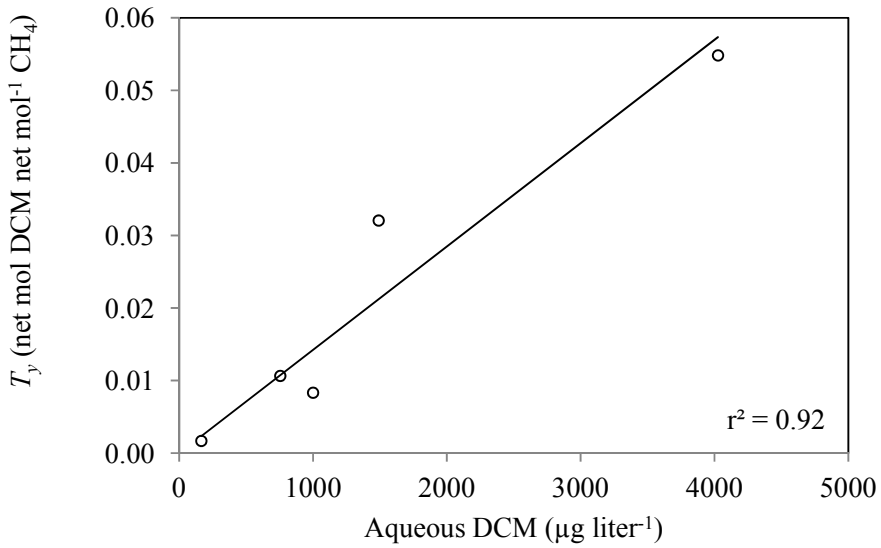

Figure 1.7 Transformation Yield (T_y), net mol dichloromethane (DCM) degraded net mol^{-1} methane (CH_4) consumed, for sub-cycles of experiments one, two, and three in Phase V. Initial aqueous CH_4 for sub-cycles was 1.1 mg liter^{-1} (0.12 mmol). Aqueous DCM values were determined by totaling the calculated concentration added throughout a sub-cycle.

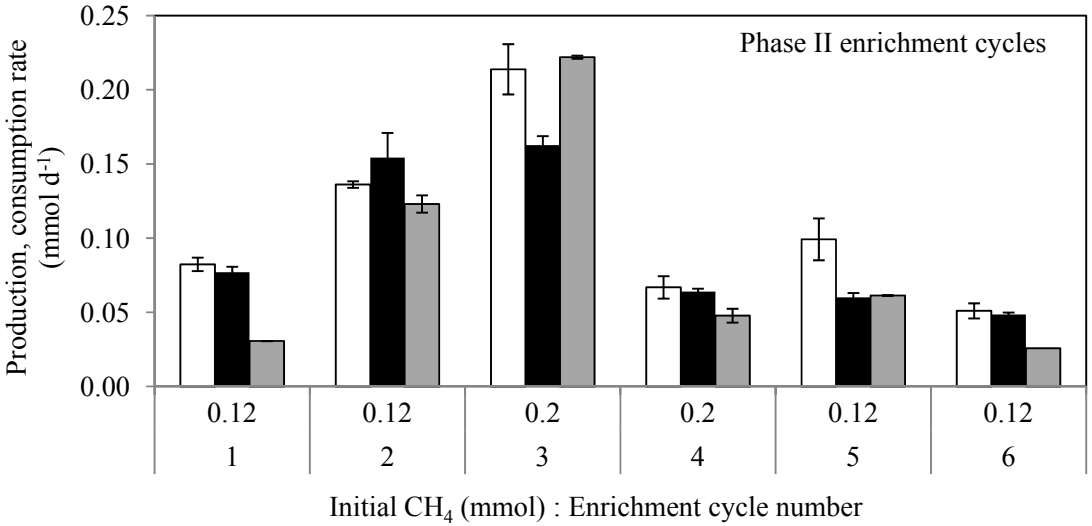

Figure 1.8 Average daily production or consumption rate (mmol d^{-1}) in live Phase II microcosms is shown: total inorganic carbon, open bars; total oxygen, black bars; and methane (CH_4), gray bars. Initial aqueous CH_4 concentration was 1.1 mg $liter^{-1}$ (0.12 mmol) for all cycles except three and four, which had increased CH_4 additions of 1.8 mg $liter^{-1}$ (0.20 mmol). The mixing regime was switched from end-over-end to gentle horizontal between cycles three and four. Error bars give standard deviation of three samples.

Table 1.1 Overview of experimental systems for the study of cometabolic CAH degradation by methanotrophic bacteria naturally associated with *Carex comosa* roots[a]

Experiment name	Date			
	Plant harvest	Experimental set up	CAH[b]	Experimental variable[c]
Phase I	09/--/2008	08/19/2010	TCE	$[CH_4]$[d]
Phase II	03/18/2011	03/24/2011	TCE	[TCE]
Phase III	03/18/2011	04/07/2011	*cis* 1,2-DCE	[*cis* 1,2-DCE]
Phase IV	07/29/2011	08/04/2011	1,2-DCA	[1,2-DCA]
Phase V	09/27/2011	10/06/2011	DCM	[DCM]

[a] – All microcosm sets had 1.0-g *Carex comosa* roots, with the exception of Phase III, which had 0.5-g.

[b] – HAH – halogenated aliphatic hydrocarbon: TCE – trichloroethene: *cis* 1,2-DCE – *cis* 1,2-dichloroethene: 1,2-DCA – 1,2-dichloroethane: DCM – dichloromethane.

[c] – Brackets denote concentration.

[d] – CH_4 – methane.

Table 1.2 Steady state biomass concentration (X_{ss}, mg cell liter^{-1}); Transformation Yield (T_y, net mol TCE net mol^{-1} CH_4); initial pseudo-first order CH_4 and TCE degradation rate constants ($k_{obs\text{-}CH4,\ TCE}$, d^{-1}) and corresponding coefficient of determination (r^2); and biomass normalized rate constants ($k_{1\text{-}CH4,\ TCE}$, liter mg^{-1} cell d^{-1}) in Phase I for seven experimental CH_4 levels and their respective five-day whole cycles

	Initial CH_4[ab]				CH_4 consumption			TCE degradation		
Experiment Id	[Aqueous] (mg liter^{-1})	Amount (mmol)	Cycle	X_{ss}	$k_{obs\text{-}CH4}$	r^2	Average $k_{1\text{-}CH4}$[c]	$k_{obs\text{-}TCE}$	r^2	Average $k_{1\text{-}TCE}$[c]
Sub-phase I-1	0.36	0.041	1		1.11	1.0		0.022	0.14	
			2		1.19	1.0		0.33	1.0	
			3		1.80	0.98		0.12	0.83	
			4		1.51	1.0		0.072	0.16	
			5		1.74	1.0		0.11	0.66	
Sub-phase I-2	1.1	0.12	1	5.9	0.418	0.99	0.079 ± 0.008	0.16	0.71	0.033 ± 0.01
			2	6.5	0.565	0.99		0.26	0.99	
			3	5.7	0.446	0.99		0.18	0.90	
Sub-phase I-3	2.2	0.25	1	5.9	0.357	0.99	0.067 ± 0.01	0.16	1.0	0.039 ± 0.02
			2	4.1	0.304	1.0		0.21	0.87	
Sub-phase I-4	3.3	0.37	1	15	0.302	0.97	0.026 ± 0.008	0.057	0.89	0.0079 ± 0.01
			2	9.3	0.292	0.95		0.11	0.95	
Sub-phase I-5	2.2	0.25	1	11	0.718	1.0	0.059 ± 0.008	0.29	0.98	0.030 ± 0.01
			2	9.8	0.605	0.97		0.25	1.0	
			3	9.2	0.498	1.0		0.44	0.89	
			4	11	0.534	1.0		0.20	0.98	
Sub-phase I-6	1.1	0.12	1	7.5	0.939	1.0	0.098 ± 0.03	0.16	1.0	0.018 ± 0.004
			2	6.5	0.668	1.0		0.12	0.97	
			3	9.0	0.593	1.0		0.13	0.92	
Sub-phase I-7	0.36	0.041	1		1.89	0.98		0.069	0.90	
			2		0.827	1.0		0.053	0.79	
			3		1.15	1.0		0.043	0.71	

[a] – Initial methane (CH_4) additions represent calculated values.

[b] – Total aqueous trichloroethene (TCE) added for each cycle was 156 µg liter^{-1} (0.14 µmol).

[c] – Mean ± standard deviation

Table 1.3 Transformation Yield (T_y, net mol TCE net mol^{-1} CH_4) and biomass normalized rate constant ($k_{1\text{-TCE}}$, liter mg^{-1} cell d^{-1}) in Phase II for experiments one through six and their respective five-day whole cycles

Initial TCE[a]			
[Aqueous] (µg liter^{-1})	Amount (µmol)	T_y[b]	$k_{1\text{-TCE}}$[b]
30	0.030	0.000091 ± 0.00001	0.017 ± 0.000
60	0.060	0.00013 ± ---	0.011 ± 0.003
125	0.11	0.00025 ± 0.00003	0.0082 ± 0.001
155	0.14	0.00025 ± 0.00001	0.0087 ± 0.001
200	0.18	0.00021 ± 0.00000	0.0047 ± 0.000
250	0.22	0.00023 ± 0.0001	0.0036 ± 0.002

[a] – Initial trichloroethene (TCE) represent calculated values. Total aqueous methane (CH_4) for whole cycles was 2.2 mg liter^{-1} (0.25 mmol).
[b] – Mean ± standard deviation.

Table 1.4 Transformation Yield (T_y, net mol *cis* 1,2-DCE net mol^{-1} CH_4) and biomass normalized rate constant ($k_{1\text{-cDCE}}$, liter mg^{-1} cell d^{-1}) in Phase III for experiments one through five and their respective five-day whole cycles

Initial *cis* 1,2-DCE[a]			
[Aqueous] (µg liter^{-1})	Amount (µmol)	T_y[b]	$k_{1\text{-cDCE}}$[b]
360	0.40	0.0020 ± 0.0000	0.027 ± 0.007
545	0.60	0.0021 ± 0.0002	0.018 ± 0.002
730	0.80	0.0017 ± 0.0001	0.0084 ± 0.003
910	1.0	0.0020 ± 0.0003	0.0035 ± 0.002
1090	1.2	0.0029 ± 0.0003	0.013 ± 0.005

[a] – Initial *cis* 1,2-dichloroethene (*cis* 1,2-DCE) represent calculated values. Total aqueous methane (CH_4) for whole cycles was 2.2 mg liter^{-1} (0.25 mmol).
[b] – Mean ± standard deviation.

Table 1.5 Steady state biomass concentration (X_{ss}, mg cell liter^{-1}); initial pseudo first-order CH_4 consumption and CAH degradation rate constant ($k_{obs\text{-}CH4,\ CAH}$, d^{-1}), corresponding coefficient of determination (r^2); and biomass normalized rate constant ($k_{1\text{-}CH4,\ CAH}$, liter mg^{-1} cell d^{-1}) in Phase IV and V for experimental CAH levels and their respective three-day sub-cycles

				Initial CAH[b]								
Microcosm				[Aqueous]	Amount		CH_4 consumption[c]			CAH degradation		
set	CAH[a]	Experiment ID	Cycle	(μg liter^{-1})	(μmol)	X_{ss}	$k_{obs\text{-}CH4}$	r^2	$k_{1\text{-}CH4}$	$k_{obs\text{-}CAH}$	r^2	$k_{1\text{-}CAH}$
Phase IV	1,2-DCA	Sub-phase IV-2	1a	108	0.11	18.6	3.55	0.96	0.19	2.52	0.99	0.14
			1b	500	0.52	21.5	2.19	0.93	0.10	1.96	1.0	0.091
			2a	1010	1.03	22.5	2.97	1.0	0.13	1.51	0.98	0.067
			2b	1010	1.03	19.1	1.29	0.97	0.068	1.00	0.99	0.052
	1,2-DCA	Sub-phase IV-3	1a	2020	2.08	19.1	2.59	0.97	0.14	1.09	1.0	0.057
			1b	2020	2.08	18.9	1.17	0.95	0.062	0.545	1.0	0.029
			2a	3030	3.07	21.3	3.03	0.98	0.14	0.986	1.0	0.046
			2b	3030	3.07	15.5	0.94	0.96	0.061	0.519	1.0	0.033
			3a	4005	4.13	24.3	2.14	0.94	0.088	0.855	1.0	0.035
			3b	4005	4.13	16.2	1.08	0.97	0.067	0.544	0.98	0.034
Phase V[d]	DCM	Sub-phase V-2	1a	55, 110	0.068, 0.137	8.22	1.67	0.98	0.20			
			1b	200, 555	0.244, 0.683	2.86	0.562	1.0	0.20			
			1c	1000	1.23		0.480	1.0				
			2a	1490, 2530	1.80, 3.11		0.409	0.97				
			2b							0.959	0.96	
			3a	1490	1.80		0.231	0.92		0.948	1.0	

[a] – CAH – chlorinated aliphatic hydrocarbon: 1,2-DCA – 1,2-dichloroethane: DCM – dichloromethane.

[b] – Additions based on calculated values – sub-cycle "b" calculations may be based off of slightly higher CAH values than those given: residual compounds were common from incomplete mineralization of halogenated compounds. Commas indicate addition of CAH without microcosm reset.

[c] – Initial aqueous methane (CH_4) for sub-cycles was 1.1 mg liter^{-1} (0.12 mmol).

[d] – DCM consumption occurred too rapidly to determine kinetic parameters.

2. COMETABOLIC REMOVAL OF HALOGENATED ETHENES, ETHANES, METHANES, PROPANES, AND PROPENES BY METHANOTROPHIC BACTERIA NATURALLY ASSOCIATED WITH WETLAND PLANT ROOTS

I.2 BACKGROUND

Halogenated aliphatic hydrocarbons in groundwater

The United States Geological Survey (USGS) compiled a review to assess the quality of our nation's waters and concluded that almost 20 percent of the samples tested contained one or more of 55 priority pollutants. Seven pollutant groups were considered in the assessment and all were volatile organic compounds; these groups included fumigants, gasoline hydrocarbons, gasoline oxygenates, organic synthesis compounds, refrigerants, solvents, and trihalomethanes (THM) (Zogorski *et al.* 2006). Of the 55 compounds considered, the THM chloroform (CF) was detected most frequently, followed by the solvent, perchloroethene and the gasoline oxygenate methyl tert-butyl ether (Zogorski *et. al.* 2006).

The release of industrial chemicals often has a negative impact on the quality of groundwater as many of the pollutant groups listed are not fit for human consumption, even at trace levels – many of the given compounds are known or suspected carcinogens. Of specific interest are halogenated aliphatic hydrocarbons (HAH), which are chained molecules composed of carbon and hydrogen with chlorine, bromine, or fluorine

substituting for hydrogen. Fifteen of the 55 pollutants targeted in the USGS survey were found in one percent or more of the aquifer samples. Of these 15 most frequently detected compounds, all but two were HAHs (Zogorski *et. al.* 2006).

Bioremediation

HAHs can be degraded by microbial processes within aquatic systems by various redox reactions, which include anaerobic reductive dehalogenation, aerobic oxidation, and anaerobic or aerobic cometabolism (Bradley 2000). Cometabolism is a process that occurs in both aerobic and anaerobic zones and involves the transformation of a non-growth substrate by bacteria without the production of energy for growth. During cometabolism, HAHs are oxidized by enzymes that are produced by microorganisms for the oxidation of various growth substrates; these enzymes can oxidize a large range of substances.

There is a variety of microorganisms that are capable of cometabolism; many such organisms produce different enzymes that will oxidize HAHs and can grow on numerous substrates. Various growth substrates have been studied for their ability to support cometabolism of chlorinated compounds: butane, ethylene, toluene, propane, propene, isoprene, isopropylbenzene, methane (CH_4), ammonia, phenol, and other chlorinated hydrocarbons such as vinyl chloride and chloroethane (Frascari *et al*. 2006; Alvarez-Cohen and Speitel 2001; Arp *et al.* 2001).

Methanotrophs generate a non-specific enzyme for the metabolism of CH_4 called methane monooxygenase (MMO), which catalyzes the oxidation reactions of CH_4 (Jiang *et al.* 2010). Two forms of MMO have been identified, a soluble cytoplasmic form (sMMO) and a particulate membrane-associated form (pMMO) (Anderson and McCarty

1997; Jiang *et al.* 2010). When certain HAHs come in contact with these non-specific MMO enzymes they can fortuitously react and the HAHs can be oxidized to carbon dioxide (CO_2), similar to the oxidation of CH_4 to CO_2.

Treatment wetlands

Wetlands are areas of water saturated soil and are used frequently in bioremediation because they provide the ideal environment for degradation of numerous pollutants (Amon *et al*. 2007). The waterlogged soils of wetlands are mainly anaerobic, while aquatic vegetation provide oxygen to a thin layer surrounding plant roots, called the rhizosphere. In this way, wetlands provide both anaerobic (reducing) and aerobic (oxidative) environments for the complete breakdown of harmful HAHs. Results from previous studies suggested that roots of some wetland plant species may support methanotrophic populations and, therefore, will be well suited for application towards establishing treatment wetlands (King 1994).

Research objectives

This study explored the natural attenuation of HAHs in vegetated, aquatic environments. The aim was to examine the degradation potential of numerous HAHs by methanotrophic bacteria naturally associated with the roots of a common wetland plant; past studies have shown that methanotrophic bacteria naturally associated with the common wetland plant, *Carex comosa* (*C. comosa*), expressed the ability to cometabolically degrade TCE (Powell and Agrawal 2011; Powell *et al.* 2011). HAHs of interest included 1,1-dichloroethene (1,1-DCE); 1,1,2-trichloroethane (1,1,2-TCA); 1,2-dichloroethane (1,2-DCA); 1,2-dibromoethane (1,2-DBA); 1,2-dichloropropane (1,2-

DCP); 1,3-dichloropropene (1,3-DCPe); and four THMs: CF; bromodichloromethane (BDCM); dibromochloromethane (DBCM); and bromoform (BF).

Results of this study may be applied to constructed or restored wetlands for pollutant mitigation and site management: i) removal of chemicals from microcosms reveals the potential for aerobic degradation of key halogenated compounds and emerging contaminants within wetland systems; ii) results from microcosm studies provide further insight into rhizospheric processes; and iii) microcosm studies in which plant roots are present along with a mixed microbial population provide realistic experiments that more closely resemble natural settings.

II.2 MATERIALS AND METHOD

Experimental design

Five sets of six microcosms were created to identify HAHs that will cometabolically degrade by methanotrophic bacteria naturally associated with *C. comosa* roots (Table 2.1). The experiments were conducted in numerous phases in which various HAHs were added to microcosms with 1.0-g or 0.5-g of *C. comosa* roots with active methanotrophic microbial populations.

Growth media

Growth media "A" was prepared for addition to live microcosms as described in Fogel *et al.* (1986). Growth media "A" consisted of the following salts dissolved in one liter of deionized water (DIW) 98 mg $MgSO_4$, 20 mg $CaCl_2 \cdot 2H_2O$, 1000 mg $NaNO_3$, 40 mg KCl, 160 mg KH_2PO_4, 180 mg $NaH_2PO_4 \cdot H_2O$, 20 µg $MnCl_2 \cdot 4H_2O$, 20 µg H_3BO_4, 100 µg $CoCl_2 \cdot 6H_2O$, 10 µg $CuCl_2$, 20 µg $NiCl_2 \cdot 6H_2O$, 700 µg $ZnSO_4 \cdot 7H_2O$, 3000 µg $FeSO_4 \cdot 7H_2O$. In some instances, 180 mg NaH_2PO_4 was substituted with 184 mg

Na_2HPO_4 and NaOH was added for pH adjustment. Control microcosms received mineral media "B", which was prepared similar to media "A", but with 100 mg sodium azide (NaN_3) liter^{-1}. NaN_3 is a known microbicide for gram-negative bacteria. Both solutions had a final pH of 6.80.

Microcosm set-up

C. comosa plants were harvested from a natural wetland located in Beavercreek, OH (USA). The plants were maintained in a greenhouse at Wright State University, Dayton, OH (USA) until use, if necessary. As needed, roots from *C. comosa* plant were pulled/clipped, washed with deionized water to remove all soil, and patted dry with paper towel prior to addition to microcosms.

Collected wetland plant roots were weighed and equal amounts were added to six, 160 milliliter (mL) borosilicate glass serum bottles (Wheaton, Millville, NJ). Three bottles were prepared as live microcosms and amended with 100 mL of media "A" and three control bottles were prepared with 100 mL of media "B". Four enrichment cycles were initially carried out, where each cycle started with removal of old growth media while retaining roots. After the addition of 100 mL of fresh media, all microcosms were bubbled with air for ~15 minutes to ensure that the experimental bottles contained enough oxygen (O_2) to maintain aerobic conditions throughout the course of the experiment; initial dissolved oxygen (DO) concentrations were ~8 mg liter^{-1}. All bottles were wrapped in aluminum foil to simulate natural conditions and placed upside down on a rotary shaker (Glas-Col, Terre Haute, IN) at 30 revolutions minute^{-1} (rpm) for gentle, horizontal mixing. Microcosms were then capped with Teflon-lined butyl rubber stoppers and sealed with aluminum crimp seals.

Enrichment cycles with CH_4

In all phases, there were at least four cycles of microbial enrichment with CH_4 as a substrate, where each cycle corresponded to a period during which CH_4 degraded nearly completely and needed to be replenished. During enrichment cycles, pure gaseous CH_4 was added to each live and control bottle by use of a gas-tight glass syringe; before addition of CH_4, an equal amount of headspace was removed. For each enrichment cycle CH_4, O_2, and carbon dioxide (CO_2) levels were monitored until all CH_4 degraded to aqueous concentrations of 0.05 to 0.001 mg liter^{-1}.

HAH additions

Following enrichment cycles, various HAHs were added to the microcosms; five- or seven-day (weekly) experimental cycles followed where initial aqueous CH_4 was approximately 1.1 mg liter^{-1}. More CH_4 was added after sampling throughout the cycle as needed (typically on day three and day five). Each halogenated substrate concentration was tested for at least two cycles. Experimental set up followed the same procedures as the enrichment cycles, but with added HAH (Table 2.1). After each cycle, between HAH additions, the microcosms were reset by exchanging 100 mL media and bubbling with air for ~15 minutes to remove any remaining volatiles and to oxygenate the system. After bubbling, the microcosms were sealed, amended with CH_4 only, and incubated on the rotator for 2 days.

Chemicals and analysis

HAH stock solutions were prepared by adding 20 μL of the organic compound to a 160 mL borosilicate glass serum bottle containing organic-free Milli-Q water, and sealed with a Teflon-lined rubber stopper and aluminum crimp without headspace. The

stock solution was then placed on a rotary shaker for 48 h to allow HAH compounds to dissolve completely (see APPENDIX A for complete calculation procedure and chemicals examined).

Concentrations of CH_4, DO, dissolved inorganic carbon (DIC), and HAH were measured daily in each cycle; headspace samples were analyzed by gas chromatography (GC). CH_4 and HAH were analyzed by an Agilent 7890A GC system with flame ionization (FID) and electron capture detectors (ECD). CH_4 was separated on a capillary column (GS GasPro, 30 m × 0.32 mm; J&W Scientific) connected to the FID, and HAHs were separated on a capillary column (HP-624, 30 m × 0.32 mm; Agilent Technologies) connected to the ECD.

Aqueous concentrations of CH_4 and HAH at equilibrium were calculated using the Ideal Gas law and Henry's law and a published method (USEPA 2012; Sander 1999; Burris *et al.* 1996; Gossett 1987).

The partial pressures of O_2 and CO_2 were determined by analysis on a 5890 Series II GC system with a thermal conductivity detector and a packed column (Shin Carbon 100/120, 2 m× 1 mm; Restek, Bellefonte, PA). pH values were collected on the first and last day of each cycle (AP10 pH 10/mV/temp, Denver Instrument, Bohemia, NY). DO and DIC concentrations were then calculated by application of Henry's Law and carbonate system equilibrium relationships at measured pH values.

All concentrations for CH_4, DIC, DO, and HAH were determined from standard calibration curves that encompassed the concentration(s) of interest.

Data treatment

The amount of volatile compound lost in control microcosms was subtracted from the live microcosms to account for amount loss by microbial activity due to methanotrophic bacteria present along with the plant roots. Average loss of total oxygen (TO), CH_4, and HAH (mmol) for live and control bottles was calculated by taking the difference between the average measured mass on day one and the average measured mass on day five. Similarly, average total inorganic carbon (TIC) production was determined by subtracting the average measured mass on day five from the average initial mass on day one.

In all systems experimental cycles were subdivided into sub-cycles, each ~2 days long, where CH_4 was added on day one and allowed to degrade for ~48 hours, until day three. After sampling on the third day, additional CH_4 was added and allowed to degrade for two more days. These CH_4 addition approaches lead to the creation of sub-cycles within the experiments. Initial CH_4 was held constant for sub-cycles at aqueous concentrations of 1.1 mg liter^{-1}; whole cycle aqueous CH_4 concentrations were 2.2 mg liter^{-1}.

CH_4 consumption and HAH degradation in live and control microcosms was calculated two ways: sub-cycles and whole cycles. Halogenated compounds were not analyzed on the day that they were injected into the microcosms to allow for a 24 hour equilibration period between the headspace and liquid. When HAH was added to the microcosms more than once in a cycle (i.e., without microcosm reset) consumption of DO and CH_4, degradation of HAH, and production of TIC were computed by sub-cycles.

Transformation Yield (T_y) was determined by dividing average net HAH degradation (mol) by average net CH_4 consumption (mol).

The microbial biomass during whole or sub-cycles was estimated using the stoichiometry of O_2 and CH_4 consumption, as outlined in Jenal-Wanner and McCarty (1997) and Powell *et al.* (in review). Similar to Powell *et al.* (in review), biomass may be assumed to reach a steady state (X_{ss}; mg liter^{-1}) after the enrichment period due to the balance between biomass growth and decay (Noguera *et al.* 2001; Clapp *et al.* 1999; Arvin 1991) (see APPENDIX A for complete calculations).

The pseudo first-order degradation rate constants ($k_{obs\text{-}HAH}$; d^{-1}) were determined from the slope of ln[HAH amount (mmol)] versus time (day) scatter plots for the first three days of each HAH whole cycle and CH_4 sub-cycle. $k_{obs\text{-}HAH}$ was then normalized with respect to steady-state biomass concentration (X_{ss}; mg cell liter^{-1}), now termed "biomass normalized rate constant", $k_{1\text{-}HAH}$, expressed as liter mg cell^{-1} d^{-1}. A similar approach was used to obtain degradation rate constants for CH_4 consumption ($k_{obs\text{-}CH4}$), and then normalized with respect to steady-state biomass concentration to obtain $k_{1\text{-}CH4}$ (liter mg^{-1} cell d^{-1}).

III.2 RESULTS AND DISCUSSION

Transformation and kinetics with respect to published work

Past studies that have provided transformation extent and kinetics in methanotrophic systems for the compounds analyzed in this work have been summarized in table format in APPENDIX B (Table S2.1).

Similar studies of the root microcosm systems indicate that the methanotrophs are growing in a biofilm, rather than in a suspended culture (Powell *et al*., in review). Faster methane consumption rate constants were seen when the microcosms were rotated end-over-end, rather than the gentle horizontal mixing used in this study; rate constants of

methane consumption and HAH cometabolism may be slower in these systems when compared to published rates because many published experiments have been conducted with pure cultures in suspension. Generally, biofilm kinetics are slower than suspended culture kinetics because of diffusion limitations of substrates across the biofilm (Anderson and McCarty 1994).

Trihalomethanes

Four THMs were examined in Phase III microcosms: CF, BDCM, DBCM, and BF. All compounds were found to degrade to some extent in the methanotrophic systems (Figures 2.1–2.4). Individual HAHs and their respective concentrations appeared to yield similar $k_{1\text{-HAH}}$ and T_y values (Table 2.2); the ability for repeated removal indicates that the methanotrophic bacteria associated with *C. comosa* roots are able to sustain cometabolic removal of emerging contaminants. Degradation of these THMs is believed to be cometabolism because control microcosms did not exhibit CH_4 or THM removal, while live microcosms had complete CH_4 removal and significantly more THM loss than the controls.

Few reports have been published on the cometabolism of BDCM, DBCM, and BF by methanotrophic microorganisms, though studies with nitrifying bacteria revealed that individual THM rate constants increased with increasing bromination: BF > DBCM > BDCM > CF (Wahman *et al.* 2006). In the methanotrophic systems studied here, rates were two orders of magnitude slower and did not follow the above pattern. In methanotrophic systems, mainly pure cultures of resting cells have been shown to cometabolically degrade brominated and chlorinated THMs (Han *et al.* 1999; Bartricki and Castro 1994).

There have not been any scientific reports on T_y from the cometabolism of these four THMs by methanotrophic cultures – Transformation Capacity (T_c), which measures the extent of toxicity effects on cometabolism, has been reported for CF in methanotrophic systems (Alvarez-Cohen and McCarty 1991) and T_c by nitrifying bacteria for the four THMs has been reported (Wahman *et al.* 2006).

Results of THM cometabolism in methanotrophic microcosms provides a proof of concept that such microbial populations, naturally associated with wetland plant roots, have the potential to attenuate chlorinated and brominated hydrocarbons. Rates of degradation of THMs by methanotrophs have not been consistently reported in the literature.

Halogenated ethanes and ethenes

1,2-DCA; 1,2-DBA; and 1,1-DCE were found to degrade in Phase IV microcosms (Figures 2.5–2.7).

1,2-DCA has been shown to degrade by methanotrophic bacteria (Chang and Alvarez -Cohen 1996; Lanzarone and McCarty 1990), though T_y was not reported and most commonly maximum degradation rates (k, mg substrate mg^{-1} cell d^{-1}) were determined instead.

One recent peer reviewed publication has noted methanotrophic microorganisms as an avenue for cometabolic removal of 1,2-DBA from contaminated systems (McKeever *et al.* 2012). Initial pseudo-first order degradation rates were given though they were not normalized with respect to biomass: In aerobic microcosms with soil from a contaminated aquifer, 2.4 aqueous mg $liter^{-1}$ CH_4 was added along with 80 µg $liter^{-1}$ 1,2-DBA. The first-order decay rate was found to be 3.49 ± 3.29 yr^{-1}.

The T_y values obtained for 1,1-DCE removal are comparable to those found in the literature (Anderson and McCarty 1997). In a mixed culture of methanotrophs that were expressing pMMO and grown in the presence of CH_4, a T_y of 0.00022 mol 1,1-DCE mol^{-1} CH_4 was obtained for 1,1-DCE degradation. The mixed microbial culture in the root microcosms studied here produced a T_y of 0.00024 mol 1,1-DCE mol^{-1} CH_4.

The $k_{1\text{-HAH}}$ and T_y values reported here help provide more realistic insight into what level of remediation is possible in a natural setting. At present, there have not been many reports on mixed microbial cultures. The values given in this work may more adequately reflect the expected removal rates from a constructed mitigation system.

Cometabolic removal

Ten chlorinated and/or brominated compounds were analyzed in the methanotrophic root-microcosms (Table 2.1). Of the compounds analyzed only 1,1,2-TCA and 1,2-DCP did not degrade, Phases I and II, respectfully (Figures 2.1 and 2.2); significantly more CH_4 removal within the live microcosms as compared to the control microcosms indicates that methanotrophic bacteria were successfully inactivated in the control systems. However, there appeared to be little to no loss of 1,1,2-TCA and 1,2-DCP in the live and control microcosms (Figures 2.8 and 2.9), which indicates that these two compounds do not degrade in these methanotrophic root systems.

1,3-DCPe was found to degrade very quickly in Phase V microcosms; however, degradation may not have been tied to methanotrophy as killed controls, which did not exhibit any CH_4 consumption, had 1,3-DCPe loss comparable to the live microcosms (Figure 2.10). This suggests that 1,3-DCPe was degrading as a result of competing biological processes or from an abiotic process. Interestingly, it has been reported that

1,3-DCPe can degrade metabolically by aerobic, gram positive bacteria (Olaniran *et al.* 2007).

The fact that 8 HAHs did degrade in these methanotrophic systems shows the potential for natural attenuation of key and emerging halogenated compounds by wetland processes.

HAH degradation kinetics

$k_{1\text{-HAH}}$ for chlorinated and brominated THMs were one order of magnitude slower than those of chlorinated ethenes and ethanes; this may indicate that THMs have less efficiency for the MMO enzyme that was being expressed in the root microcosms (Han *et al.* 1999). In addition, THMs may have been affected by diffusion limitations across the biofilm as slower kinetics are often attributed to biofilm transfer efficiency and the type of MMO enzyme that is expressed (Noguera *et al.* 2001; Anderson and McCarty 1994; Arvin 1990).

CH_4 consumption kinetics

In all live microcosms initial CH_4 consumption followed pseudo first-order rate kinetics; linear fitting of ln[HAH concentration] versus time plots produced coefficient of determination (r^2) values around 0.95 to 1.0; acceptable r^2 values indicate that first-order decay was taking place. When possible, pseudo first-order degradation rates ($k_{\text{obs-CH4}}$) were normalized to biomass ($k_{1\text{-CH4}}$) (Table 2.3). Though values were not statistically significantly different, in all live systems sub-cycle one had consistently faster $k_{1\text{-CH4}}$ than sub-cycle two. This may be attributed to periodic microcosm reset (see methods). The two-day recovery period after each HAH addition may have allowed for the methanotrophic population to rebuild after toxic effects of HAH degradation; the increase

in microbial population would account for the observed increased CH_4 consumption rates in the first sub-cycle. $k_{1\text{-}CH4}$ may have been slower in the second half of the experimental cycles due to build up of toxic intermediates from incomplete HAH mineralization.

However, because this phenomenon was also seen in live microcosms that did not degrade 1,1,2-TCA and 1,2-DCP, this slowing in rates during the second half of the cycle is more likely the results of decreased O_2 levels over the weekly cycle. It has been suggested that methanotrophy is most affected by the concentration of O_2, rather than the concentration of CH_4 (King 1996). O_2 levels fell throughout the experimental cycle and lower O_2 in the second half of the experiments may have caused the apparent slowing in CH_4 consumption.

The effect of O_2 on CH_4 consumption within these systems is important to understand because, within the wetland system, O_2 and CH_4 concentrations may fluctuate daily and seasonally. The interaction between O_2 and CH_4 concentration may adversely affect the amount of HAH degraded at a given time.

IV.2 CONCLUSIONS

This study explored the role of the aerobic microenvironment in wetland systems. When compared to the majority of scientific research on cometabolism by methanotrophic bacteria, the root microcosm experimental approach used here provides a more realistic understanding of the natural attenuation of HAHs by methanotrophic bacteria. Wetland settings will more likely contain a mixed microbial population growing both on biofilms and in suspension, and growth substrate will be continually present.

Results of this study help to fill in data gaps for wetland processes particularly regarding cometabolism of emerging pollutants by methanotrophic bacteria naturally associated with wetland plant roots. Much of the research previously conducted for methanotrophic systems has been done in pure cultures; there is also a lack of data for degradation of the emerging THMs, BF; BDCM; and DBCM. Kinetics of cometabolism can add to the understanding of cometabolic limitations and feasibility for the use of enhanced bioremediation and natural attenuation as options for remediation.

V.2 REFERENCES

Alvarez-Cohen, L. A.; McCarty, P. L. Product toxicity and cometabolic competitive inhibition modeling of chloroform and trichloroethylene transformation by methanotrophic resting cells. *Applied and Environmental Microbiology* **1991**, *57* (4), 1031–1037.

Alvarez- Cohen, L.; Speitel, G. E., Jr. Kinetics of aerobic cometabolism of chlorinated solvents. *Biodegradation* **2001**, *12*, 105–126.

Amon, J. P.; Agrawal, A.; Shelley, M. L.; Opperman, B. C.; Enright, M. P.; Clemmer, N. D.; Slusser, T.; Lach, J.; Sobolewski, T.; Gruner, W.; Entingh, A. C. Development of a wetland constructed for the treatment of groundwater contaminated by chlorinated ethenes. *Ecological Engineering* **2007**, *30*, 51–66.

Anderson, J. E.; McCarty, P. L. Model for treatment of trichloroethylene by methanotrophic biofilms. *Journal of Environmental Engineering-ASCE* **1994**, *120* (2), 379–400.

Anderson, J. E.; McCarty, P. L. Transformation yields of chlorinated ethenes by a methanotrophic mixed culture expressing particulate methane monooxygenase. *Applied and Environmental Microbiology* **1997**, *63* (2), 687–693.

Arp, D. J.; Yeager, C. M.; Hyman, M. R. Molecular and cellular fundamentals of aerobic cometabolism of trichloroethylene. *Biodegradation* **2001**, *12*, 81–103.

Arvin, E. Biodegradation kinetics of chlorinated aliphatic hydrocarbons with methane oxidizing bacteria in an aerobic fixed biofilm reactor. *Water Resources* **1991**, *25* (7), 873–881.

Bartnicki, E. W.; Castro, C. E. Biodehalogenation- rapid oxidative-metabolism of monohalomethanes and polyhalomethanes by *Methylosinus-trichosporium* OB-3b. *Environmental Toxicology and Chemistry* **1994**, *13* (2), 241–245.

Bradley, P. M. Microbial degradation of chloroethenes in groundwater systems. *Hydrogeology Journal* **2000**, *8*, 104–111.

Chang, H.; Alvarez-Cohen, L. Biodegradation of individual and multiple chlorinated aliphatic hydrocarbons by methane-oxidizing cultures. *Applied and Environmental Microbiology* **1996**, *62* (9), 3371–3377.

Chang H.; Alvarez-Cohen, L. Transformation capacities of chlorinated organics by mixed cultures enriched on methane, propane, toluene, or phenol. *Biotechnology and Bioengineering* **1995**, *45* (5), 440–449.

Clapp, L. W.; Regan, J. M.; Ali, F.; Newman, J. D.; Park, J. K.; Noguera, D. R. Activity, structure, and stratification of membrane-attached methanotrophic biofilms cometabolically degrading trichloroethylene. *Water Science and Technology* **1999**, *39* (7), 153–161.

Dolan, M. E.; McCarty, P. L. Methanotrophic chloroethene transformation capacities and 1,1-dichloroethene transformation product toxicity. *Environmental Science and Technology* **1997**, *29* (11), 2741–2747.

Frascari, D.; Pinelli, D.; Nocentini, M.; Zannoni, A.; Fedi, S.; Baleani, E.; Zannoni, D.; Farneti, A.; Battistelli, A. Long-term aerobic cometabolism of a chlorinated

solvent mixture by vinyl chloride-, methane- and propane- utilizing biomasses. *Journal of Hazardous Materials* **2006**, *B 138*, 29–39; DOI: 10.1016/j.jhazmat.2006.05.009.

Han, J.; Lontoh, S.; Semrau, J. D. Degradation of chlorinated and brominated hydrocarbons by *Methylomicrobium album* BG8. *Archives of Microbiology* **1999**, *172* (6), 393–400.

Jiang, H.; Chen, Y.; Jiang, P.; Zhang, C.; Smith, T. J.; Murrell, C.; Xing, X. Methanotrophs: Multifunctional bacteria with promising applications in environmental bioengineering. *Biochemical Engineering Journal* **2010**, *49*, 277–288.

Jenal-Wanner, U.; McCarty, P. L. Development and evaluation of semicontinuous slurry microcosms to stimulate *in situ* biodegradation of trichloroethylene in contaminated aquifers. *Environmental Science and Technology* **1997**, *31* (10), 2915–2922.

King, G. M. Associations of methanotrophs with the roots and rhizomes of aquatic vegetation. *Applied Environmental Microbiology* **1994**, *60* (9), 3220–3227.

King, G. M. In situ analyses of methane oxidation associated with the roots and rhizomes of a bur reed, *Sparganium eurycarpum*, in a Maine wetland. *Applied and Environmental Microbiology* **1996**, *62* (12), 4548–4555.

Lanzarone, N. A; McCarty, P. L. Column studies on methanotrophic degradation of trichloroethene and 1,2-dichloroethane. *Ground water* **1990**, *28* (6), 910–919.

McKeever, R.; Sheppard, D.; Nüsslein, K.; Baek, K.; Rieber, K.; Ergas, S. J.; Forbes, R.; Hilyard, M.; Park, C. Biodegradation of ethylene dibromide (1,2-dibromoethane

[EDB]) in microcosms simulating in situ and biostimulated conditions. *Journal of Hazardous Materials* **2012**, *209*, 92–98.

Noguera, D. R.; Pizarro, G.; Clapp, L. W. Mathematical modeling of trichloroethylene (TCE) degradation in membrane-attached biofilms. *Water Science and Technology* **2001**, *41* (4), 239–244.

Oldenhuis, R.; Oedzes, J. Y.; van der Waarde, J. J.; Janssen D. B. Kinetics of chlorinated hydrocarbon degradation by *Mythylosinus tichosporium* OB3b and toxicity of trichloroethylene. *Applied and Environmental Microbiology* **1991**, *57* (1), 7–14.

Olaniran, A. O.; Naidoo, S.; Masango, M. G.; Pillay, B. Aerobic biodegradation of 1,2-Dichloroethane and 1,3-Dichloropropene by bacteria isolated from a pulp mill wastewater effluent in South America. *Biotechnology and Bioprocesses Engineering* **2007**, *12* (3), 276–281.

Powell, C. L.; Agrawal, A. Biodegradation of trichloroethene by methane oxidizers naturally associated with wetland plant roots. *Wetlands* **2011**, *31* (1), 45–52.

Powell, C. L.; Nogaro, G.; Agrawal, A. Aerobic cometabolic degradation of trichloroethene by methane and ammonia oxidizing microorganisms naturally associated with *Carex comosa* roots. *Biodegradation* **2011**, *22* (3), 527–538; DOI: 10.1007/s10532-010-9425-1

Sander, R. Compilation of Henry's Law constant for inorganic and organic species of potential importance in environmental chemistry, 1999. Web. 28 Feb. 2012. <http://www.mpch-mainz.mpg.de/~sander/res/henry.html>

Speitel G. E. Jr.; Thompson, R. C.; Weissman, D. Biodegradation kinetics of Methylosinus trichosporium OB3b at low concentrations of chloroform in the

presence and absence of enzyme competition by methane. *Water Resources* **1993**, *27* (1), 15–24.

USEPA. EPA On-line Tools for Site Assessment Calculation. Ecosystems Research, Athens GA, 05 Jan. 2012. Web. 20 Mar. 2012. <http://www.epa.gov/athens/learn2model/part-two/onsite/esthenry.html>

van Hylckama Vlieg, J. E.; de Koning, W.; Janssen, D. B. Transformation kinetics of chlorinated ethenes by *Methylosinus trichosporium* OB3b and detection of unstable epoxides by on-line gas chromatography. *Applied Environmental Microbiology* **1996**, *62* (9), 3304–3312.

Wahman, D. G.; Henry, A. E.; Katz, L. E.; Speitel G. E. Jr. Cometabolism of trihalomethanes by mixed culture nitrifiers. *Water Research* **2006**, *40*, 3349–3358.

Zogorski, J. S.; Carter, J. M.; Ivahnenko, T.; Lapham, W. W.; Moran, M. J.; Rowe, B. L.; Squillace, P. J.; Toccalino, P. L. **2006**. The quality of our Nation's waters–Volatile organic compounds in the nation's ground water and drinking-water supply wells: U.S. Geological Survery Circular 1292, 101 p.

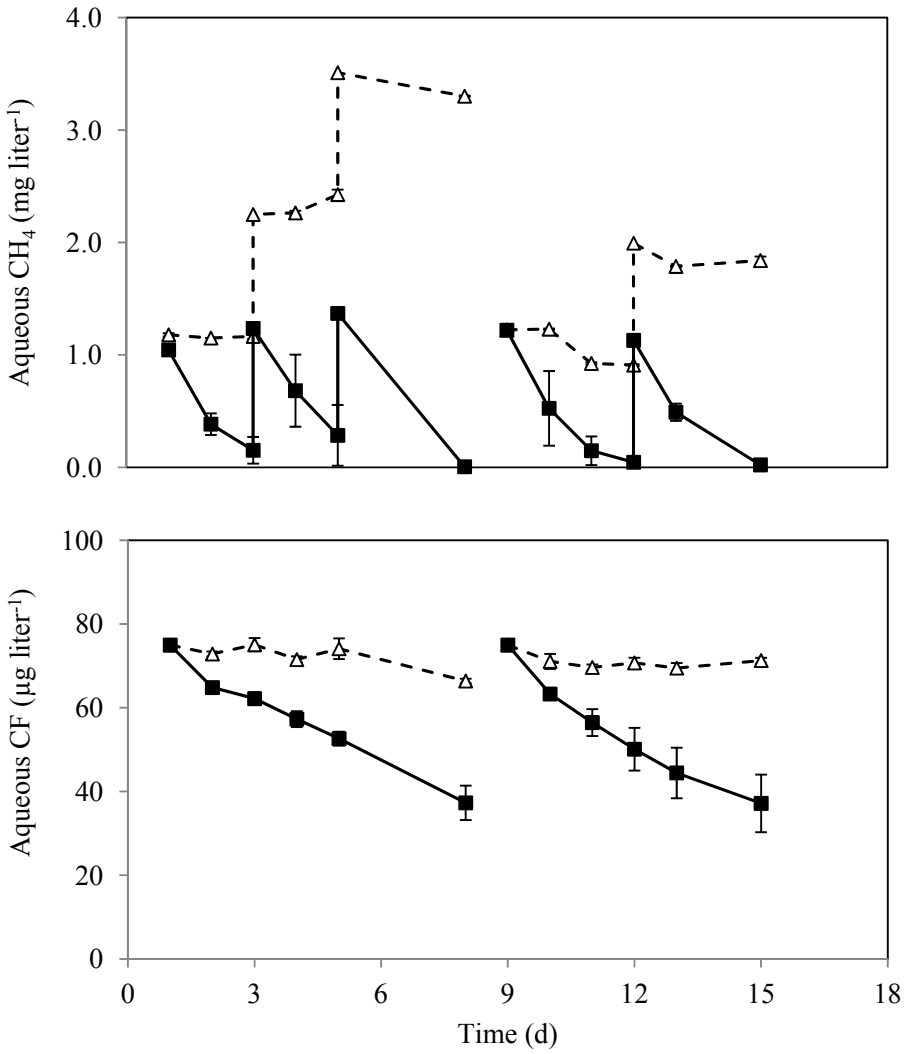

Figure 2.1 Average methane (CH_4) consumption and chloroform (CF) degradation in control (open triangle) and live (closed square) Phase III microcosms. Initial CF concentrations represent calculated values. Error bars give standard deviation of three samples.

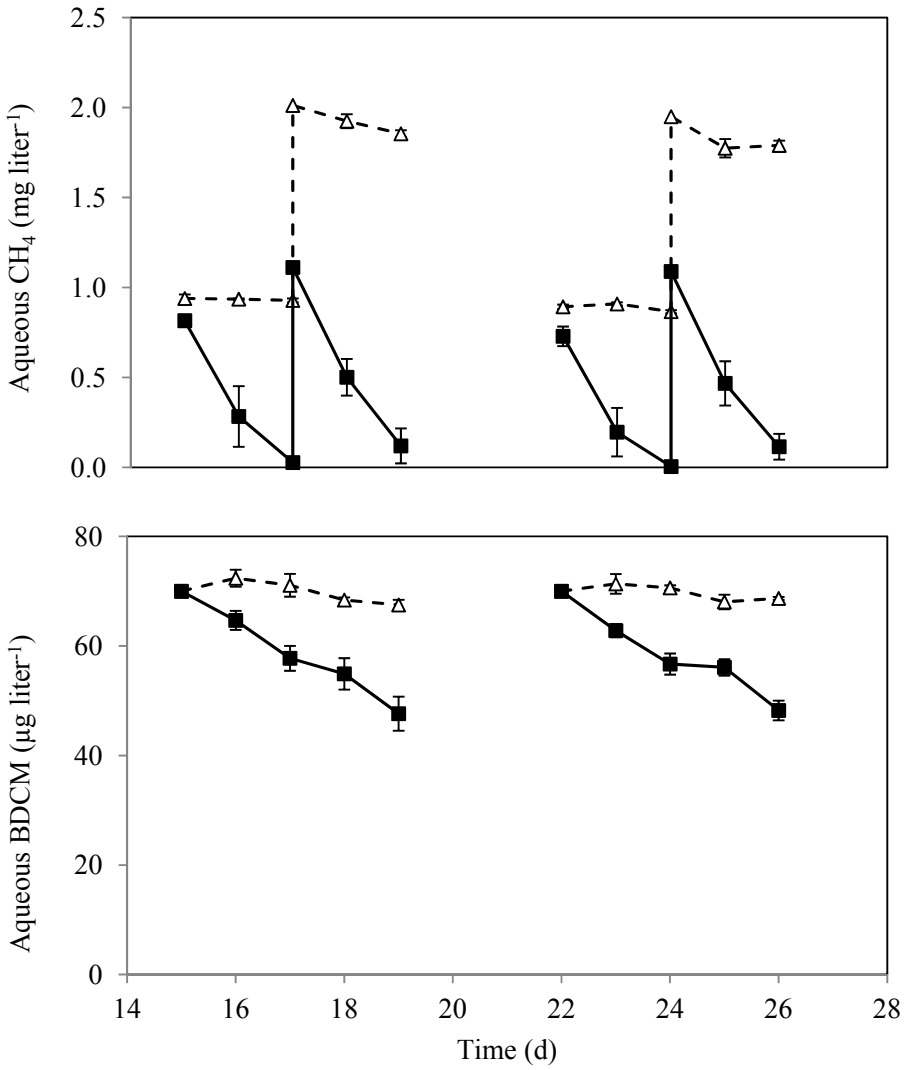

Figure 2.2 Average methane (CH_4) consumption and bromodichloromethane (BDCM) degradation in control (open triangle) and live (closed square) Phase III microcosms. Initial BDCM concentrations represent calculated values. Error bars give standard deviation of three samples.

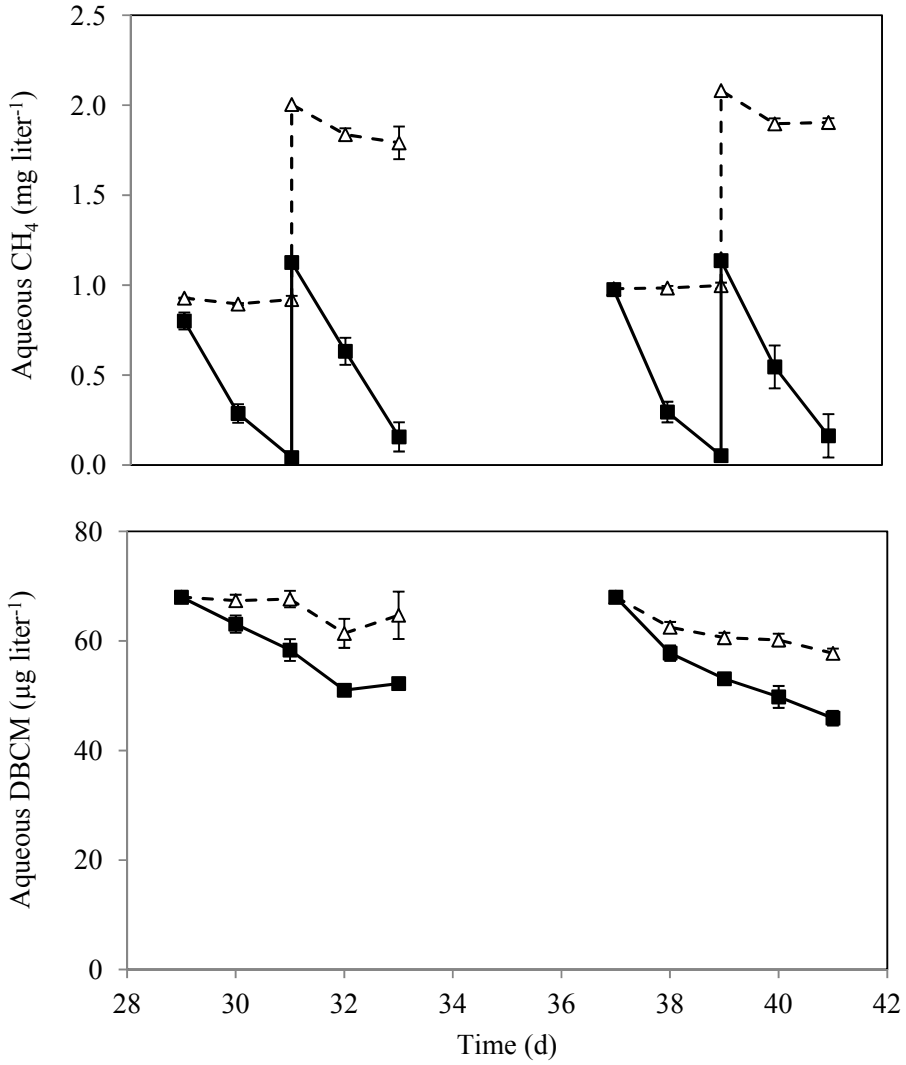

Figure 2.3 Average methane (CH_4) consumption and dibromochloromethane (DBCM) degradation in control (open triangle) and live (closed square) Phase III microcosms. Initial DBCM concentrations represent calculated values. Error bars give standard deviation of three samples.

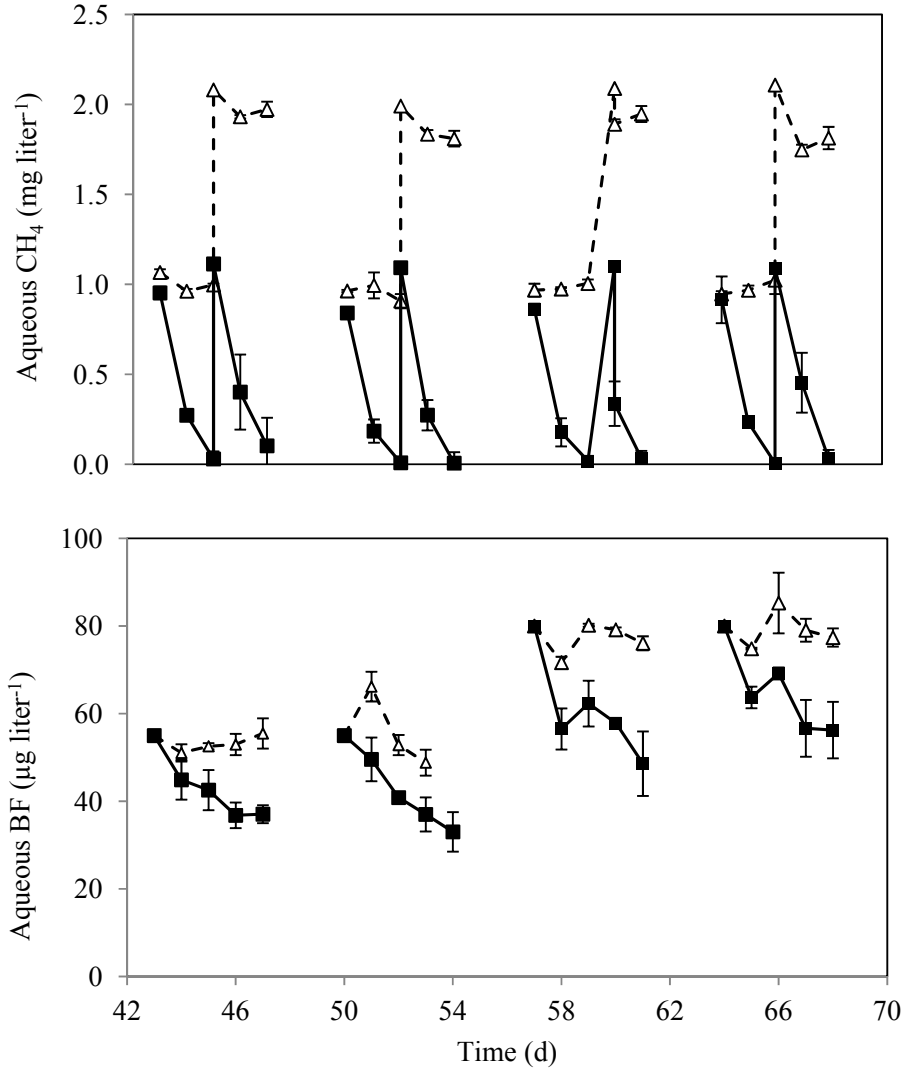

Figure 2.4 Average methane (CH_4) consumption and bromoform (BF) degradation in control (open triangle) and live (closed square) Phase III microcosms. Initial BF concentrations represent calculated values. Error bars give standard deviation of three samples.

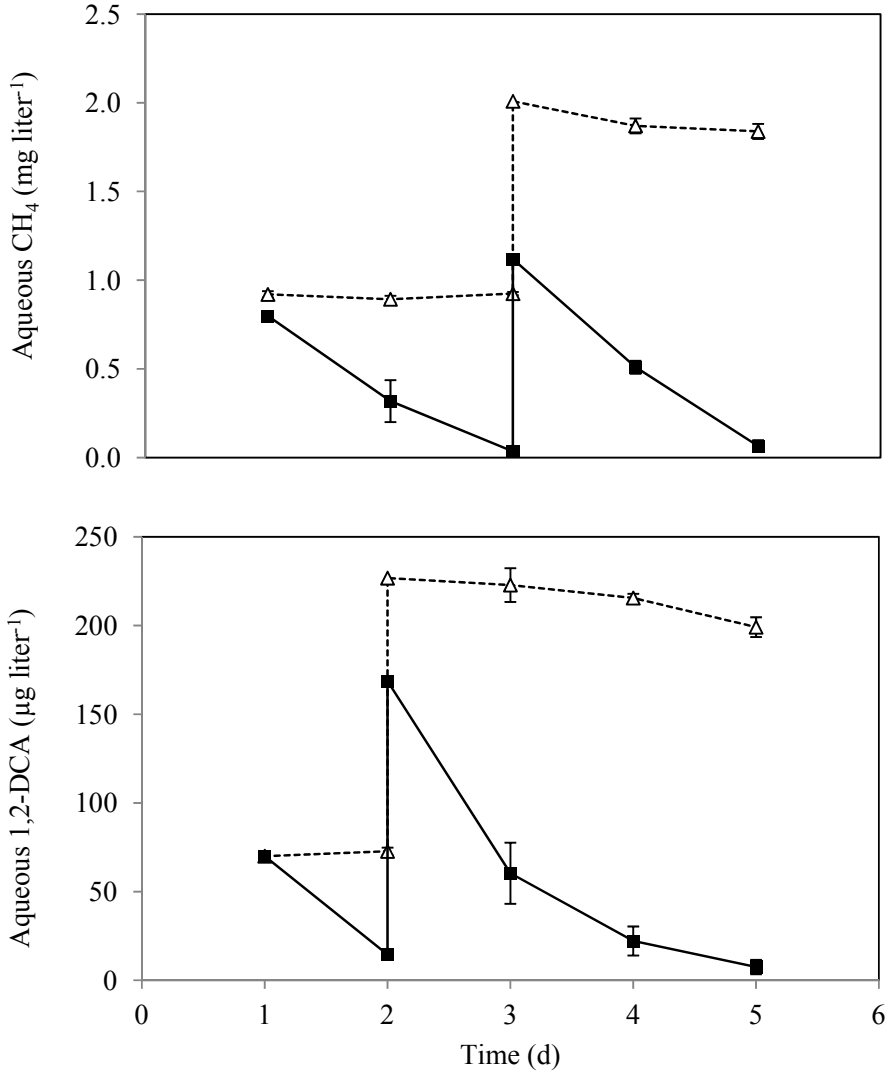

Figure 2.5 Average methane (CH_4) consumption and 1,2-dichloroethane (1,2-DCA) degradation in control (open triangle) and live (closed square) Phase IV microcosms. Initial 1,2-DCA concentrations represent calculated values. Error bars give standard deviation of three samples.

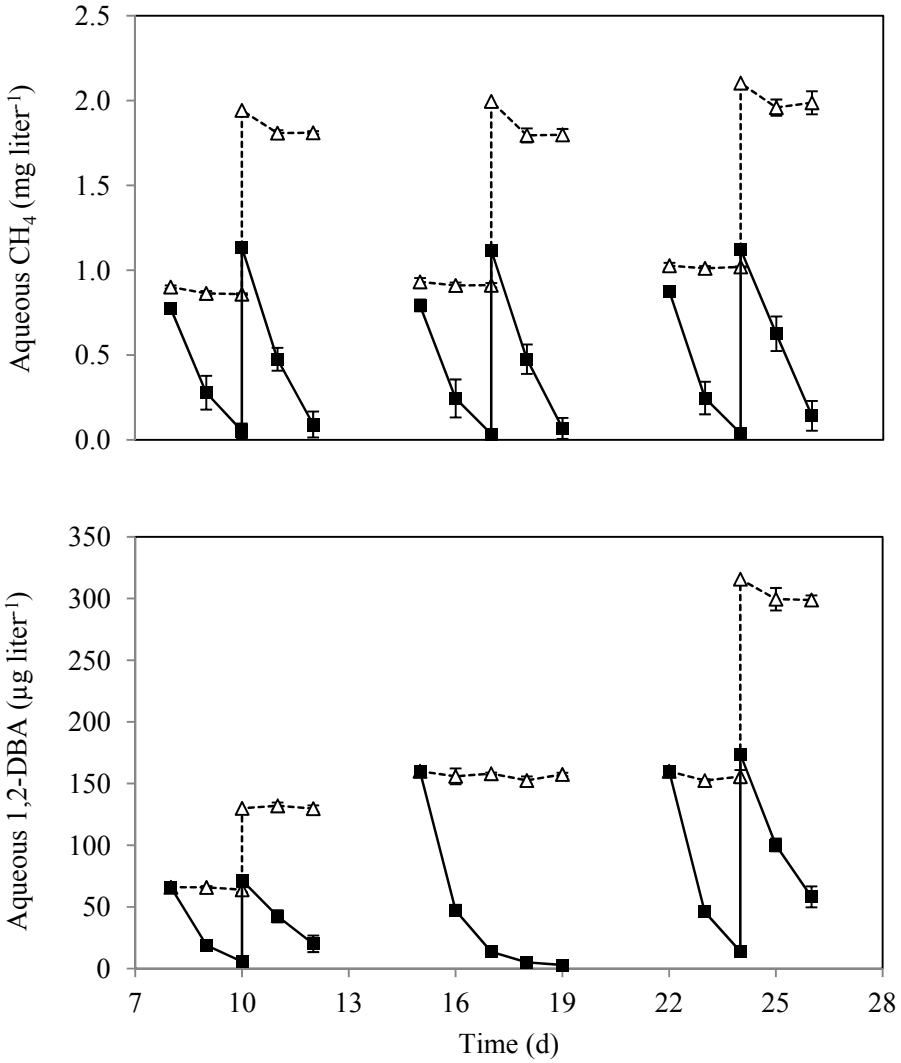

Figure 2.6 Average methane (CH_4) consumption and 1,2-dibromoethane (1,2-DBA) degradation in control (open triangle) and live (closed square) Phase IV microcosms. Initial 1,2-DBA concentrations represent calculated values. Error bars give standard deviation of three samples.

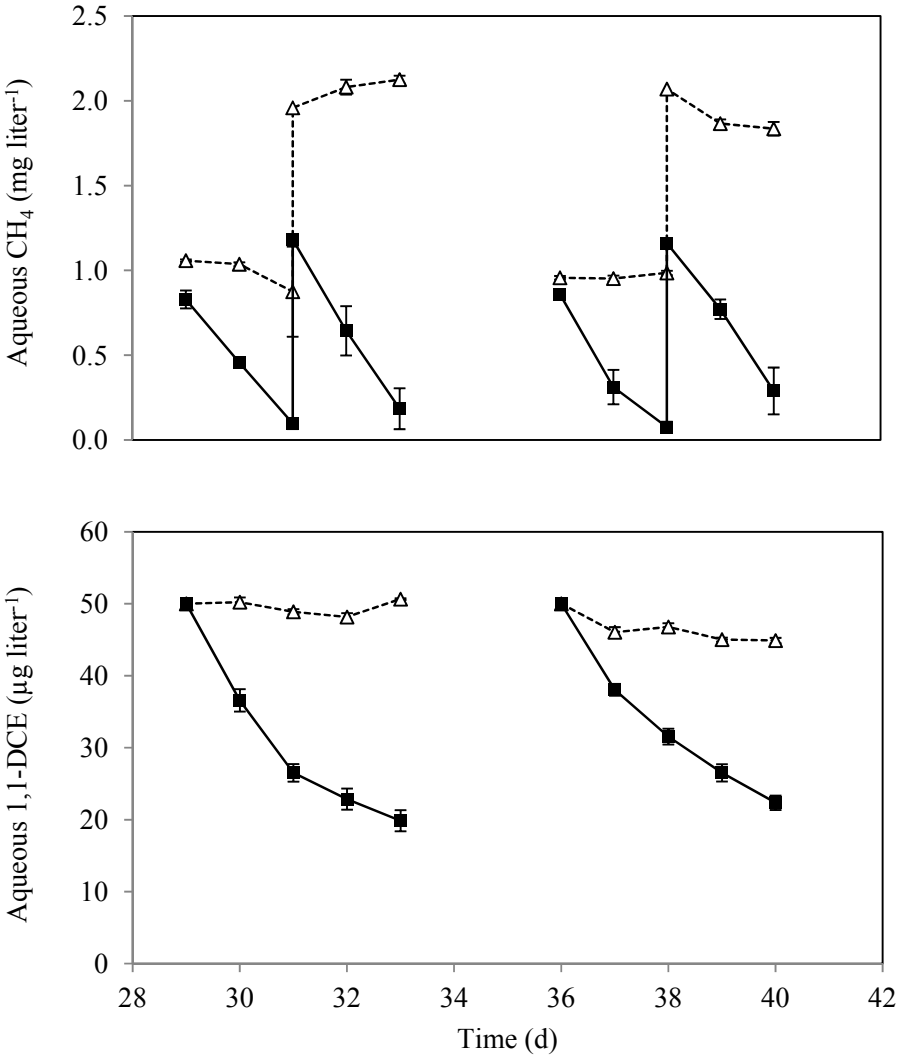

Figure 2.7 Average methane (CH_4) consumption and 1,1-dichloroethene (1,1-DCE) degradation in control (open triangle) and live (closed square) Phase IV microcosms. Initial 1,1-DCE concentrations represent calculated values. Error bars give standard deviation of three samples.

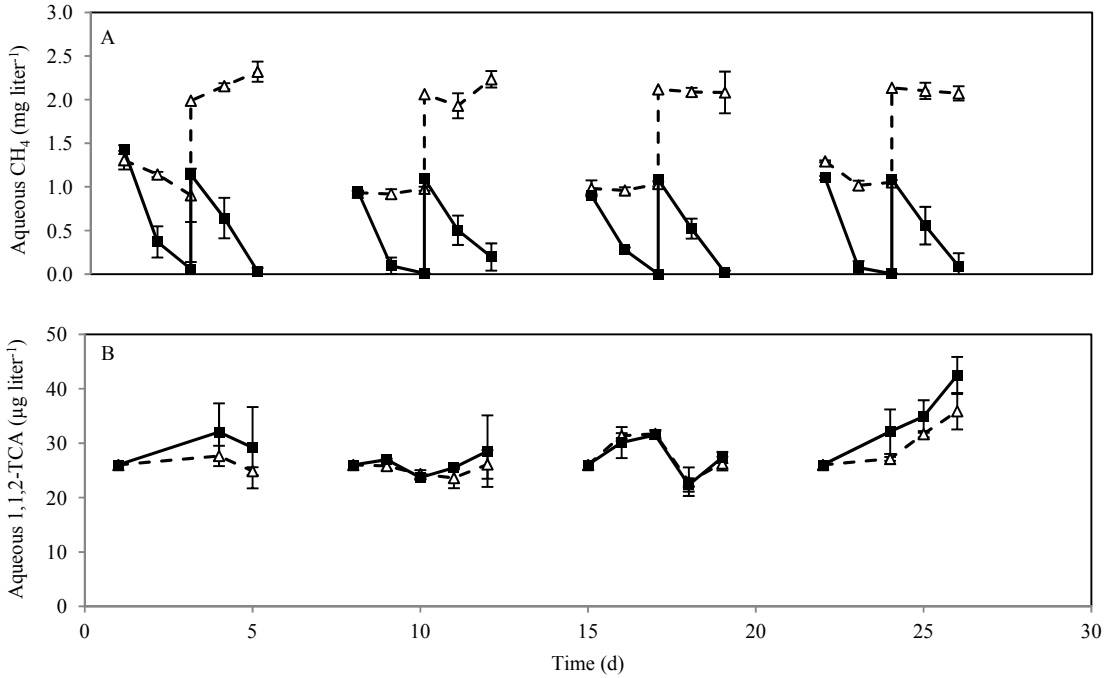

Figure 2.8 A) Methane (CH_4) consumption and B) 1,1,2-trichloroethane (1,1,2-TCA) degradation in control (open triangles) and live (closed circles) Phase I microcosms for experiments one and two, 1,1,2-TCA additions. Error bars give standard deviation of three samples.

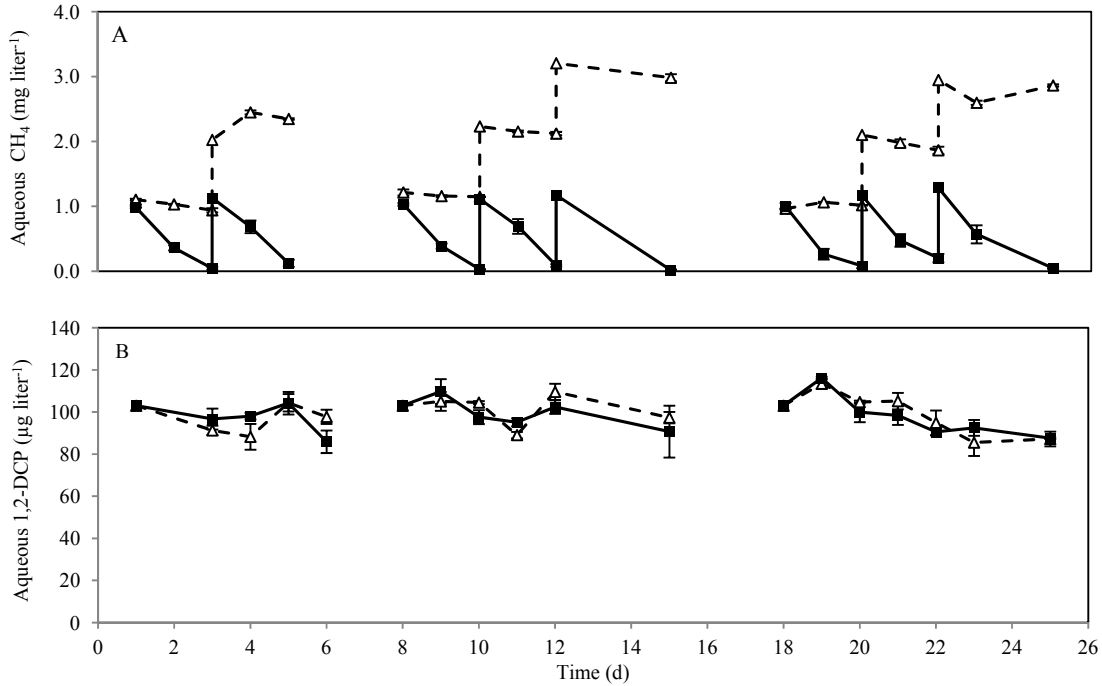

Figure 2.9 A) Methane (CH_4) consumption and B) 1,2-dichloropropane (1,2-DCP) degradation in control (open triangles) and live (closed squares) Phase II microcosms for experiment one, 1,2-DCP additions. Error bars give standard deviation of three samples.

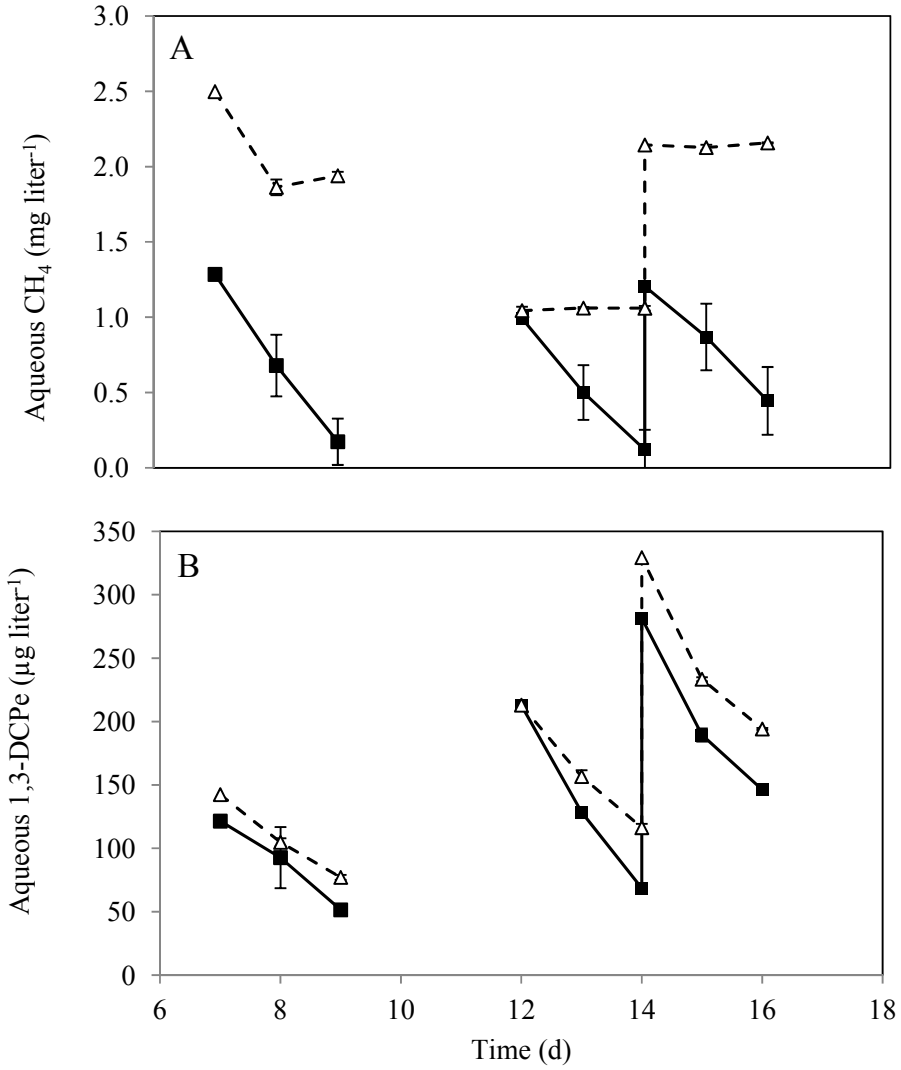

Figure 2.10. A) Methane (CH_4) consumption and B) 1,3-dichloropropene (1,3-DCPe) degradation in control (open triangles) and live (closed squares) Phase V microcosms for experiment one, 1,2-DCPe additions. Error bars give standard deviation of three samples.

Table 2.1 HAH additions to microcosms with 1.0-g *Carex comosa* roots

Microcosm set	Date: Plant harvest	Date: Experimental set up	Experiment	Cycle[a]	HAH[b]	HAH additions[c]: [Aqueous] (μg liter^{-1})	HAH additions[c]: Amount (μmol)
Phase I	07/29/2011	08/04/2011	1	1	1,1,2-TCA	26	0.020
				2		26	0.020
			2	1	1,1,2-TCA	26	0.020
				2		26	0.020
Phase II	09/27/2011	10/06/2011	1	1	1,2-DCP	100	0.096
				2		100	0.096
				3		100	0.096
Phase III	12/02/2011	12/15/2011	1	1	CF	75	0.067
				2		75	0.067
			2	1	BDCM	70	0.045
				2		70	0.045
			3	1	DBCM	70	0.033
				2		70	0.033
			4	1	BF	55	0.021
				2		55	0.021
				3		80	0.032
				4		80	0.032
Phase IV	12/02/2011	12/15/2011	1	1	1,2-DCA	70	0.071
				2		155	0.16
			2	1	1,2-DBA	70, 70	0.036, 0.036
				2		160	0.087
				3		160, 160	0.087, 0.087
			3	1	1,1-DCE	50	0.078
				2		50	0.078
Phase V	03/05/2012	03/26/2012	1	2	1,3-DCPe	100	0.12
			2	1		200, 200	0.25, 0.25

[a]- Initial aqueous CH_4 concentration was 1.1 mg liter^{-1} (0.12 mmol). All cycles had at least one sub-cycle where additional CH_4 was added without microcosm reset.

[b]- HAH – halogenated aliphatic hydrocarbon: 1,1,2-TCA – 1,1,2-trichlorethane: 1,2-DCP – 1,2-dichloropropane: CF – chloroform: BDCM – bromodichloromethane: DBCM – dibromochloromethane: BF – bromoform: 1,2-DCA – 1,2-dichloroethane: 1,2-DBA – 1,2-dibromoethane: 1,1-DCE – 1,1-dichloroethene: 1,3-DCPe – 1,3- dichloropropene.

[c]- Commas indicate HAH additions without microcosm reset.

Table 2.2 Transformation Yield (T_y, net mol HAH net mol^{-1} CH_4); steady state biomass concentration (X_{ss}, mg cell liter^{-1}); initial HAH degradation rate constant ($k_{obs\text{-}HAH}$, d^{-1}) and corresponding coefficient of determination (r^2); and biomass normalized rate constant ($k_{1\text{-}HAH}$, liter mg^{-1} cell d^{-1}) for three-day sub-cycles or five-day whole cycles

				Initial HAH[c]						
Microcosm set	HAH[a]	Experiment	Cycle[b]	[Aqueous] (µg liter^{-1})	Amount (µmol)	T_y	X_{ss}	$k_{obs\text{-}HAH}$	r^2	$k_{1\text{-}HAH}$
Phase I	1,1,2-TCA	1	1a	26	0.020	[d]	20.0			
			1b				20.5			
			2a	26	0.020		19.8			
			2b				18.5			
	1,1,2-TCA	2	1a	26	0.020		18.6			
			1b				21.5			
			2a	26	0.020		22.5			
			2b				19.1			
Phase II	1,2-DCP	1	1	100	0.096		18.6			
			2	100	0.096		19.1			
			3	100	0.096		17.3			
Phase III	CF	1	1	75	0.067	0.000090	12.4	0.105	0.96	0.0085
			2	75	0.067	0.00015	13.4	0.130	0.99	0.0097
	BDCM	2	1	70	0.045	0.000064	19.0	0.0963	0.92	0.0051
			2	70	0.045	0.000068	19.0	0.129	0.98	0.0068
	DBCM	3	1	70	0.033	0.000033	19.4	0.0832	1.0	0.0043
			2	70	0.033	0.000029	19.3	0.126	0.96	0.0065
	BF	4	1	55	0.021	0.000029	18.1	0.069	0.71	0.0038
			2	55	0.021	0.000036	17.3	0.145	0.93	0.0084
			3	80	0.033	0.000050	16.7	0.135	0.45	0.0081
			4	80	0.033	0.000042	16.8	0.0618	0.29	0.0037
Phase IV	1,2-DCA	1	1a	70	0.071	0.00086	37.3	2.24	1.0	0.060
			1b	155	0.16	0.0010	17.0	1.04	1.0	0.061
	1,2-DBA	2	1a	70	0.036	0.00035	18.3	1.39	0.99	0.076
			1b	70	0.036	0.00027		0.644	0.99	
			2	160	0.087	0.00079	17.7	1.41	0.99	0.080
			3a	160	0.087	0.00069	24.1	1.40	0.99	0.058
			3b	160	0.087	0.00055	16.9	0.542	1.0	0.032
	1,1-DCE	3	1	50	0.078	0.00024	16.1	0.350	0.99	0.022
			2	50	0.078	0.00021	16.7	0.258	0.96	0.015
Phase V	1,3-DCPe	1	2b	100	0.12	0.00019		0.574	0.99	
		2	1a	200	0.25	0.00054	16.2	0.523	1.0	0.032
			1b	200	0.25	0.0000021	18.6	0.383	1.0	0.021

[a] – HAH – halogenated aliphatic hydrocarbon: 1,1,2-TCA – 1,1,2-trichloroethane: 1,2-DCA – 1,2-dichloroethane: 1,2-DCP – 1,2-dichloropropane: DCM – dichloromethane: CF – chloroform: BDCM – bromodichloromethane: DBCM – dibromochloromethane: BF – bromoform: 1,2-DBA – 1,2-dibromoethane: 1,1,-DCE – 1,1-dichloroethene; 1,3-DCPe – 1,3-dichloropropene

[b] – Initial aqueous methane (CH_4) for sub-cycles was 1.1 mg liter^{-1} (0.12 mmol); total aqueous CH_4 for whole cycles was 2.2 mg liter^{-1} (0.25 mmol).

[c] – Additions based on calculated values – sub-cycle "b" calculations may be based off of slightly higher HAH values than those given; residual compounds were common from incomplete mineralization of halogenated compounds.

[d] – No significant degradation of the analyzed HAH was observed.

Table 2.3 Biomass normalized rate constant (liter mg^{-1} cell d^{-1}) for CH_4 consumption in methanotrophic microcosms

Microcosm set	"a" Sub-cycle[a]	"b" Sub-cycle[a]
Phase I	0.13 ± 0.05	0.076 ± 0.02
Phase II	0.084 ± 0.004	0.073 ± 0.02
Phase III	0.096 ± 0.03	0.074 ± 0.03
Phase IV	0.080 ± 0.02	0.061 ± 0.02

[a] – Mean ± standard deviation. Sub-cycles were three days long and had initial aqueous methane (CH_4) additions of 1.1 mg $liter^{-1}$ (0.12 mmol).

3. COMETABOLISM OF CHLORINATED ALIPHATIC HYDROCARBONS BY AEROBIC BACTERIA NATURALLY ASSOCIATED WITH WETLAND PLANT ROOTS

I.3 BACKGROUND

Treatment wetlands and bioremediation

Chlorinated aliphatic hydrocarbons (CAH) are a major source of groundwater pollution in the United States (ATSDR 1997). These chemicals can be removed from the environment through chemical/physical methods and bioremediation (Amon *et al*. 2007). Pump-and-treat and air sparging can facilitate physical removal of volatile organic compounds. While often successful, such physical methods often run continually for decades and have long-term costs that often make bioremediation a more attractive option (Kuiper *et al*. 2004).

Bioremediation is the use of microorganisms or plants for the decomposition and removal of harmful pollutants (Kuiper *et al.* 2004). Wetlands are areas of water saturated soil and are used frequently in bioremediation because they provide the ideal environment for degradation of numerous pollutants (Amon *et al*. 2007). The waterlogged soils of wetlands are mainly anaerobic, while aquatic vegetation provides oxygen to a thin layer surrounding plant roots, called the rhizosphere. In this way

wetlands provide both anaerobic (reducing) and aerobic (oxidative) environments for the complete breakdown of harmful CAHs.

Degradation pathways and microbiology

CAHs can be degraded by microbial processes within aquatic systems by various redox reactions, which include anaerobic reductive dehalogenation, aerobic oxidation, and anaerobic or aerobic cometabolism (Bradley 2000). Cometabolism is a process that occurs in both aerobic and anaerobic zones and involves the transformation of a non-growth substrate by bacteria without the production of energy for growth. Dehalogenation of CAHs by reductive dechlorination may occur slowly and often results in the buildup of harmful daughter products, such as vinyl chloride, whereas cometabolism may successfully mineralize chlorinated compounds into harmless carbon dioxide (CO_2) (Bradley 2000; Conrad *et al*. 2010; Powell *et al*. 2011). During cometabolism, CAHs are oxidized by enzymes that are produced by microorganisms for the oxidation of various growth substrates; these enzymes can often oxidize a large range of substances (Arp *et al.* 2001).

There is a variety of microorganisms that are capable of cometabolism; some bacteria can grow on numerous substrates and produce different enzymes that will oxidize CAHs. Growth substrates include butane, ethylene, toluene, propane, propene, isoprene, isopropylbenzene, methane, ammonia, phenol, and other chlorinated hydrocarbons such as vinyl chloride and chloroethane (Frascari *et al*. 2006; Alvarez-Cohen and Speitel 2001; Arp *et al.* 2001).

Root exudates and plant-microbe interactions

Past studies have explored the possibility of plant-microbe interactions for the bioremediation of harmful pollutants in soil. The root-microbial relationship is mutually beneficial (Anderson *et al*. 1993). Potential interactions that promote the biological breakdown of pollutants in soil include an increase in microbial growth and population; catabolic enzyme generation; co-oxidation of high-molecular weight compounds; and improved bioavailability of contaminants (Rentz *et. al.* 2004).

One subset of bioremediation occurs in the rhizosphere, which is the volume of soil that is influenced by root activity and typically extends from zero to two millimeters out from the plant roots (Bertin *et al*. 2003). The nutrients within this region are affected by the presence of roots, which withdraw dissolved nutrients directly from the surrounding soil and help to spread bacteria through the soil (Kuiper *et. al.* 2004; Bertin *et al*. 2003).

Plants further enhance the growth of microorganisms in the root zone through secretion of nutrients by plant roots; this process creates a nutrient rich environment, which in turn stimulates microbial activity (Kuiper *et. al.* 2006). Exudates include released ions; free oxygen and water; enzymes; mucilage (Bais *et al*. 2006); and numerous carbon-containing low- and high-molecular weight metabolites: Such metabolites include polysaccharides; organic, fatty and amino acids; carbohydrates; phenolic, aliphatic and aromatic compounds; and sugars (Badri and Vivanco 2009; Bertin *et al*. 2003).

In return, root-associated bacteria will degrade pollutants that could be harmful to the plant, such as herbicides (Anderson *et al.* 1993); facilitate plant growth through fixation of atmospheric nitrogen by different classes of Proteobacteria; and protect plants

against potential pathogens by the production of protective biofilms or antibiotics (Bais *et al*. 2006).

Research objectives

This study explored the natural attenuation of CAHs in near-surface, vegetated, aquatic environments. Root microcosms were created in which mineral media, oxygen, and CAHs were added; microcosms were monitored for the loss of CAH with time. The aim was to expand upon recent studies that discovered the cometabolic removal of trichloroethene (TCE) and *cis* 1,2-dichloroethene (*cis* 1,2-DCE) by aerobic bacteria naturally associated with the roots of the common wetland plant, *Carex comosa* (*C. comosa*); methanotrophic bacteria present initially with the *C. comosa* roots have shown the ability to cometabolize numerous CAHs (Powell et al. 2011).

TCE, *cis* 1,2-DCE, 1,1-dichloroethene (1,1-DCE), *trans* 1,2-dichloroethene (*trans* 1,2-DCE), carbon tetrachloride (CT), chloroform (CF), and 1,2-dichloroethane (1,2-DCA) were added to root microcosm systems without any outside source of growth substrates to examine the CAH's potential for biological removal by the aerobic microorganisms naturally associated with the *C. comosa* roots. The growth substrate naturally present in the system

Results of this study may be applied to constructed or restored wetlands for pollutant mitigation and site management: i) aerobic bacteria naturally present on wetland plant roots have the ability to degrade harmful chemicals; ii) the root microcosm approach used in this study provides insight into root-microbe interactions; and iii) provides a more realistic approach to understanding rhizospheric processes with respect to their potential for pollutant mitigation.

II.3 MATERIALS AND METHOD

Experimental design

Experiments were conducted in six phases. Six sets of six microcosms were created in which 2.0-g or 4.0-g of freshly harvested *C. comosa* roots were added along with a mineral media; microcosms were oxygenated and a CAH was added and monitored for loss (Table 3.1). All media was filter sterilized and microcosms and utensils were autoclaved. No outside growth substrate was added; therefore, microbial growth is hypothesized to have been taking place by metabolism of root-derived carbon substrates, herein termed dissolved organic carbon (DOC).

Growth media

Mineral media "A" was modified from Hartmans *et al*. (1992) and Coleman *et al*. (2002). The growth media consisted of 1210 mg KH_2PO_4, 1580 mg Na_2HPO_4, 170 mg $NaNO_3$, 59 mg $MgSO_4$, 10 mg EDTA, 5 mg $FeSO_4 \cdot 7H_2O$, 2 mg $ZnSO_4 \cdot 7H_2O$, 1 mg $CaCl_2 \cdot 2H_2O$, 1 mg $MnCl_2 \cdot 2H_2O$, 0.2 mg $Na_2MoO_4 \cdot 2H_2O$, 0.2 mg $CuSO_4 \cdot 5H_2O$, and 0.4 mg $CoCl_2 \cdot 6H_2O$ brought up to a final volume of 1.0 liter with nanopure water. The media solution was modified from literature by replacing ammonium with an equimolar amount of nitrate (Hartmans *et al.*1992; Coleman *et al.* 2002). Control microcosms received mineral media "B", which was prepared similar to media "A", but with 10 mg sodium azide (NaN_3) $liter^{-1}$; NaN_3 is a known gram negative microbicide. Both media had a final pH of 7.00.

Microcosm set-up

C. comosa was harvested from a natural wetland located in Beavercreek, OH (USA). The plants were maintained in a greenhouse at Wright State University, Dayton,

OH (USA) until use, one to four weeks. As needed, roots from *C. comosa* were removed from the greenhouse, washed with de-ionized water to remove all soil, and patted dry prior to use for preparing microcosms.

Collected wetland plant roots were weighed and equal amounts were added to six, 160 milliliter (mL) borosilicate glass serum bottles (Wheaton, Millville, NJ). Three bottles were prepared as live microcosms and amended with 100 mL of media "A" and three control bottles were prepared with 100 mL of media "B". After the addition of media, all microcosms were bubbled with air for approximately 15 minutes to ensure that the experimental bottles contained enough oxygen (O_2) to maintain aerobic conditions throughout the course of the experiment; initial dissolved oxygen (DO) concentrations were ~8 mg liter^{-1}. Microcosms were then capped with Teflon-lined butyl rubber stoppers and sealed with aluminum crimp seals. Bottles were wrapped in aluminum foil to simulate natural conditions, placed upside down on a rotary shaker (Glas-Col, Terre Haute, IN), and mixed end-over-end at 30 revolutions minute^{-1} for complete mixing. Microcosm systems were held at a temperature of 22 ± 1 ^{o}C.

At the start and end of each CAH experiment 50 mL of nutrient solution was discarded and 50 mL of new solution was added. In Phase III, IV, and V, experimental bottles were bubbled with pure O_2 for two timed minutes after approximately 15 minutes of bubbling with air.

No enrichment cycles were observed for studying the effect of root-derived DOC on the degradation of CAHs. On the first day of microcosm set up, CAH was added and monitored for removal.

Analysis

CAH stock solutions were prepared by adding 20 μL of the organic compound to a 160 mL borosilicate glass serum bottle containing organic-free Milli-Q water, and sealed with a Teflon-lined rubber stopper and aluminum crimp without headspace. The stock solution was then placed on a rotary shaker for 48 h to allow CAH compounds to dissolve completely.

Concentrations of dissolved inorganic carbon (DIC), dissolved oxygen (DO), and CAH were measured periodically in each experimental cycle; headspace samples were analyzed by gas chromatography (GC). Two GC systems were used throughout analysis of CAHs in DOC systems: HP 6890 series II and Agilent 7890A (Table 3.1). Both systems had the same type of column and electron capture detector. A switch from analysis on the HP 6890 to the AG 7890 was made between experiments because of technical problems with the HP 6890.

Aqueous concentrations of CAH at equilibrium were calculated using the Ideal Gas law and Henry's law (EPA 2012; Sander 1999; Burris *et al.* 1996; Gossett 1987). pH values were collected on the first and last day of each cycle (AP10 pH 10/mV/temp, Denver Instrument, Bohemia, NY). The partial pressures of O_2 and carbon dioxide (CO_2) were determined by analysis on a 5890 Series II GC system with a thermal conductivity detector and a packed column (Shin Carbon 100/120, 2 m× 1 mm; Restek, Bellefonte, PA). pH values were collected on the first and last day of each cycle (AP10 pH 10/mV/temp, Denver Instrument, Bohemia, NY). DO and DIC concentrations were then calculated by application of Henry's Law and carbonate system equilibrium relationships at measured pH values.

All concentrations for DIC, DO, and CAH were determined from standard calibration curves that encompassed the concentration(s) of interest.

To determine the presence of organic acids, Phase VI microcosms were set up as described above and allowed to rotate for two hours. After two hours, and again on day six and 13, 1.5 mL solution was withdrawn from each microcosm. Liquid samples from live and control bottles, as well as live and control mineral solutions, were filtered with XPertek 0.2 μm NYL filter tips and analyzed on a Varian 920 liquid chromatograph. Microcosms were then reset and 1 mL pure gaseous ethylene was added to each microcosm and monitored periodically for loss on a 7890A GC.

Data treatment

For all bottles, average consumption of DO (mmol) for live and control bottles was calculated by taking the difference between the average measured mass on day one and the average measured mass on day five. DIC production was determined by subtracting the average measured mass on day five from the average initial mass on day one. CAH degradation for whole cycles was determined by adding the difference in initial and final masses of all sub-cycles. Chlorinated compounds were not analyzed on the day that they were injected into the microcosms to allow for a 24 hour equilibration period between the headspace and liquid.

Transformation yield (T_y) was determined by dividing average live CAH degradation (μmol) by average live total inorganic carbon (TIC) production (mmol) or total O_2 (TO) consumption.

III.3 RESULTS AND DISCUSSION

Chloroform and carbon tetrachloride

In Phase I experimental one, 2.0-g root microcosms were amended with CF and CT (720 and 500 aqueous μg liter^{-1}, respectively). Over a five day period, there was no significant removal of either compound. Similar results were obtained in experiment two, two additional cycles were conducted in which the microcosms were amended with 77 μg liter^{-1} aqueous CF; though there was significant removal in live microcosms during the second cycle, the overall CF degraded was negligible (approximately two aqueous μg liter^{-1}).

In experiment three, two cycles were run in which 60 μg liter^{-1} aqueous TCE was added to the Phase I systems and allowed to degrade. T_y was computed by two methods: μmol TCE degraded mmol^{-1} TIC produced and μmol TCE degraded mmol^{-1} TO produced. T_y based off of TIC production yielded 0.031 and 0.048, while T_y computed by TO production resulted in slightly larger values: 0.046 and 0.053.

The lack of CT and CF degradation in Phase I microcosms may stem from initial toxicity of 720 and 500 aqueous μg liter^{-1} CF and CT, respectively – perhaps the cometabolic population was initially killed off by levels of CF and CT that were toxic. The lack of degradation could also mean that there was no initial cometabolic microbial population; this possibility seems unlikely as there was some loss of TCE in experiment three, cycles one and two.

The lack of degradation of CF and CT could stem from these compounds being chlorinated methanes, which differs from experiments with TCE and *cis* 1,2-DCE. TCE and *cis* 1,2-DCE have carbon-carbon double bonds and may more readily degrade cometabolically, which could account for the marginal degradation of TCE and lack of degradation of CF and CT in the Phase I systems.

Total inorganic carbon and total oxygen dynamics

In the microcosm systems, TIC is produced from the conversion of DOC into energy by heterotrophic bacteria. In this process, one O_2 atom is consumed for every TIC molecule produced: The ratio of TIC production to TO consumption should therefore be one (Figure 3.1). A consistent 1:1 ratio of TIC production and TO consumption indicates that, stoichiometrically, all the O_2 consumed went towards DOC oxidation to produce CO_2. When the ratio was greater than 1.0, another process was taking place to produce CO_2, without the consumption and subsequential sink of O_2. The production of CO_2 without O_2 consumption most likely occurred from fermentation processes within anaerobic zones of the roots. During fermentation, organic matter from within the roots would be converted to acetate, which in turn would create CO_2 and CH_4.

TIC production versus TO consumption was fairly consistent within Phase I microcosm systems and indicates that over time, there was not a notable shift in DOC and O_2 demand by the microbial populations present (Figure 3.1). Similar results of this 1:1 ratio were seen in other microcosm sets (Tables 3.2, 3.3, and 3.4).

cis 1,2-DCE was added to Phase II microcosms in increasing concentration over a 35 day period. Within the experimental cycles a significant amount of *cis* 1,2-DCE was cometabolically removed, while TIC was rapidly produced and TO was rapidly consumed (Figure 3.2). TIC production and TO consumption leveled off with time in the Phase II control microcosms. Though the trend was less pronounced, live Phase II microcosms also exhibited a slowing in TIC production and TO consumption with time and increasing *cis* 1,2-DCE concentration. The marked loss of TIC production and TO consumption capability in control Phase II microcosms may indicate (i) a shift in

microbial population, (ii) successful repression of cometabolic microorganisms by NaN_3 and (iii) toxicity of *cis* 1,2-DCE with increasing concentration. A similar slowing in daily rates of TIC production, TO consumption, and *cis* 1,2-DCE degradation was seen in live microcosms. This slowing of biological activity may have resulted from a shift in microbial population due to toxicity from *cis* 1,2-DCE cometabolic intermediates or from a loss in total cometabolic microbial biomass as DOC from *C. comosa* roots was depleted. DOC consumption would affect the amount of available energy for population growth and in turn, less cometabolic bacteria would be present with time. Both explanations may have occurred together to account for the apparent loss of activity.

This phenomenon of slowing production and consumption with time was also seen in Phase III and IV microcosms; however, the above reasons for this slowing may not apply to these systems. For example, it is unlikely that a drop in rates was due to toxicity of cometabolic intermediates in Phase III and IV microcosms as little to no cometabolism occurred throughout the experimental cycles within these systems. Instead, reasons for the loss of biologic activity in these systems may stem from loss of biomass with continued consumption of root derived DOC without replacement. This may be a more appropriate assessment as both control and live microcosms exhibited the same phenomenon, with marked shut down occurring in control microcosms with time.

Effect of oxygen concentration

1,1-Dichlorethene and trans 1,2-dichloroethene – pure oxygen

Sustained significant loss of 1,1-DCE and *trans* 1,2-DCE did not occur in Phase III microcosms. In experiment one, cycle one there was significant removal of 1,1-DCE – from aqueous concentration of 110 μg $liter^{-1}$ to 76 ± 17 (Figure 3.3). However, O_2 was

consumed rapidly during this first cycle. To combat rapid O_2 removal and allow the experimental cycles to run for an extended period, the microcosms were bubbled with pure O_2. After this bubbling, cycles two and three were run during which there was minimal to no significant loss of 1,1-DCE: Cycle 2) 110–92 ± 2, live and control not significantly different; Cycle 3) 110–91 ± 3.

trans 1,2-DCE was added in a second experiment in Phase III microcosms at an aqueous concentration of 110 μg liter^{-1}. Though significant removal of *trans* 1,2-DCE did occur, degradation rates were very slow and after a period of 27 days the aqueous concentration had fallen from 110 μg liter^{-1} to 102 μg liter^{-1}.

1,2-Dichloroethane and trichloroethene – pure oxygen

Cometabolic degradation of 1,2-DCA in Phase IV microcosms (Figure 3.4) followed a similar trend to 1,1-DCE loss in Phase III. In the first cycle of experiment one 108 aqueous μg 1,2-DCA liter^{-1} was added to the microcosms and allowed to degrade over a five day period at atmospheric O_2 levels. The average final concentration in the live Phase IV microcosms was 70 ± 24 aqueous μg liter^{-1}. After the first cycle of experiment one, the microcosms were bubbled with pure O_2 to allow for higher O_2 concentrations and longer cycle lengths. In cycles two and three of experiment one 108 aqueous μg 1,2-DCA liter^{-1} was again added to the microcosms, though minimal to no loss was observed over 10 and 18 day period.

Loss of microbial ability to degrade 1,1-DCE and 1,2-DCA in Phase III and IV microcosms indicates that the bacteria present in the microcosms may not be suitable for use in constructed remediation systems.

In experiment two of Phase IV microcosms, two cycles were run in which microcosms were bubbled with pure O_2 and amended with 110 and 140 aqueous µg TCE liter^{-1} (Figure 3.5). In the first cycle TCE was degraded from 110 to 54 ± 9 aqueous µg liter^{-1} over a 20 day period. It appeared that in the final days of experiment two, cycle one TCE removal leveled off; however, rates of degradation picked back up for the first three days of cycle two, which had an aqueous TCE concentration of 140 µg liter^{-1}. Though initially there was loss of TCE, values in live microcosms were not significantly different from control values, and after three days removal ceased.

Initial TCE degradation followed pseudo-first order kinetics: cycle one had an initial pseudo first-order degradation rate constant (k_{obs}, d^{-1}) of 0.099 (r^2 – 1.0) and cycle two had a k_{obs} of 0.071 (r^2 – 1.0). Coefficient of determination (r^2) values that are ~1.0 indicate that the data is reasonably expressed by a linear fit and that TCE loss within the system can be considered first-order.

1,1-Dichloroethene; trans 1,2-dichloroethene; and 1,2-dichloroethane – ambient oxygen

After analysis of 1,1-DCE and 1,2-DCA in Phase III and IV systems, respectively, it was suggested that bubbling with pure O_2 may have offset the microbial population and could have significantly hindered the cometabolic bacteria initially present. To investigate this claim, Phase V microcosms were set up in which 2.0-g roots were taken from a freshly harvested *C. comosa* plant. Three, five-day cycles were run with 110 aqueous µg liter^{-1} CAH: Cycle 1) 1,1-DCE; Cycle 2) *trans* 1,2-DCE; and Cycle 3) 1,2-DCA (Figure 3.6).

It was expected that these compounds would show similar degradation trends as the first cycle of each corresponding experiment in Phase III and IV microcosms;

however, limited removal of all three compounds was seen (Figure 3.6); results further indicate that such root-microbe systems are not suitable for the remediation of these specific CAHs.

Toxicity

The microbial population was able to sustain TCE and *cis* 1,2-DCE removal over long periods of time. Minimal cometabolic removal of the other CAHs may have occurred from (i) *C. comosa* roots lacking the initial cometabolic bacteria, (ii) toxic effects from the breakdown of CAH in the first experimental cycle, or (iii) destruction of the cometabolic bacteria after the bubbling with pure O_2.

It is unlikely that these compounds did not degrade due to a lack of cometabolic bacteria being initially present along with the *C. comosa* roots for two reasons: In experiment one, cycle one for Phase III and IV, there was significant removal of the chlorinated compound added. Furthermore, cometabolic bacteria must have been present in at least the Phase IV microcosms as, though 1,2-DCA had limited removal, TCE was degraded to half of its starting aqueous concentration over a 20 day period.

There may have been irreversible toxicity that occurred from initial removal of 1,1-DCE and 1,2-DCA in Phase III and IV microcosms, respectively. This toxicity effect is seen in slowing of overall TIC production and TO consumption with time. There is further evidence of toxicity by cometabolism in the shutdown of TCE removal in experiment two, cycles one and two of Phase IV microcosms (Figure 3.5). Initially TCE was degraded from 110 aqueous μg liter^{-1} to 70 ± 24. However, after microcosm reset in cycle two, 140 aqueous μg TCE liter^{-1} was added and no significant removal occurred.

The shutdown of cometabolic removal of CAHs in Phases III and IV could have occurred from bubbling with pure O_2. In the wetland, O_2 levels would never be above atmospheric levels; it has also been suggested in the literature that bench scale experiments often have too high of O_2 levels and therefore results that occur in the lab may not always be what will occur in nature (King 1996). However, bubbling with pure O_2 may not have been the sole culprit in loss of cometabolic degradation in the Phase III and IV systems as there was also no loss of 1,1-DCE, *trans* 1,2-DCE, or 1,2-DCA in Phase V microcosms, which were not bubbled with pure O_2 (Figure 3.6).

Organic acid and ethene analysis

Phase VI microcosms were created to identify the growth substrate that the cometabolic bacteria were consuming. Analysis of microcosm liquid for live and control bottles on the 920 LC did not reveal the presence of formic acid, acetic acid, propionic acid, or lactic acid. 920 LC retention times for the compounds include lactic acid, 5.5 minutes; propionic acid, 15.61 minutes; acetic acid, 6.33 minutes; and formic acid, 3.85 minutes.

Live and control microcosms had similar chromatographic read outs except for small peaks farther out in the run in live bottles. These peaks came at 6.4, 13.9, 15.1, and 15.7 minutes and were not present in the starting mineral solution or in the microcosms on day one of set up. In both live and kill solutions there was a significant peak at 2.8 minutes that depleted over time in the live microcosms only. This peak came before the analyzed organic acids and is hypothesized to be phosphate, which is present in significant amounts in the mineral solution. Small peaks appeared at a time of 6.25 in both live and control mineral solutions as well as live microcosms after approximately 2

hours of initial set up – this peak was not present on day 13 in live microcosms and was not present at any time in the control microcosms.

A peak at time 5.6 was present in the control bottles and kill solution only. This peak is hypothesized to be sodium azide and is fairly constant in concentration from day one through day 13 in the control bottles. A peak at time 6.2 was present in control microcosms from day one through day 13. A peak at time 6.13 and 6.4 appeared on day 13 in the live microcosms.

Ethene is a simple hydrocarbon that is produced by plants most specifically for the ripening of fruit. Pure gaseous ethane was added to the Phase VI microcosms on day two of the second reset – 1.87 aqueous mg liter^{-1}. Over a period of six days ethene levels as well as CO_2 and O_2 were monitored on a gas chromatograph. Throughout the six day cycle, no significant removal of ethane was observed (Figure 3.7).

The results for organic acid analysis in Phase VI microcosms were inconclusive. There did not appear to be formic acid, acetic acid, propionic acid, or lactic acid present in the control or live bottles at any stage in the sampling cycle. There also did not appear to be any degradation of ethylene in the live or control rootcosms, which suggests that cometabolism within the rootcosms does not occur from enzymes associated with the oxidation of ethylene. It is still unclear as to what compound the cometabolic bacteria are consuming.

IV.3 CONCLUSIONS

Immediate degradation of chlorinated ethenes and removal of low levels of other types of CAHs indicates that cometabolic microorganisms are naturally present in and around the roots of wetland plants – even if the wetland system has not been previously

exposed to chemical pollutants. These results provide support to the use of wetland systems as means of natural attenuation of contaminated groundwater: i) in these systems, the aerobic microorganisms naturally present with wetland plant roots did not require an incubation period before they could sustain TCE and *cis* 1,2-DCE degradation; and ii) results indicate that the bacteria capable of CAH degradation would not need to be added to a wetland remediation system, they would be there naturally.

V.3 REFERENCES

Alvarez- Cohen, L.; Speitel, G. E., Jr. Kinetics of aerobic cometabolism of chlorinated solvents. *Biodegradation* **2001**, *12*, 105–126.

Amon, J. P.; Agrawal, A.; Shelley, M. L.; Opperman, B. C.; Enright, M. P.; Clemmer, N. D.; Slusser, T.; Lach, J.; Sobolewski, T.; Gruner, W.; Entingh, A. C. Development of a wetland constructed for the treatment of groundwater contaminated by chlorinated ethenes. *Ecological Engineering* **2007**, *30*, 51–66.

Anderson, T. A.; Guthrie, E. A.; Walton, B. T. Bioremediation. *Environmental Science and Technology* **1993**, *27* (13), 2630–2636.

Arp, D. J.; Yeager, C. M.; Hyman, M. R. Molecular and cellular fundamentals of aerobic cometabolism of trichloroethylene. *Biodegradation* **2001**, *12*, 81–103.

ATSDR. Toxicological profile for trichloroethylene (update). ATSDR 1997, Atlanta.

Badri, D. V.; Vivanco, J. M. Regulation and function of root exudates. *Plant, Cell and Environment* **2009**, *32*, 666–681.

Bais, H. P.; Weir, T. L.; Perry, L. G.; Gilroy, S.; Vivanco, J. M. The role of root exudates in rhizosphere interactions with plants and other organisms. *Annual Review of Plant Biology* **2006**, *57* (2), 233–266.

Bertin, C.; Yang, X.; Weston, L. A. The role of root exudates and allelochemicals in the rhizosphere. *Plant and Soil* **2003**, *256*, 67–83.

Bradley, P. M. Microbial degradation of chloroethenes in groundwater systems. *Hydrogeology Journal* **2000**, *8*, 104–111.

Burris, D. R.; Delcomyn, C. A.; Smith, M. H.; Roberts, A. L. Reductive dechlorination of tetrachloroethylene and trichloroethylene catalyzed by vitamin B-12 in homogenous and heterogeneous systems. *Environmental Science and Technology* **1996**, *30*, 3047–3052.

Coleman, N. V.; Mattes, T. E.; Gossett, J. M.; Spain, J. C. Biodegradation of *cis*-dichloroethene as the sole carbon source by a β-Proteobacterium. *Applied and Environmental Microbiology* **2002**, *68* (6), 2726–2730.

Conrad, M. E.; Brodie, E. L.; Radtke, C. W.; Bill, M.; Delwiche, M. E.; Lee, H.; Swift, D. L.;Colwell, F. S. Field evidence for co-metabolism of trichloroethene stimulated by addition of electron donor to groundwater. *Environmental Science and Technology* **2010**, *44*, 4697–4704.

Frascari, D.; Pinelli, D.; Nocentini, M.; Zannoni, A.; Fedi, S.; Baleani, E.; Zannoni, D.; Farneti,A.; Battistelli, A. Long-term aerobic cometabolism of a chlorinated solvent mixture by vinyl chloride-, methane- and propane- utilizing biomasses. *Journal of Hazardous Materials* **2006**, *B 138*, 29–39; DOI: 10.1016/j.jhazmat.2006.05.009.

Gossett, J. M. Measurement of Henry's Law constants for C_1 and C_2 chlorinated hydrocarbons. *Environmental Science and Technology* **1987**, *21* (2), 202–208.

Hartmans, S.; Kaptein, A.; Tramper, J.; de Bont, J. A. M. Characterization of a *Mycobacterium* sp. and a *Xanthobacter* sp. for the removal of vinyl chloride and 1,2-dichloroethane from waste gases. *Applied Microbiology and Biotechnology* **1992**, *37*, 796–801.

King, G. M. In situ analyses of methane oxidation associated with the roots and rhizomes of a bur reed, *Sparganium eurycarpum*, in a Maine wetland. *Applied and Environmental Microbiology* **1996**, *62* (12), 4548–4555.

Kuiper, I.; Lagendijk, E. L.; Bloemberg, G. V.; Lugtenberg, B. J. J. Rhizoremediation: A beneficial plant-microbe interaction. *Molecular Plant-Microbe Interactions* **2004**, 17 (1), 6–15.

Powell, C. L.; Nogaro, G.; Agrawal, A. Aerobic cometabolic degradation of trichloroethene by methane and ammonia oxidizing microorganisms naturally associated with *Carex comosa* roots. *Biodegradation* **2011**, *22* (3), 527–538; DOI: 10.1007/s10532-010-9425-1

Rentz, J. A.; Alvarez, P. J. J.; Schnoor, J. L. Repression of Pseudomonas Putida Phenanthrene-Degrading Activity by Plant Root Extracts and Exudates. *Environmental Microbiology* **2004**, *6* (6), 574–583.

Sander, R. Compilation of Henry's Law constants for inorganic and organic species of potential importance in environmental chemistry, 1999. Web. 28 Feb. 2012. <http://www.mpch-mainz.mpg.de/~sander/res/henry.html>

USEPA. EPA On-line Tools for Site Assessment Calculation. Ecosystems Research, Athens GA, 05 Jan. 2012. Web. 20 Mar. 2012. <http://www.epa.gov/athens/learn2model/part-two/onsite/esthenry.html>

Zogorski, J. S.; Carter, J. M.; Ivahnenko, T.; Lapham, W. W.; Moran, M. J.; Rowe, B. L.; Squillace, P. J.; Toccalino, P. L. **2006**. The quality of our Nation's waters–Volatile organic compounds in the nation's ground water and drinking-water supply wells: U.S. Geological Survery Circular 1292, 101 p.

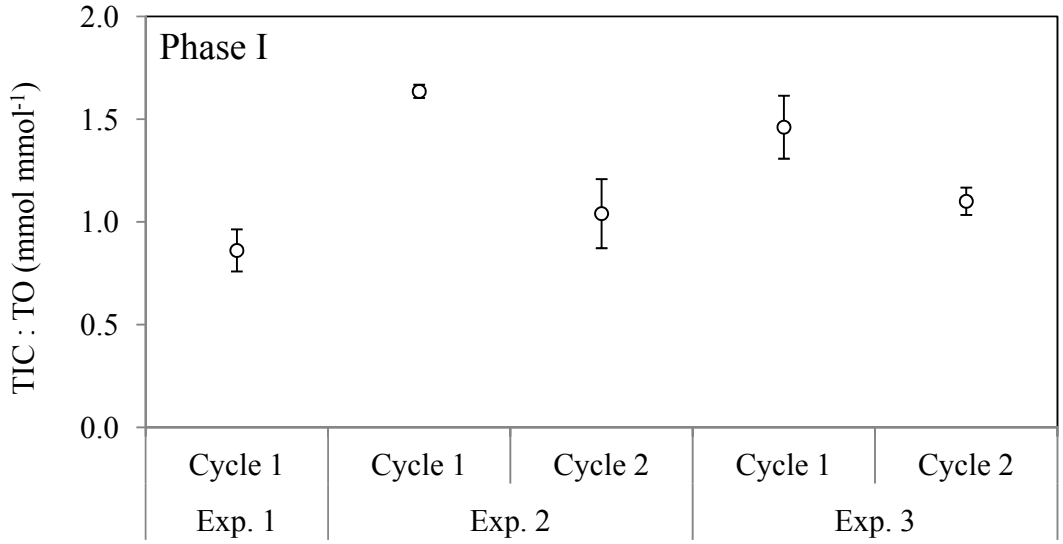

Figure 3.1 Average ratio of total inorganic carbon (TIC) production (mmol) versus total oxygen (TO) consumption (mmol) in live Phase I microcosms for experiments one, two, and three. Microcosms were amended with varying aqueous concentrations (μg liter^{-1}) of chlorinated aliphatic hyrdocrabons (CAH): Exp.1) chloroform, 720 and carbon tetrachloride, 500; Exp.2) chloroform, 77; and Exp. 3) trichloroethene, 60. Error bars give standard deviation of three samples.

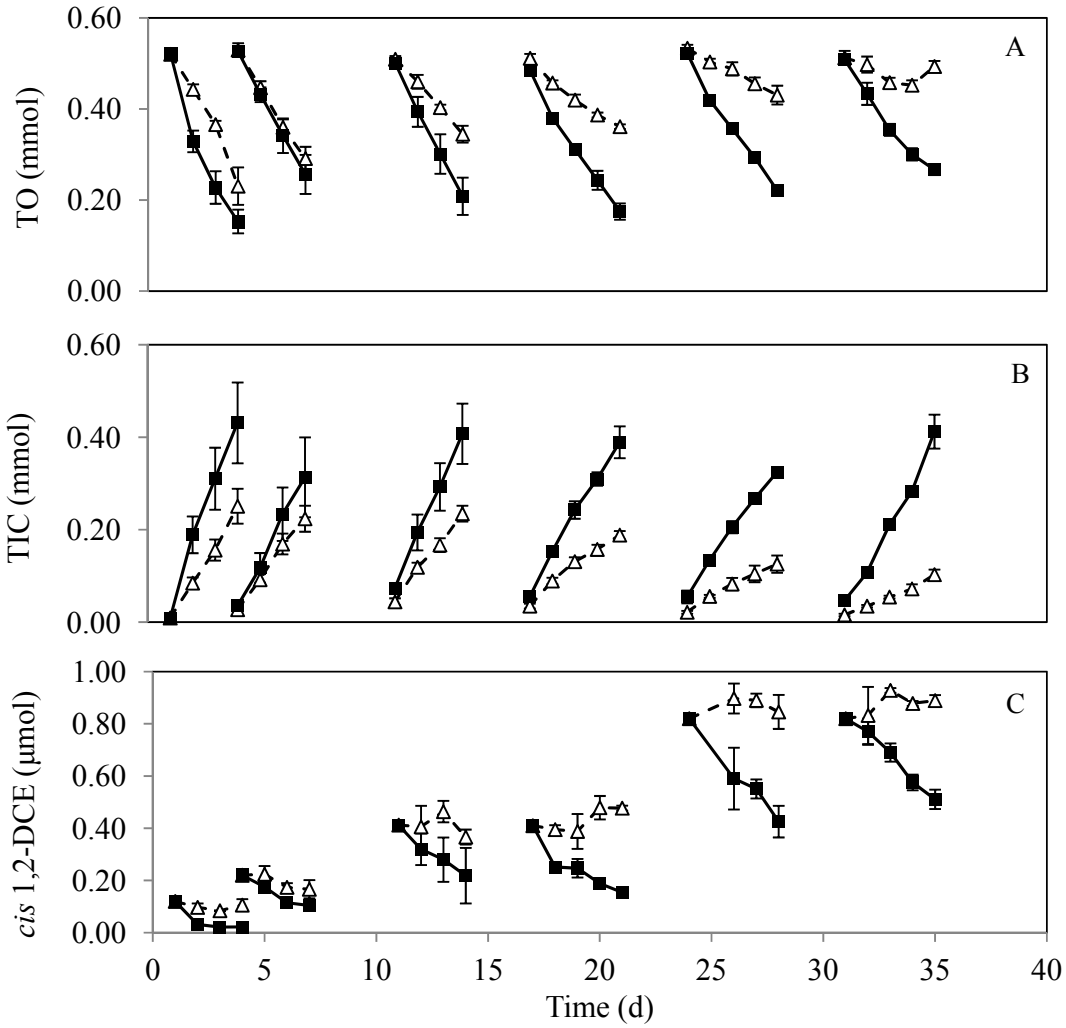

Figure 3.2 A) Total oxygen (TO) consumption; B) total inorganic carbon (TIC) production; and C) *cis* 1,2-dichloroethene (*cis* 1,2-DCE) degradation in control (open triangles) and live (closed squares) Phase II microcosms for experiments one through four. Initial *cis* 1,2-DCE additions represent calculated values. Error bars give standard deviation of three samples.

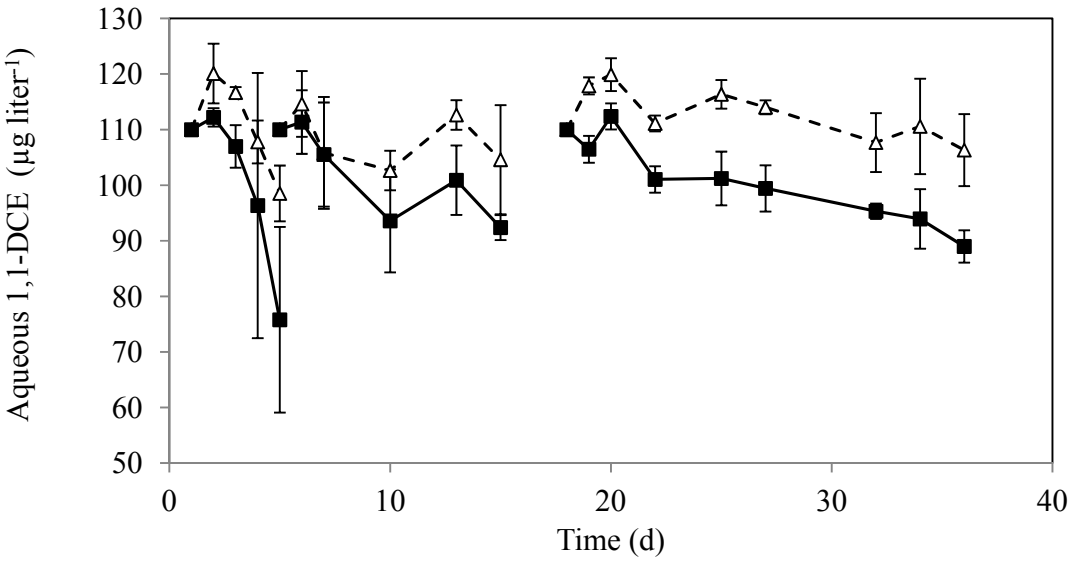

Figure 3.3 1,1-Dichloroethene (1,1-DCE) degradation in control (open triangles) and live (closed squares) Phase III microcosms for experiment one, cycles one, two, and three. Initial 1,1-DCE additions represent calculated values. Error bars give standard deviation of three samples.

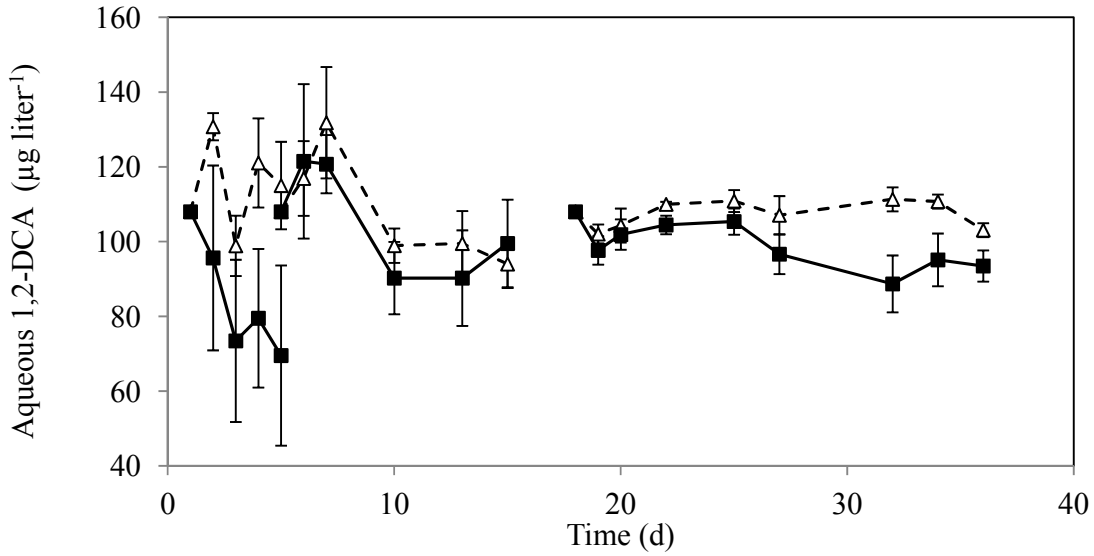

Figure 3.4 1,2-Dichloroethane (1,2-DCA) degradation in control (open triangles) and live (closed squares) Phase IV microcosms for experiment one, cycles one, two, and three. Initial 1,2-DCA additions represent calculated values. Error bars give standard deviation of three samples.

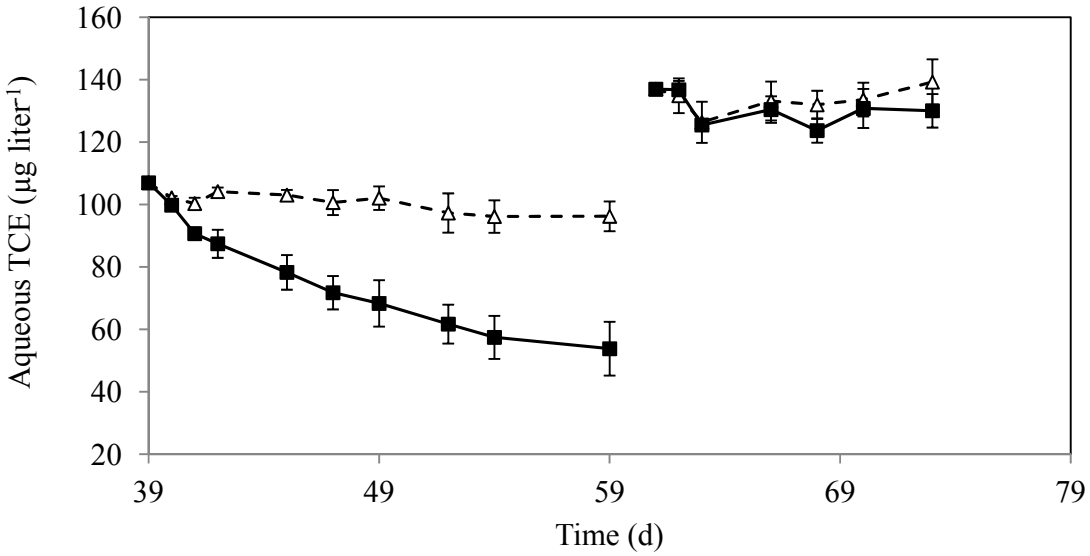

Figure 3.5 Cometabolic trichloroethene (TCE) removal in control (open triangles) and live (closed squares) Phase IV microcosms for experiment two, cycles one and two. Initial TCE additions represent calculated values. Error bars give standard deviation of three samples.

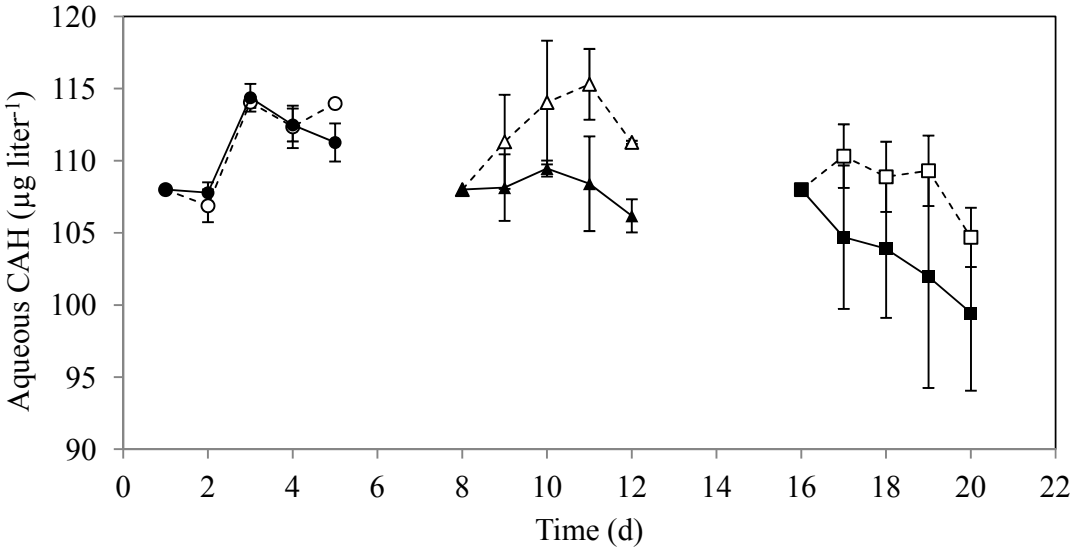

Figure 3.6 Cometabolic removal of chlorinated aliphatic hydrocarbons (CAH) in control (open symbols) and live (closed symbols) Phase V microcosms for experiments one, two, and three and their respective five-day cycles. Initial CAH additions represent calculated values: 1,1-dichloroethene (circles), *trans* 1,2-dichloroethene (triangles), and 1,2-dichloroethane (squares). Error bars give standard deviation of three samples.

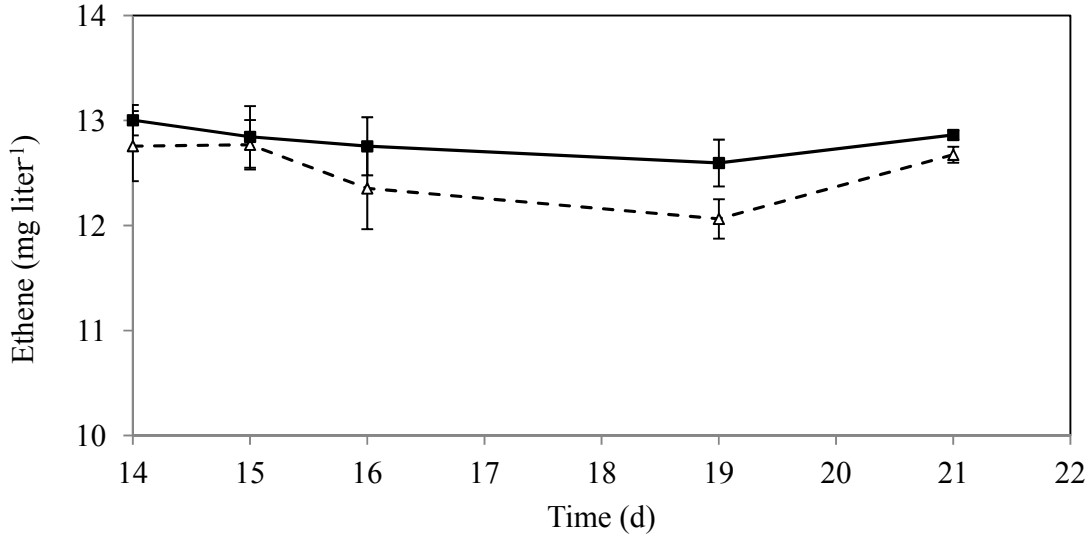

Figure 3.7 Aqueous ethane concentration in control (open triangles) and live (closed squares) Phase VI microcosms. Error bars give standard deviation of three samples.

Table 3.1. CAH additions to microcosms with 4.0-g[a] *Carex comosa* roots and no added growth substrate

	Date						CAH additions[b]	
Microcosm set up	Plant harvest	Experimental set up	Experiment	Number of cycles	CAH[c]	GC system[d]	[Aqueous] (µg liter^{-1})	Amount (µmol)
Phase I	07/29/2011	08/01/2011	1	1	CF: CT	HP 6890	720: 500	0.65: 0.52
			2	2	CF	HP 6890	50	0.069
			3	2	TCE	HP 6890	60	0.056
Phase II	07/09/2011	08/27/2011	1	1	*cis* 1,2-DCE	HP 6890	110	0.12
			2	1	*cis* 1,2-DCE	HP 6890	200	0.22
			3	2	*cis* 1,2-DCE	HP 6890	400	0.41
			4	2	*cis* 1,2-DCE	AG 7890	800	0.82
Phase III	09/27/2011	10/01/2011	1	3	1,1-DCE	HP 6890, AG 7890	110	0.18
			2	1	*trans* 1,2-DCE	AG 7890	110	0.12
Phase IV	09/27/2011	10/01/2011	1	3	1,2-DCA	HP 6890, AG 7890	110	0.18
			2	2	TCE	AG 7890	110, 140	0.10, 0.13
Phase V	03/05/2011	03/05/2012	1	1	1,1-DCE	AG 7890	110	0.17
			2	1	*trans* 1,2-DCE	AG 7890	110	0.17
			3	1	1,2-DCA	AG 7890	110	0.11
Phase VI	12/01/2011	12/15/2011	1	2	---[e]	AG 7890		

[a] – Phase I and v had 2.0-g *Carex comosa* roots.

[b] – Initial CAH additions represent theoretical values.

[c] – CAH – chlorinated aliphatic hydrocarbon: CF – chloroform: CT – carbon tetrachloride: TCE – trichloroethene: *cis* 1,2-DCE – *cis* 1,2-dichloroethene. 1,1,-DCE – 1,1-dichloroethene: *trans* 1,2-DCE – *trans* 1,2-dichloroethene: 1,2-DCA – 1,2-dichloroethane.

[d] – GC – gas chromatograph.

[e] – Rootcosms were set up for analysis of organic acids to determine cometabolic growth substrate.

Table 3.2 Transformation Yield (T_y, µmol *cis* 1,2-DCE mmol^{-1} TIC, TO); total inorganic carbon (TIC) production (mmol); and total oxygen (TO) consumption (mmol) in live Phase II microcosms

		Initial *cis* 1,2-DCE[b]						
		[Aqueous]	Amount	T_y				
Experiment	Cycle[a]	(µg liter^{-1})	(µmol)	TIC^{-1}	TO^{-1}	TIC production	TO consumption	TIC/TO
1	1	110	0.12	0.23	0.27	0.42	0.37	1.1
2	1	200	0.22	0.42	0.43	0.28	0.27	1.0
3	1	400	0.41	0.58	0.66	0.33	0.29	1.1
	2	400	0.41	0.77	0.82	0.33	0.31	1.1
4	1	800	0.82	1.5	1.3	0.27	0.30	0.09
	2	800	0.82	0.85	1.3	0.37	0.24	1.5

[a] – Each cycle was run for a total of five days.

[b] – Initial *cis* 1,2-dichloroethene (*cis* 1,2-DCE) additions represent calculated values.

Table 3.3 Transformation Yield (T_y, µmol CAH mmol^{-1} TIC, TO); total inorganic carbon (TIC) production (mmol); and total oxygen (TO) consumption (mmol) in live Phase III microcosms

			T_y				
Experiment	Cycle[a]	CAH[bc]	TIC^{-1}	TO^{-1}	TIC production	TO consumption	TIC/TO
1	1	1,1-DCE	0.073	0.084	0.76	0.66	1.14
	2		0.013	0.014	2.27	2.01	1.13
	3		0.012	0.013	2.60	2.39	1.09
2	1	*trans* 1,2-DCE	0.004	0.004	2.03	1.99	1.02

[a] – Each cycle was run for five days.

[b] – CAH – chlorinated aliphatic hydrocarbon: 1,1-DCE – 1,1-dichloroethene: *trans* 1,2-DCE – *trans* 1,2-dichloroethene.

[c] – Initial aqueous 1,1-DCE for all cycles of experiment one, and *trans* 1,2-DCE for cycle one of experiment two was 110 µg liter^{-1} (0.18 and 0.12 µmol, respectively).

Table 3.4 Transformation Yield (T_y, µmol CAH mmol^{-1} TIC, TO); total inorganic carbon (TIC) production (mmol); and total oxygen (TO) consumption (mmol) in live Phase IV microcosms

			Initial CAH[b]						
					T_y		TIC	TO	
Experiment	Cycle	CAH[a]	[Aqueous] (µg liter^{-1})	Amount (µmol)	TIC^{-1}	TO^{-1}	production	consumption	TIC/TO
1	1	1,2-DCA	108	0.18	0.086	0.096	0.76	0.68	1.1
	2		108	0.18	0.008	0.010	2.30	1.82	1.3
	3		108	0.18	0.011	0.012	2.57	2.28	1.1
2	1	TCE	110	0.10	0.026	0.026	1.93	1.90	1.0
	2		140	0.13	0.022	0.023	0.60	0.58	1.0

[a] – CAH – chlorinated aliphatic hydrocarbon: 1,2-DCA – 1,2-dichloroethane: TCE – trichloroethene.
[b] – Initial CAH additions represent calculated values.

APPENDIX A ANALYSIS AND CALCULATIONS

A.1 CALCULATIONS FOR DETERMINING AQUEOUS CONCENTRATIONS AND MASS OF VOLATILES IN MICROCOSMS (ADAPTED FROM POWELL AND AGRAWAL 2011)

A.1.1 **Methane**

1. Using the ideal gas law, determine the number of moles (n)
   a. $n = \frac{PV}{RT}$

      where R = gas constant, 0.0821 atm liter mole^{-1} K^{-1}; T = temperature, 298 K; P = Pressure, 1 atm; V = volume of gas injected
2. Find the total mass of methane (m_t) in mg
   a. $m_t = (n * FW)(1000)$

      where FW = formula weight of methane, 16 g mole^{-1}; 1000 = conversion factor
3. Find the water partitioning coefficient (f_w)
   a. $f_w = \frac{1}{(1+k'_H(\frac{V_a}{V_w}))}$

      where k'_H = Henry's Constant for methane (C_{air}/C_{water}) at 20^{o}C, 28.5 [D] (Schwarzenbach *et al.* 1995); V_a = volume of head space; V_w = volume of liquid

4. Find mass of methane, in mg, for aqueous phase (m_w) and gas phase (m_a)
    a. $m_w = m_t * f_w$
    b. $m_a = m_t(1 - f_w)$
5. Find the methane concentration, in mg liter^{-1}, for aqueous phase (C_w) and gas phase (C_a)
    a. $C_w = \frac{m_w}{V_w}$
    b. $C_a = \frac{m_a}{V_a}$
6. Plot a standard curve with peak areas on the x-axis and C_a on the y-axis
    a. Determine C_a in a microcosm sample by plugging the peak area into the best fit line equation (y = mx + b, where peak area is x).

A.1.2 **Oxygen**

1. Create a calibration curve of ambient air samples
    a. Analyze 10, 30, and 50 µL ambient air samples ($Samp._v$) with a 50 µL gas-tight syringe ($Syr._v$) on a HP 5890 series gas chromatograph system with a thermal conductivity detector, and a packed column with N_2 as carrier gas
    b. Determine partial pressure, in atm, of air in samples (Pi)
        i. $Pi = \left(\frac{Samp._v}{Syr._v}\right) 0.21$

            where 0.21 = percent oxygen in air
2. Plot a standard curve with peak area on the y-axis and Pi on the x-axis
3. Find aqueous concentration, in mg liter^{-1}, of oxygen (C_w)
    a. $C_w = k_H * Pi(FW * 1000)$

where k_H = Henry's constant for oxygen (C_{water}/C_{air}) at 20 ^{o}C, 1.3x10^{-3} mole liter^{-1} atm^{-1} (Lide and Frederikse 1995); Pi = partial pressure in headspace, atm; FW = formula weight of oxygen, 32 g mole^{-1}; 1000 = conversion factor

or

a. Add a known amount of pure oxygen to system; use ideal gas law to find moles of oxygen added, convert to grams for total mass (m_t)

b. Find the aqueous partitioning coefficient (f_w)

i. $f_w = \frac{1}{\left(1+\frac{1}{k'_H}\right)*\frac{V_a}{V_w}}$

where k'_H = Dimensionless Henry's constant for oxygen (C_{water}/C_{air}) at 20 ^{o}C, 0.0318 [D] (Sander 1999); V_a = volume of headspace; V_w = volume of liquid

c. Find aqueous mass, in mg, of oxygen (m_w) and aqueous concentration (C_w)

i. $m_w = m_t * f_w$

ii. $C_w = \frac{m_w}{V_a}$

4. Find the total mass, in mg, of oxygen (m_t)

a. $m_t = \left(\frac{Pi*V_a}{RT}\right)(FW * 1000) + (C_w * V_w)$

where Pi = partial pressure of oxygen in headspace sample, atm; R = gas constant, 0.0821 atm liter mole^{-1} K^{-1}; T = temperature, 298 K; FW = formula weight of oxygen, 32 g mole^{-1}; 1000 = conversion factor

A.1.3 **Carbon dioxide**

1. The aqueous concentration of CO_2 or dissolved inorganic carbonate (DIC) can be calculated using the following relationships (Pankow 1991)
   a. $[DIC] = ([H_2CO_3^*] + [HCO_3^-] + [CO_3^{2-}])$
   b. $If\ pH{\sim}7, then\ [DIC] = ([H_2CO_3^*] + [HCO_3^-])$
      i. $[H_2CO_3^*] = k_H * pCO_2$

         where k_H = $10^{-1.47}$; pCO_2 = partial pressure of CO_2, atm
      ii. $[HCO_3^-] = \frac{k_1 * k_H * pCO_2}{10^{-pH}}$

         where k_1 = $10^{-6.35}$
2. Determine aqueous concentration, in mg liter^{-1}, of CO_2 (C_w)
   a. $C_w = \left(\left[H_2CO_3^* + [HCO_3^-]\right]\right)(FW * 1000)$

      where FW = formula weight of CO_2, 44 mg liter^{-1}; 1000 = conversion factor
3. Find total mass, in mg, of CO_2 (m_t)
   a. $m_t = \left(\frac{Pi * V_a}{RT}\right)(FW * 1000) + (C_w * V_w)$

      where Pi = partial pressure of CO2 in headspace sample, atm; R = gas constant, 0.0821 atm liter mole^{-1} K^{-1}; T = temperature, 298 K

A.1.4 **Chlorinated aliphatic hydrocarbon**

1. Prepare CAH stock solution by adding a known amount of pure compound to a 160 mL glass serum bottle filled completely with Milli-Q water. Seal bottle with Teflon lined rubber septa and aluminum crimp. Rotate bottle, end-over-end at 30 rpm for 48 hours to allow compound to completely dissolve (Burris *et al.* 1996).
2. Calculate the concentration, in mg liter^{-1}, of the stock solution (C_s)
   a. $m_t = \rho_{CAH} * V_{pure}$

      where ρ_{CAH} = density of CAH, g/cc; V_{pure} = volume of pure CAH added by gas tight syringe
   b. $C_s = m_t * V_w$

      where V_w = volume of water, liter
3. Remove CAH stock solution with gas-tight, glass syringe and add to microbial system.
4. Calculate the concentration (C_t), in µmol liter^{-1}, and total mass (m_t), in µg, of CAH in microbial system before partitioning
   a. $C_t = \frac{V_{stock} * C_s}{V_w * (FW)}$

      where V_{stock} = volume of stock solution added, µL; V_w = volume of liquid in microcosm, mL; FW = formula weight of CAH, g mol^{-1}
   b. $m_t = C_t * V_w$
5. Find the water partitioning coefficient (f_w)

a. $f_w = \frac{1}{(1+k'_H(\frac{V_a}{V_w}))}$

where k'_H = Henry's Constant for CAH (C_{air}/C_{water}) at 20°C, [D]; V_a = volume of head space; V_w = volume of liquid in microcosm

6. Determine the mass in aqueous phase (m_w) and mass in head space (m_a), in µg
   a. $m_w = m_t * f_w$
   b. $m_a = m_t * (1 - f_w)$
7. Convert the mass in aqueous phase to aqueous concentration (C_w), µg liter^{-1}, and mass in head space to concentration in air (C_a), µg liter^{-1}
   a. $C_w = \frac{m_w}{V_w}$
   b. $C_a = \frac{m_a}{V_a}$

A.1 Properties and purity of HAHs evaluated in this work

HAH[a]	Chemical name	Provider	Values computed at 20 °C: Density (g/cm^3)	Values computed at 20 °C: Henry's constant [D][b]	Purity (%)
TCE	Trichloroethene	Acros Organics	1.470	0.299[a]	99.6
cis 1,2-DCE	*cis* 1,2-Dichloroethene	Acros Organics	1.280	0.167[a]	97.0
1,1-DCE	1,1,-Dichloroethene	Aldrich Chemical Co.	1.213	0.904	99.0
1,1,2-TCA	1,1,2-Trichloroethane	Aldrich Chemical Co.	1.435	0.0287	98.0
1,2-DCA	1,2-Dichloroethane	Aldrich Chemical Co.	1.256	0.0318	99.0
1,2-DBA	1,2-Dibromoethane	Sigma-Aldrich	2.170	26.42[c]	98.0
CF	Chloroform	Fisher Scientific	1.472	0.122	--
BF	Bromoform	Sigma-Aldrich	2.889	0.0161	99.0
DCM	Dichloromethane	Fisher Scientific	1.325	0.0745	99.9
BDCM	Bromodichloromethane	Sigma-Aldrich	1.980	0.0517	98.0
DBCM	Dibromochloromethane	Sigma-Aldrich	2.451	0.0267	98.0
1,2-DCP	1,2-Dichloropropane	Arcos Organics	1.156	0.0907	98.0
1,3-DCPe	1,3-Dichloropropene	Arcos Organics	1.220	0.566	90.0

[a]- HAH – halogenated aliphatic hydrocarbon.
[b]- Dimensionless Henry's constants were obtained from USEPA (2012).
[c]- Dimensionless Henry's constant computed with $C_{Liquid}\ C_{Air}^{-1}$ (Sander 1999).

A.1.5 **References**

Burris, D. R.; Delcomyn, C. A.; Smith, M. H.; Roberts, A. L. Reductive dechlorination of tetrachloroethylene and trichloroethylene catalyzed by vitamin B-12 in homogeneous and heterogeneous systems. *Environmental Science and Technology* ***1996***, *30* (10), 3047–3052.

Jenal-Wanner, U.; McCarty, P. L. Development and evaluation of semicontinuous slurry microcosms to stimulate *in situ* biodegradation of trichloroethylene in contaminated aquifers. *Environmental Science and Technology* **1997**, *31* (10), 2915–2922.

Lide, D. R.; Frederikse, H. P. R. *CRC Handbook of Chemistry and Physics, 76th Edition*. 76th Edition, ed.; CRC Press, Inc.: Boca Raton, FL, 1995.

Pankow, J. F. *Aquatic Chemistry Concepts*. CFC Press, Inc.: Boca Raton, FL, 1991; p. 683.

Powell, C. L.; Agrawal, A. Biodegradation of trichloroethene by methane oxidizers naturally associated with wetland plant roots. *Wetlands* **2011**, *31* (1), 45–52.

Sander, R. Compilation of Henry's Law constants for inorganic and organic species of potential importance in environmental chemistry, 1999. Web. 28 Feb. 2012. <http://www.mpch-mainz.mpg.de/~sander/res/henry.html>

Schwarzenbach, R. P.; Gschwend, P. M.; Imboden, D. M. *Environmental organic chemistry illustrative examples, problems, and case studies*. John Wiley and Sons, Inc.: New York, 1995; p. 392.

A.2 BIOMASS ESTIMATION (ADAPTED FROM JENAL-WANNER AND MCCARTY 1997 AND POWELL ET AL., IN REVIEW)

1. Calculate net oxygen (O_2) loss through cycle (ΔO_2)
    a. Collect daily oxygen concentrations and calculate total oxygen loss (mmol).
    b. Subtract the amount of O_2 consumed in the control microcosms from the live microcosms to account for mass loss due to the presence of the plant roots.
2. Calculate net methane (CH_4) loss through a cycle (ΔCH_4)
    a. Collect daily methane concentrations and calculate methane loss (mmol).
    b. Subtract the amount of CH_4 lost in the control microcosms from the live microcosms to account for mass loss due to the presence of the plant roots.
3. Find the ratio of CH_4 loss to O_2 loss

$$\frac{\Delta CH_4}{\Delta O_2}$$

4. Calculate theoretical O_2 loss based on stoichiometry, using the following equation

$$CH_4 + \left(\tfrac{3}{5} + \tfrac{7}{5}f_e\right)O_2 + \tfrac{1}{5}f_s(H^+ + NO_3^-) \rightarrow \tfrac{1}{5}f_s C_5H_7O_2N + \left(\tfrac{7}{5}f_s + 2f_e\right)H_2O + f_eCO_2 \quad \text{Eq.1}$$

which consists of

the fraction of CH_4 oxidized to CO_2 and used for energy:

$$f_eCH_4 + 2f_eO_2 \rightarrow 2f_eH_2O + f_eCO_2 \quad \text{Eq.1a}$$

the fraction of CH_4 assimilated into biomass:

$$f_s CH_4 + \tfrac{3}{5} f_s O_2 + \tfrac{1}{5} f_s (H^+ + NO_3^-) \rightarrow \tfrac{1}{5} f_s C_5 H_7 O_2 N + \tfrac{7}{5} f_s H_2 O$$

Eq.1b

5. Determine the fraction of CH_4 oxidized for energy (f_e)
    a. set the measured ratio of CH_4 mass to O_2 mass utilized equal to the stoichiometric ratio expressed

$$\frac{3}{5} + \frac{7}{5} f_e = \frac{\Delta CH_4}{\Delta O_2}$$

6. Determine the fraction of CH_4 assimilated to biomass (f_s)

$$f_s = 1 - f_e$$

7. Calculate the biomass yield from one mol of CH_4 consumed (Y), in mmol cell mmol^{-1} CH_4
    a. Multiply f_s by the stoichiometric ratio given in Eq. 1b

$$Y = \frac{C_5 H_7 O_2 N}{CH_4} = \frac{1}{5} f_s$$

    b. Y can be converted to mg cell mg^{-1} CH_4

$$Y = \frac{1}{5} f_s \left(\frac{FW_{bio}}{FW_{GS}} \right)$$

where FW_{bio} = formula weight of biomass, 113 gram mol^{-1}; FW_{GS} = formula weight of growth substrate

8. Calculate biomass concentration (X), in mmol cell liter^{-1}
    a. Determine the amount of biomass produced from CH_4 consumed (Y')

$$Y' = Y * \Delta CH_4$$

    b. Normalize Y' by the liquid volume in the microcosm (V_w), in liters

$$X = \frac{Y'}{V_w}$$

9. Calculate steady state biomass (X_{ss}), in mmol cell liter^{-1}

    a. Assume that after the enrichment period active biomass reaches a steady state value due to balance between biomass growth and decay

$$X_{ss} = \frac{Y'}{V_w * t * b}$$

where t = total length of cycle, day; b = organism decay rate, 0.549 d^{-1} (Chang and Criddle 1997)

A.2.1 **References**

Chang, W. K.; Criddle, C. S. Experimental evaluation of a model for cometabolism: Prediction of simultaneous degradation of trichloroethylene and methane by a methanotrophic mixed culture. *Biotechnology and Bioengineering* **1997**, *56* (5), 492–501.

Powell, C. L.; Goltz, M. N.; Agrawal, A. Biodegradation kinetics of chlorinated aliphatic hydrocarbons by cometabolizing methane oxidizers naturally-associated with wetland plant roots

APPENDIX B SUPPLIMENTAL DATA

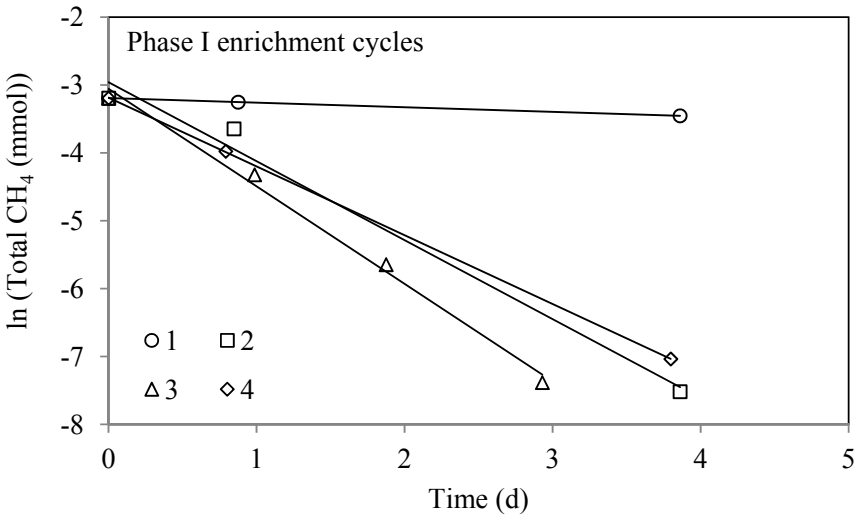

Figure S1.1 Pseudo first-order methane (CH_4) consumption rate constant (k_{obs}) in live Phase I microcosms for enrichment cycles 1 through 4. Initial aqueous [CH_4] was 0.36 mg liter^{-1} (0.041 mmol). k_{obs} and coefficient of determination (r^2) values for each cycle were determined from the best fit line: (1) 0.067, 1.0; (2) 1.16, 0.99; (3) 1.44, 0.99; (4) 1.01, 1.0.

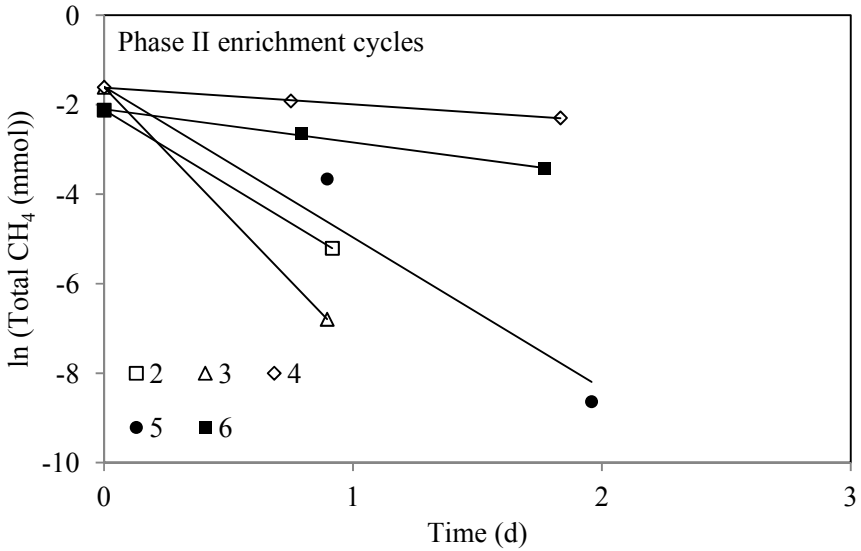

Figure S1.2 Initial pseudo first-order methane (CH_4) consumption rate constant (k_{obs}) in live Phase II microcosms for enrichment cycles two through six; a rate constant for cycle one was undeterminable. Initial aqueous CH_4 was 1.1 mg liter^{-1} (0.12 mmol) for all cycles except three and four, which had CH_4 additions of 1.8 mg liter^{-1} (0.20 mmol). Mixing regime switched from end-over-end to gentle horizontal between cycles three and four. k_{obs} (d^{-1}) and coefficient of determination (r^2) values for each cycle were determined from the best fit line and k_{obs} values were normalized with respect to biomass concentration ($k_{1\text{-}CH4}$, liter mg^{-1} cell d^{-1}): (2) 3.37, 1.0, 0.15; (3) 5.79, 1.0, 0.27; (4) 0.372, 1.0, 0.011; (5) 3.37, 0.94, 0.18; (6) 0.743, 1.0, 0.034.

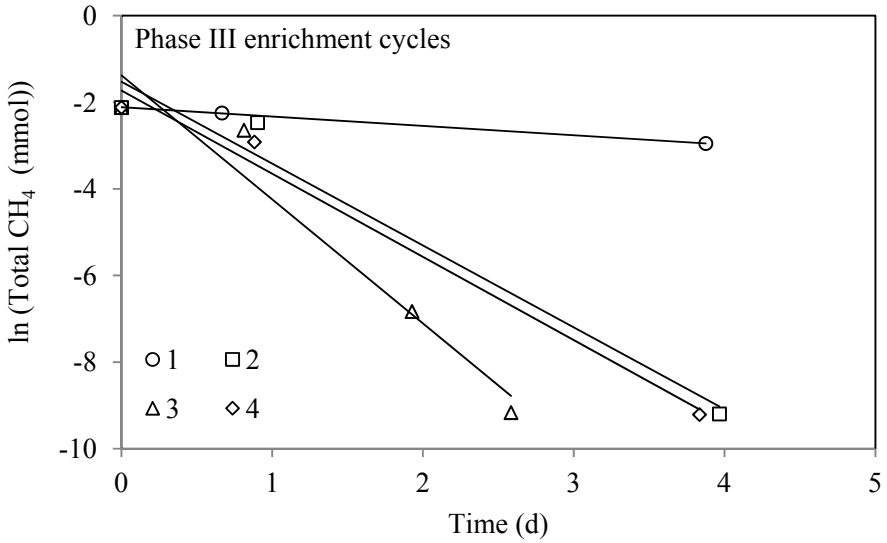

Figure S1.3 Initial pseudo first-order methane (CH_4) consumption rate constant (k_{obs}) in live Phase III microcosms for enrichment cycles one through four. Initial aqueous CH_4 was 1.1 mg liter^{-1} (0.12 mmol). k_{obs} (d^{-1}) and coefficient of determination (r^2) values for each cycle were determined from the best fit line and k_{obs} values were normalized with respect to biomass concentration ($k_{1\text{-}CH4}$, liter mg^{-1} cell d^{-1}): (1) 0.216, 1.0, 0.0091; (2) 1.89, 0.97, 0.090; (3) 2.87, 0.95, 0.14; (4) 1.92, 0.99, 0.089.

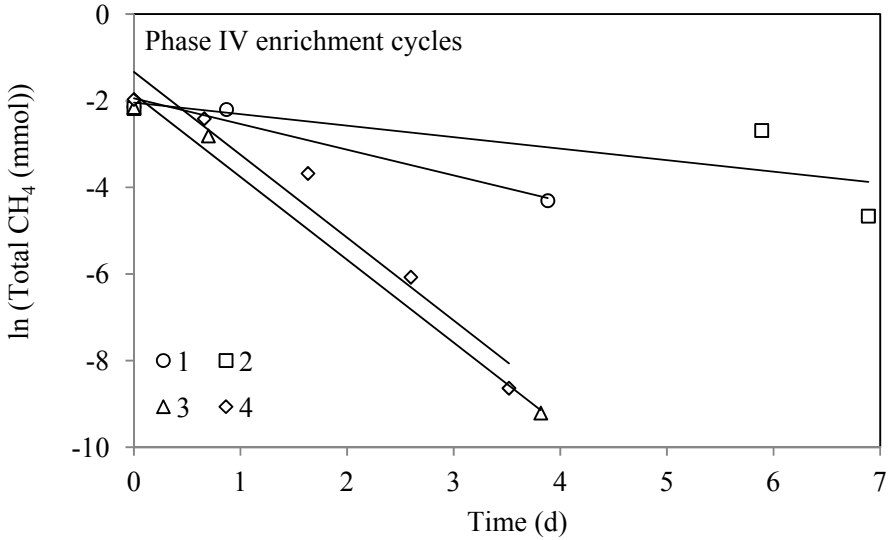

Figure S1.4 Initial pseudo first-order methane (CH_4) consumption rate constant (k_{obs}) in live Phase IV microcosms for enrichment cycles one through four. Initial aqueous CH_4 was 1.1 mg liter^{-1} (0.12 mmol). k_{obs} (d^{-1}) and coefficient of determination (r^2) values for each cycle were determined from the best fit line and k_{obs} values were normalized with respect to biomass concentration ($k_{1\text{-}CH4}$, liter mg^{-1} cell d^{-1}): (1) 0.59, 0.96, 0.024; (2) 0.27, 0.58, 0.013; (3) 1.9, 0.99, 0.073; (4) 1.9, 0.95, 0.079.

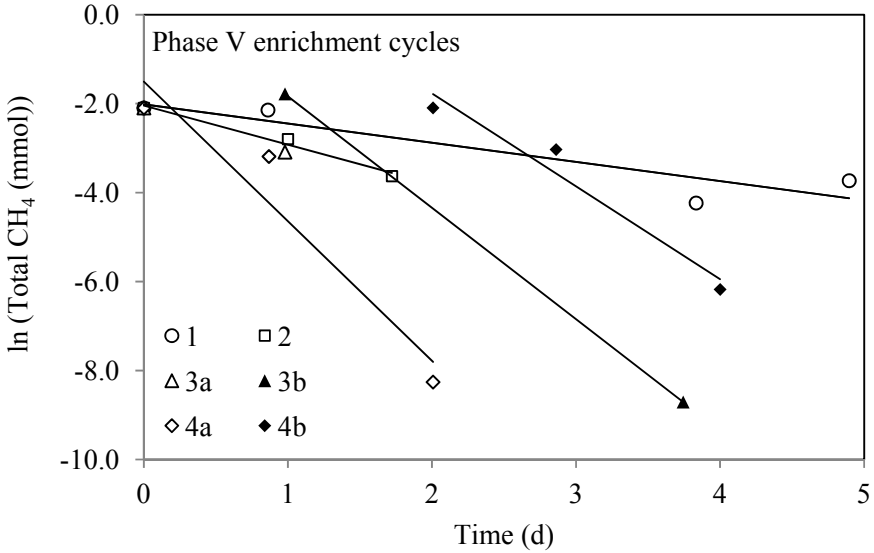

Figure S1.5 Initial pseudo first-order methane (CH_4) consumption rate constant (k_{obs}) in live Phase V microcosms for enrichment cycles one through four. Initial aqueous CH_4 was 1.1 mg liter^{-1} (0.12 mmol). k_{obs} (d^{-1}) and coefficient of determination (r^2) values for each cycle were determined from the best fit line and k_{obs} values were normalized with respect to biomass concentration ($k_{1\text{-}CH4}$, liter mg^{-1} cell d^{-1}): (1) 0.43, 0.85, ---; (2) 0.88, 0.98, 0.041; (3a) 1.01, 1, 0.074; (3b) 2.51, 1, 0.075; (4a) 3.1, 0.92, 0.13; (4b) 2.1, 0.95, 0.096.

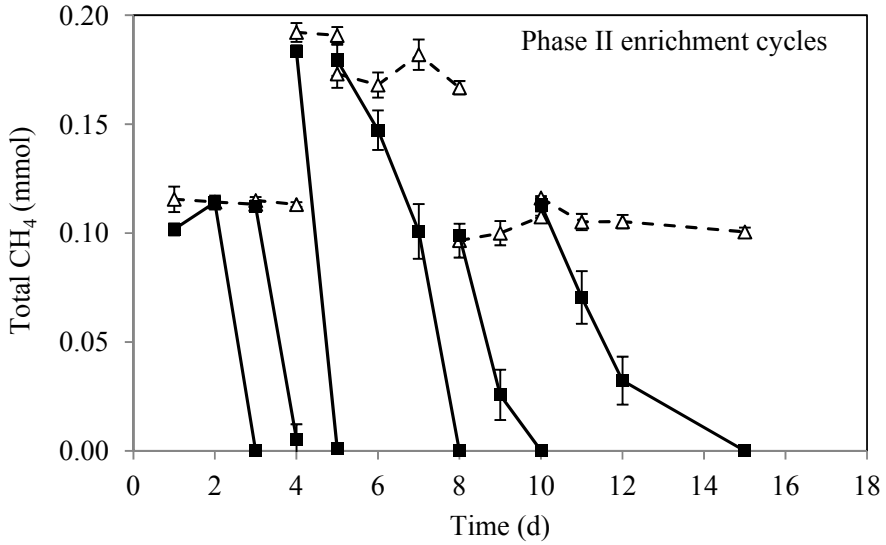

Figure S1.6 Average methane (CH_4) consumption in control (open triangles) and live (closed squares) Phase II microcosms for enrichment cycles one through six. Mixing regime was altered from end-over-end in cycles one, two, and three to gentle horizontal in cycles four, five, and six. Initial aqueous CH_4 was 1.1 mg liter^{-1} (0.12 mmol) for all cycles except three and four, where CH_4 additions were increased to 1.8 mg liter^{-1} (0.20 mmol). Error bars give standard deviation for three samples.

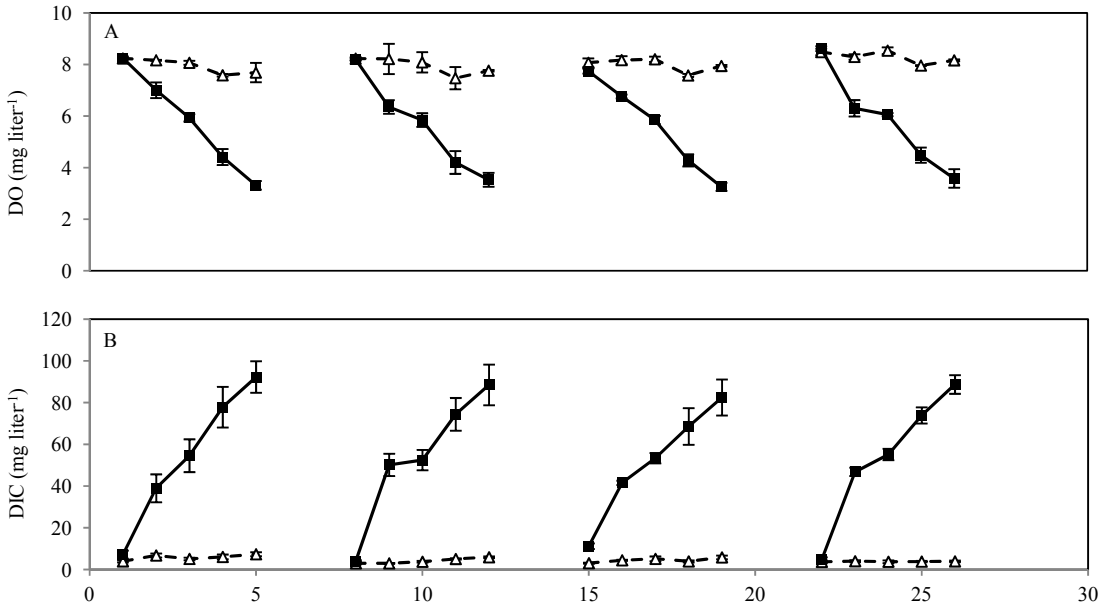

Figure S2.1 A) Dissolved oxygen (DO) consumption and B) dissolved inorganic carbon (DIC) production in control (open triangles) and live (closed circles) Phase I microcosms for experiments one and two, 1,1,2-trichloroethane additions. Error bars give standard deviation of three samples.

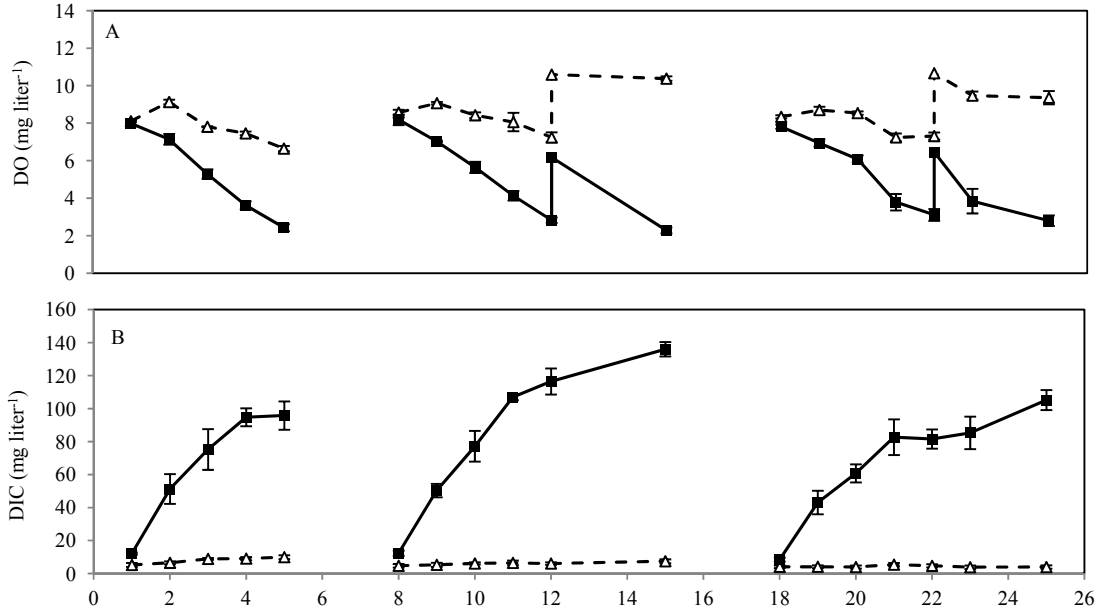

Figure S2.2 A) Dissolved oxygen (DO) consumption and B) dissolved inorganic carbon (DIC) production in control (open triangles) and live (closed squares) Phase II microcosms for experiment one, 1,2-dichloropropane additions. Error bars give standard deviation of three samples.

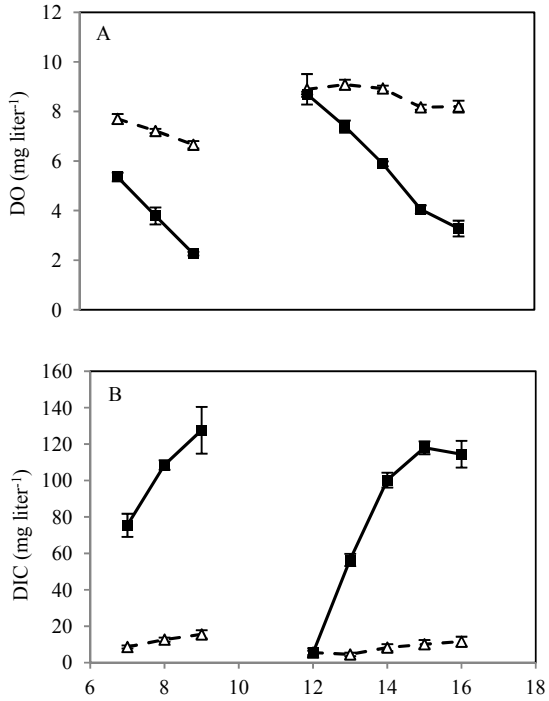

Figure S2.3 A) Dissolved oxygen (DO) consumption and B) dissolved inorganic carbon (DIC) production in control (open triangles) and live (closed squares) Phase V microcosms for experiment one, 1,2-dichloropropene additions. Error bars give standard deviation of three samples.

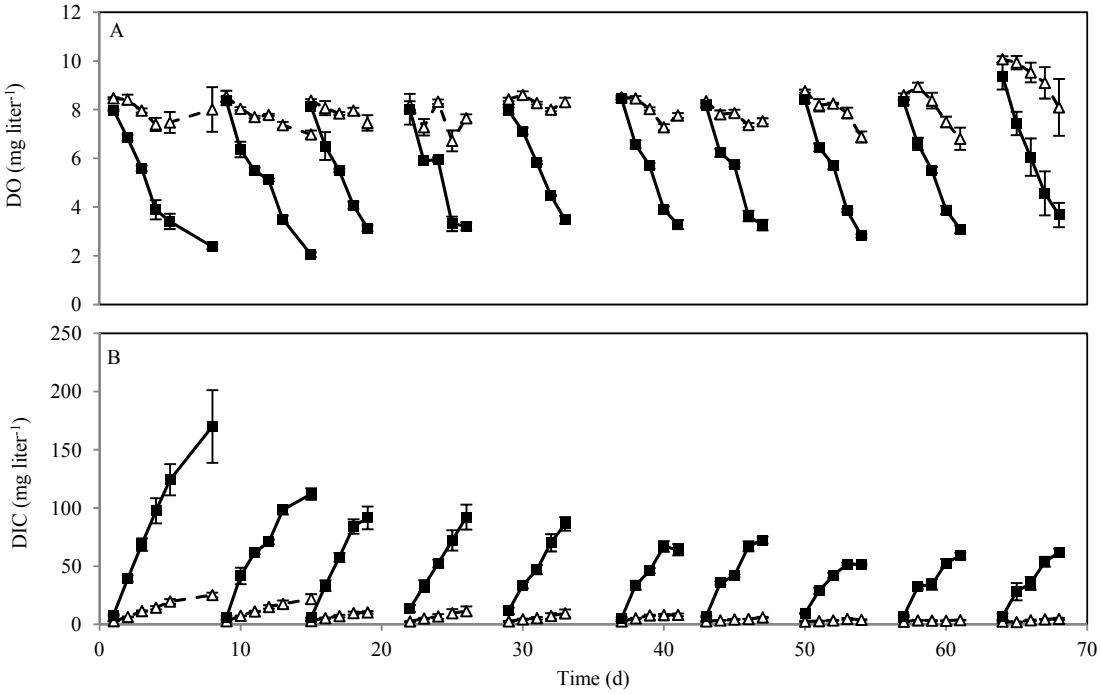

Figure S2.4 A) Dissolved oxygen (DO) consumption and B) dissolved inorganic carbon (DIC) production in control (open triangles) and live (closed squares) Phase III microcosms. Error bars give standard deviation of three samples.

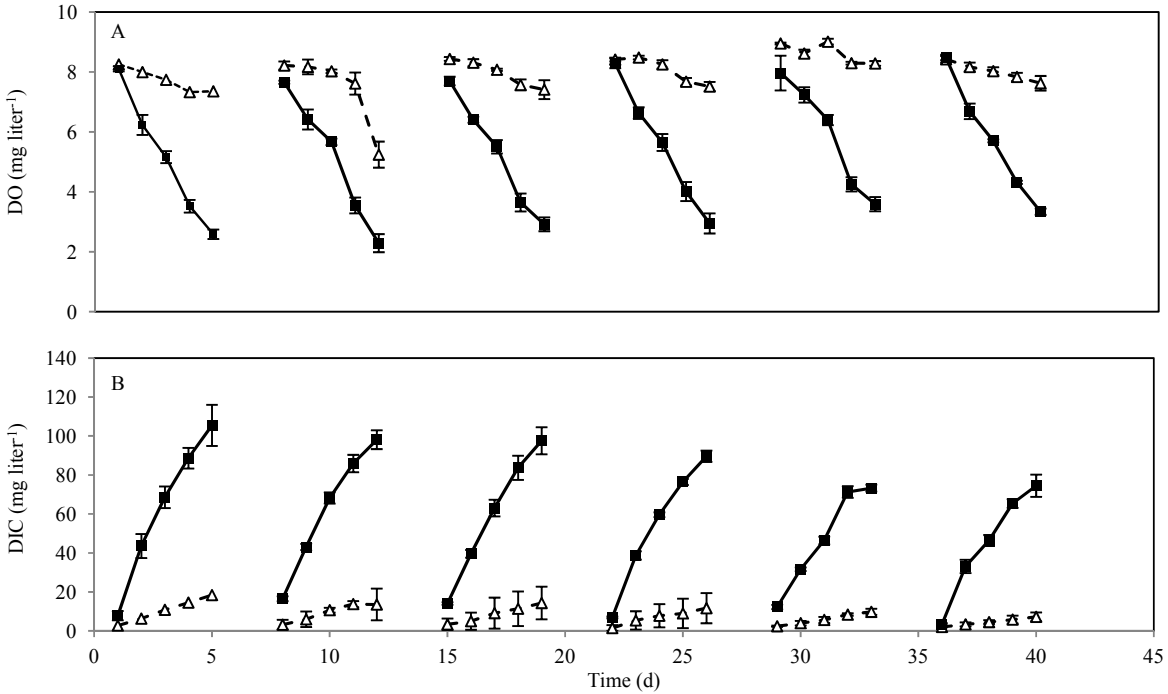

Figure S2.5 A) Dissolved oxygen (DO) consumption and B) dissolved inorganic carbon (DIC) production in (open triangles) and live (closed squares) Phase IV microcosms. Error bars give standard deviation of three samples.

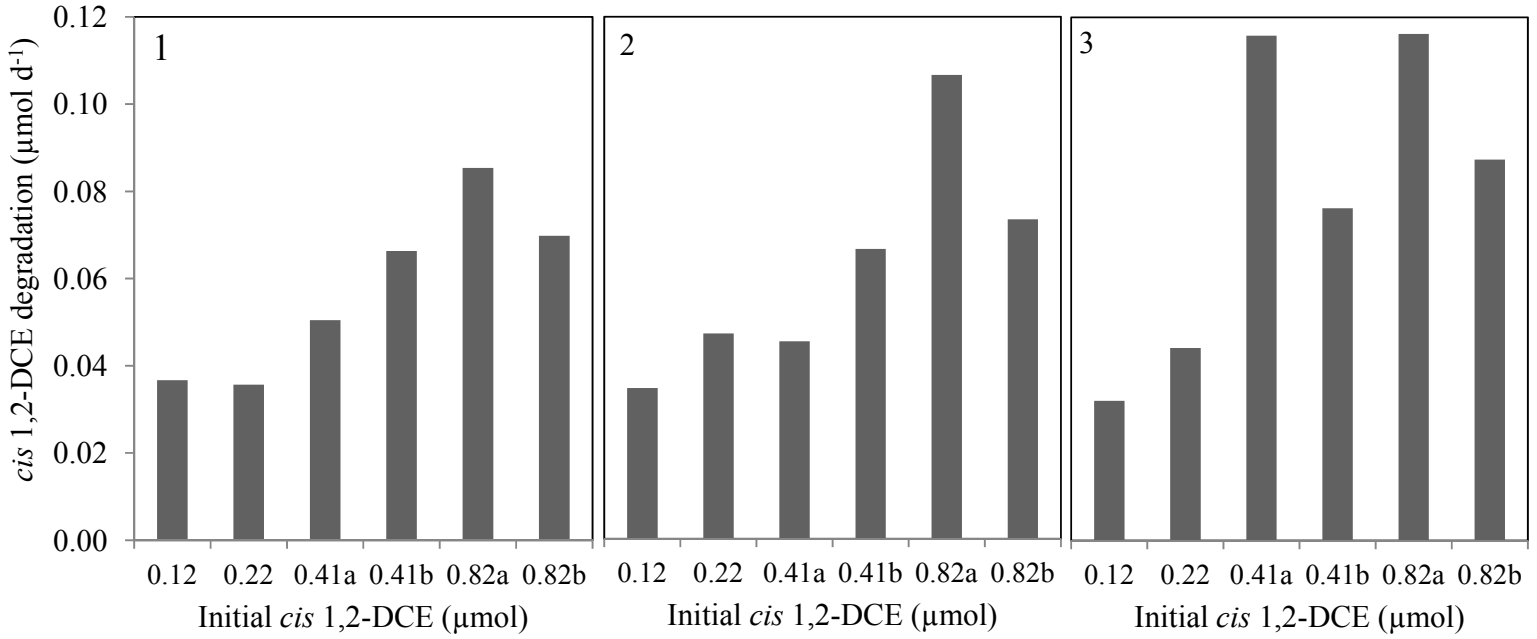

Figure S3.1 Daily *cis* 1,2-dichloroethene (*cis* 1,2-DCE) degradation rate (µmol d^{-1}) in individual live Phase II microcosms for experiments one through four. Initial *cis* 1,2-DCE additions represent calculated values.

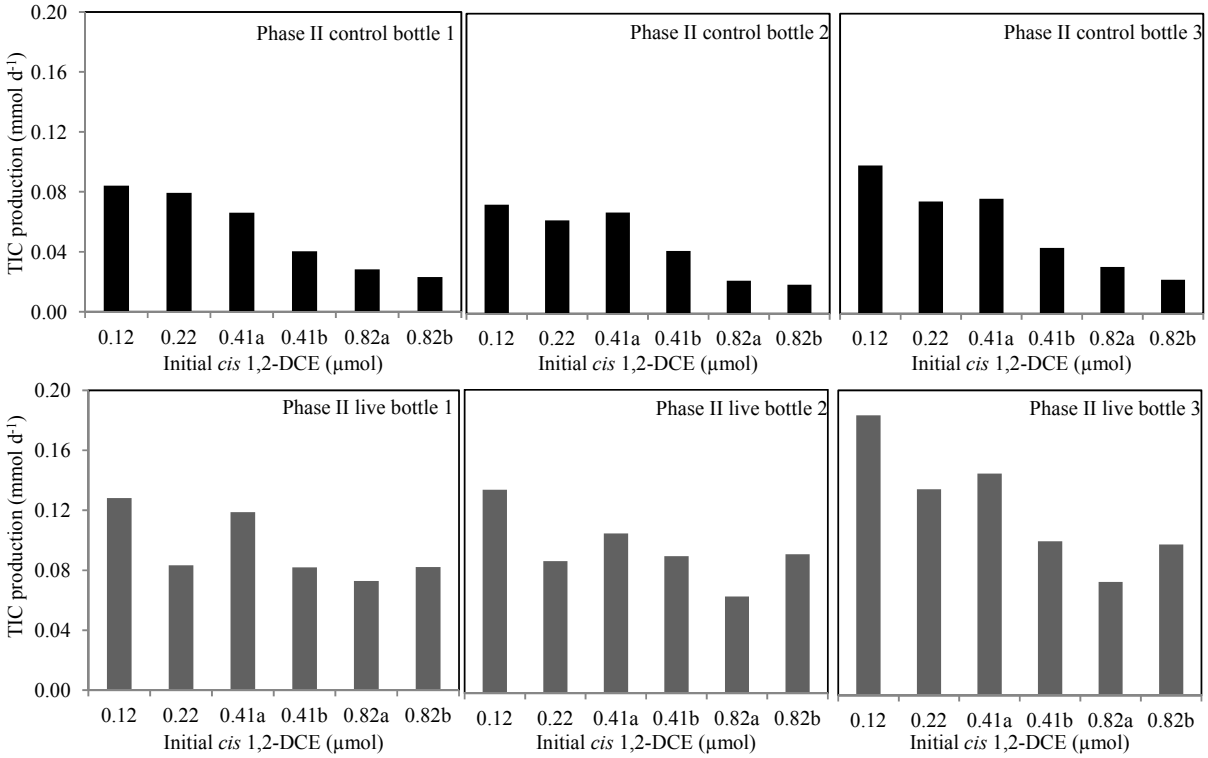

Figure S3.2 Daily total inorganic carbon (TIC) production rate (mmol d^{-1}) in control and live Phase II microcosms for experiments one through four in which *cis* 1,2-dichloroethene (*cis* 1,2-DCE) was added in increasing amount. Initial *cis* 1,2-DCE additions represent calculated values.

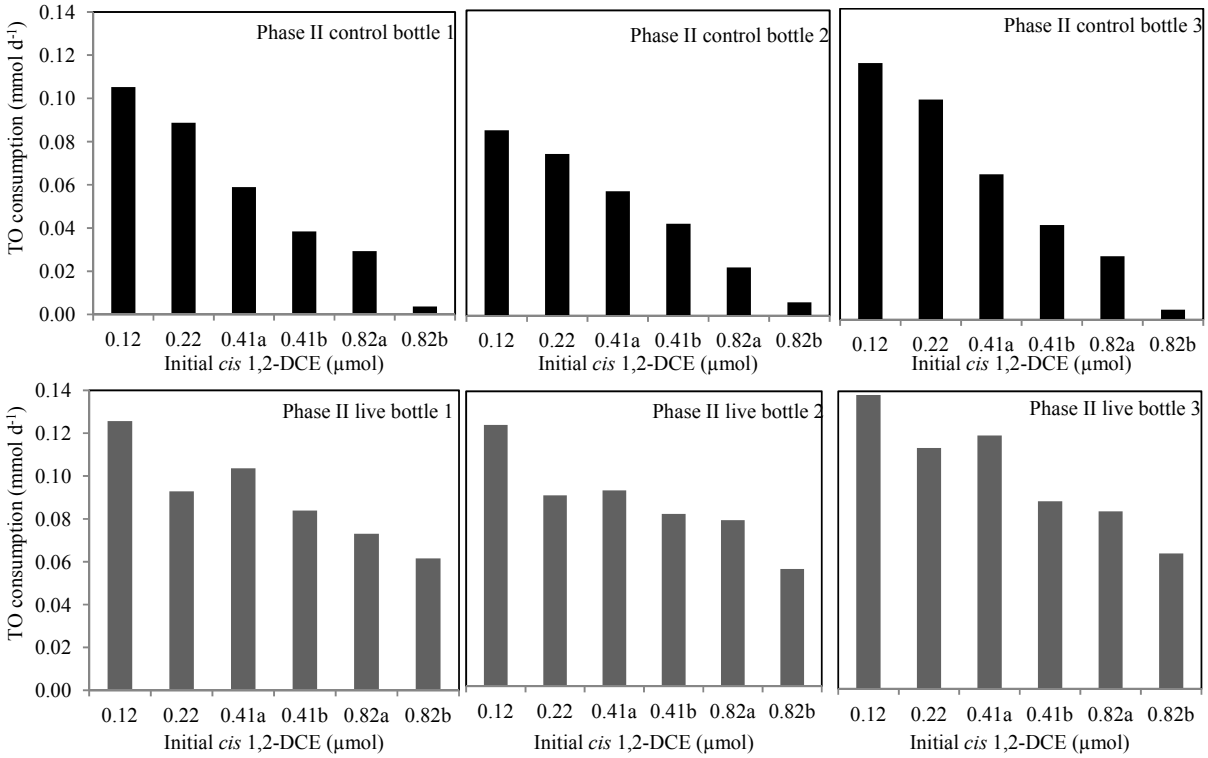

Figure S3.3 Daily total oxygen (TO) consumption rate (mmol d^{-1}) in control and live Phase II microcosms for experiments one through four in which *cis* 1,2-dichloroethene (*cis* 1,2-DCE) was added in increasing amount. Initial *cis* 1,2-DCE additions represent calculated values.

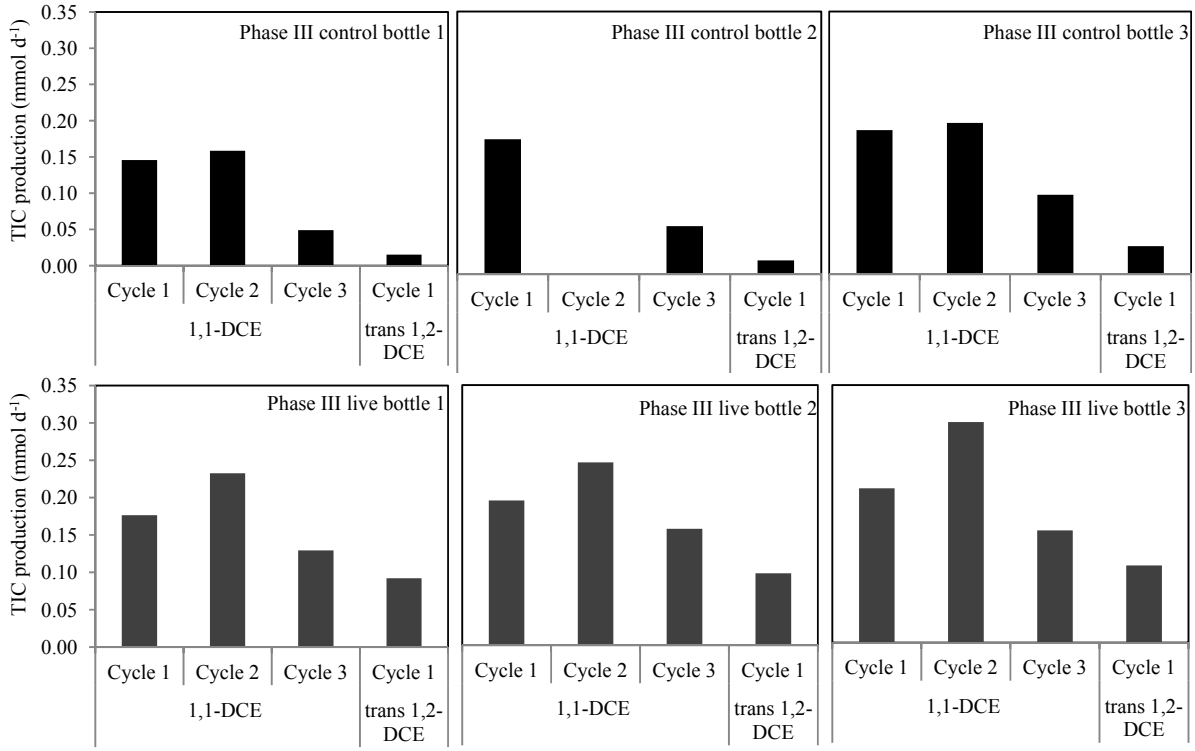

Figure S3.4 Daily total inorganic carbon (TIC) production rate (mmol d^{-1}) in control and live Phase III microcosms for experiments one and two and their respective cycles. 1,1-Dichloroethe (1,1-DCE) amount in all cycles of experiment one was 0.18 µmol. *trans* 1,2-Dichloroethene (*trans* 1,2-DCE) amount was 0.12 µmol for experiment two, cycle one.

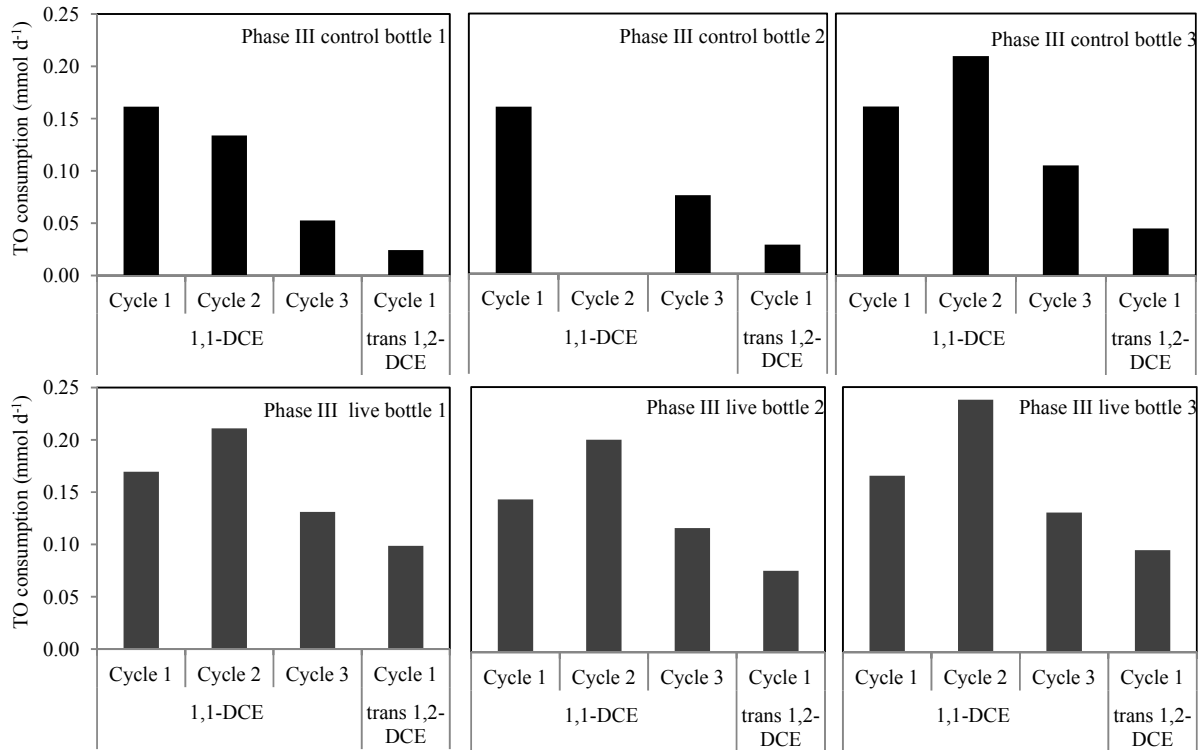

Figure S3.5 Daily total oxygen (TO) consumption rate (mmol d^{-1}) in control and live Phase III microcosms for experiments one and two and their respective cycles. Initial 1,1-dichloroethene (1,1-DCE) amount for all cycles of experiment one was 0.18 µmol. *trans* 1,2-Dichloroethene (*trans* 1,2-DCE) added for cycle one of experiment two was 0.12 µmol.

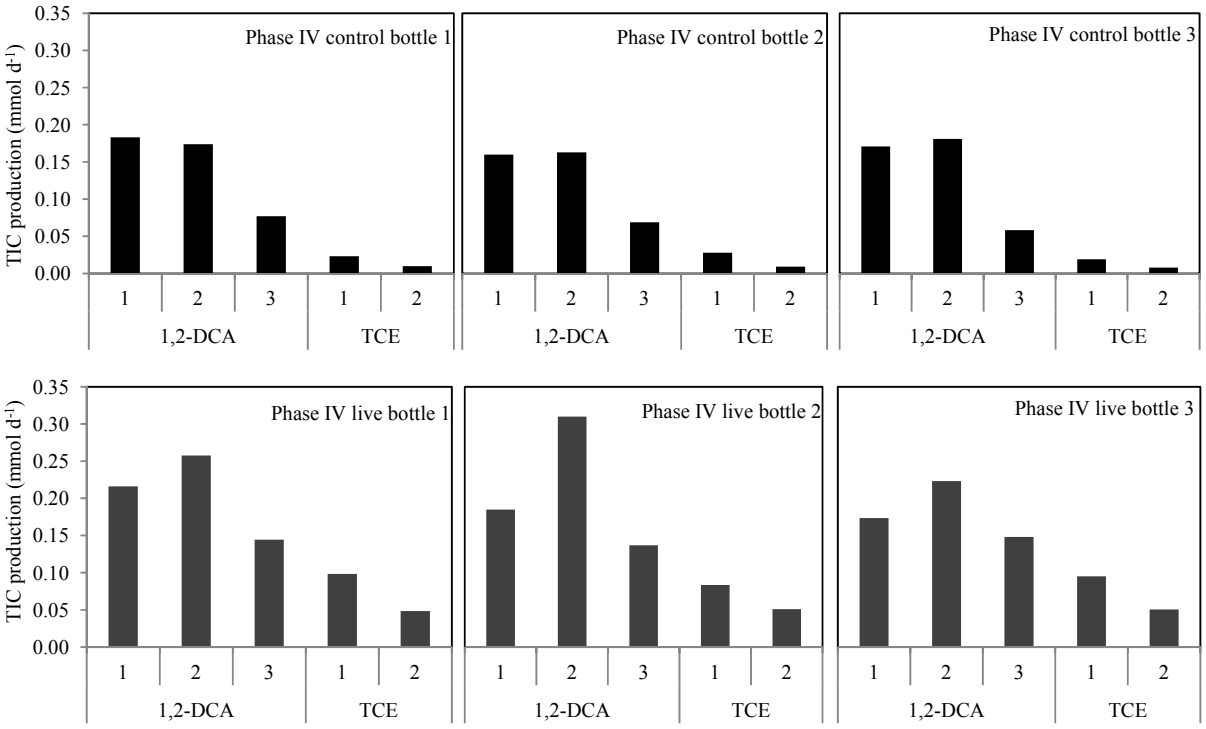

Figure S3.6 Daily total inorganic carbon (TIC) production rate (mmol d^{-1}) in control and live Phase IV microcosms for experiments one and two and their respective cycles. Initial 1,2-dichloroethane (1,2-DCA) amount for all cycles of experiment one was 0.18 µmol. Initial trichloroethene (TCE) added for experiment two, cycles one and two was 0.10 and 0.13 µmol, respectively.

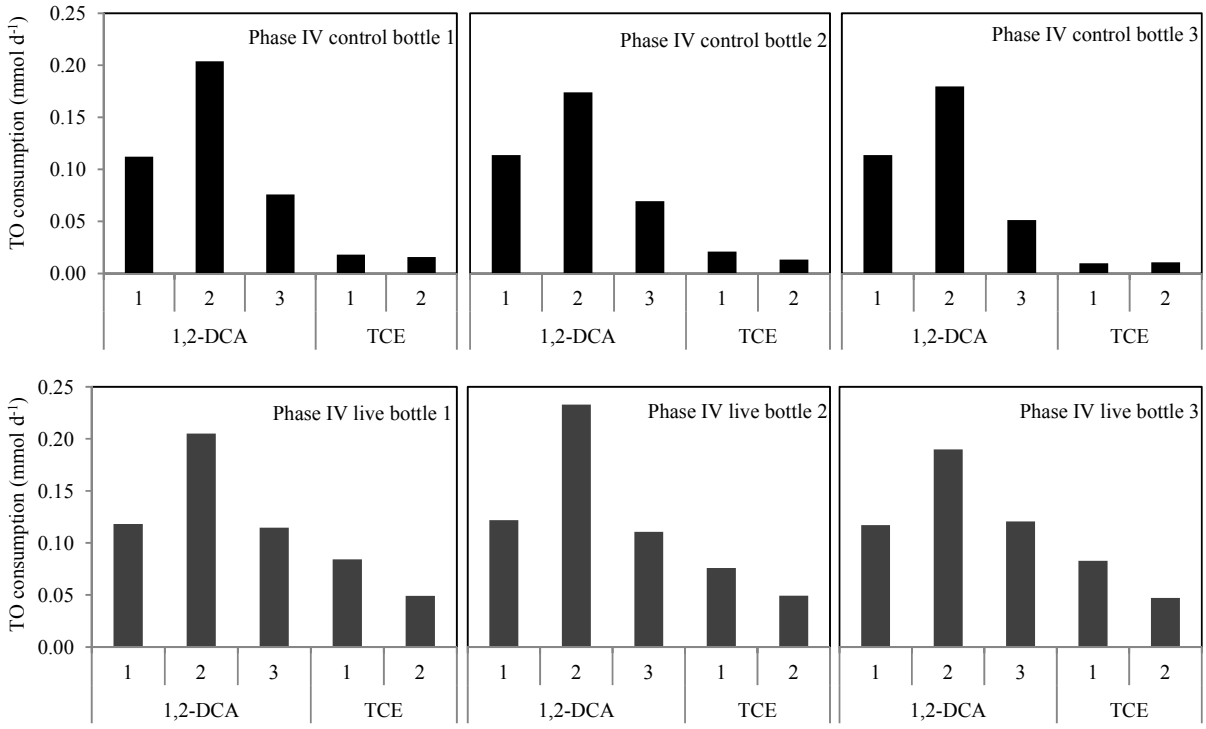

Figure S3.7 Daily total oxygen (TO) consumption rate (mmol d^{-1}) in control and live Phase IV microcosms for experiments one and two and their respective cycles. Initial 1,2-dichloroethane (1,2-DCA) amount for all cycles of experiment one was 0.18 µmol. Initial trichloroethene (TCE) added for experiment two, cycles one and two was 0.10 and 0.13 µmol, respectively.

Table S1.1 Reported Transformation Yield (T_y, mol CAH mol^{-1} growth substrate); Transformation Capacity (T_c, mg CAH mg^{-1} cell); maximum degradation rate (k, mg substrate mg^{-1} cell d^{-1}); and initial pseudo first-order degradation rate constant ($k_{1\text{-CAH}}$, liter mg^{-1} cell d^{-1})

			[Aqueous] (mg liter^{-1})					k		
CAH[1]	Source[2]	Bacteria and growth substrate	CAH	Growth substrate	Enzyme	T_y	T_c	CAH	CH_4	$k_{1\text{-CAH}}$
TCE	A, B, D	Mixed culture CH_4 fed resting cells	15	0	sMMO	0.0015	0.036	0.53	---	1.4
	B, D, I	Secondary growth substrate: formate	20	900	sMMO	0.0031	0.073	2.1	---	0.7
	A, B	Mixed culture CH_4 fed resting cells	0.6, 3, 6	0	sMMO	---	---	0.068, 0.048, 0.026	---	---
	C, I	Mixed CH_4 fed chemostat-culture resting cells	25	0	---	---	0.042	0.84	---	0.56
	D	Mixed culture CH_4 fed	1.7	0.80	pMMO	0.0019	---	---	---	---
	D, E	Mixed culture CH_4 fed resting cells	8.5	0	sMMO	0.0040	---	---	0.32	---
	D, E	Mixed culture fed secondary growth substrate: formate	35	450	sMMO	0.0048	0.11	---	0.19	---
	D, F	Mixed-chemostat culture fed secondary growth substrate: formate	NR	900	sMMO	0.022	0.54[3]	9.6	---	1.6
	G	CH_4 fed pure PM-M culture	20	NR	---	0.0075[3]	---	---	---	---
	D, H, I	Pure *M. trichosporium* OB3b culture fed secondary growth substrate: formate	6	900	sMMO	0.017	0.26	---	---	2.9
	I	Pure *M. trichosporium* OB3b culture resting cells	1	0	sMMO	---	---	---	---	0.5–3.31
	J	Mixed culture CH_4 fed resting cells	NR	0	pMMO	---	0.21	>5.0	2.2	0.35
	K	Mixed culture CH_4 fed resting cells	0–30	0	sMMO	0.0021	0.05	1.03	---	0.27
	K	Mixed culture fed secondary growth substrate: formate	0–30	900	sMMO	0.0042	0.1	4.2	---	0.60
cis 1,2-DCE	D	Mixed culture CH_4 fed	8.3	0.50	---	0.058	---	---	---	---
	D, E	CH_4 fed resting cells	10.5	0	sMMO	0.0050	---	---	0.049	---
	D, E	Secondary growth substrate: formate	47	450	sMMO	0.020	0.35	---	0.038	---

	D, F	Mixed-chemostat culture fed secondary growth substrate: formate	NR	900	sMMO	0.031	0.57[3]	8.3	---	2.7
	H	Pure *M. trichosporium* OB3b culture fed secondary growth substrate: formate	NR	900	sMMO	---	---	---	---	10
	L, M	Pure *M. trichosporium* OB3b culture fed secondary growth substrate: formate	0.4-12	NR	pMMO	---	---	---	---	0.09
DCM	F	Pure OB3b batch culture fed secondary growth substrate: formate	NR	900	sMMO	---	0.25[3]	---	---	---
	H	Pure *M. trichosporium* OB3b culture fed secondary growth substrate: formate	NR	900	sMMO	---	---	---	---	12
1,2-DCA	F	Mixed-chemostat culture fed secondary growth substrate: formate	NR	900	sMMO	---	1.5[3]	---	---	---
	H	Pure *M. trichosporium* OB3b culture fed secondary growth substrate: formate	NR	900	sMMO	---	---	---	---	1.4
	K	Mixed culture CH_4 fed resting cells	NR	0	sMMO	---	~0.10[4]	---	---	---
	K	Mixed culture fed secondary growth substrate: formate	NR	900	sMMO	---	~0.21[4]	---	---	---
	L, M	Pure *M. trichosporium* OB3b culture fed secondary growth substrate: formate	0.4-12	NR	pMMO	---	---	---	---	<0.04

[1] – CAH – chlorinated aliphatic hydrocarbon; TCE – trichloroethene; *cis* 1,2-DCE – *cis* 1,2-dichloroethene; DCM – dichloromethane; 1,2-DCA – 1,2-dichloroethane.

[2] – A . Alvarez-Cohen and McCarty 1991(a); B. Alvarez-Cohen and McCarty 1991(b); C. Alvarez-Cohen and McCarty 1991(c); D. Anderson and McCarty 1997; E. Dolan and McCarty 1997; F. Chang and Alvarez-Cohen 1996; G. Phelps *et al.* 1990; H. Oldenhuis *et al.* 1991; I. Speitel *et al.* 1993; J. Smith *et al.* 1997; K. Chang and Alvarez-Cohen 1995; L. van Hylckama Vlieg *et al.* 1996; M. Alvarez-Cohen and Speitel 2001

[3] – Largest value given.

[4] – Approximated from figure 3 in original text.

Table S1.2 Transformation Yield (T_y, net mol TCE net mol^{-1} CH_4); initial CH_4 degradation rate constant ($k_{obs\text{-}CH4}$, d^{-1}) and corresponding coefficient of determination (r^2); and biomass normalized rate constant ($k_{1\text{-}CH4}$, liter mg^{-1} cell d^{-1}) in Phase II for experiments one through six and their respective three-day sub-cycles

		Initial TCE level[ab]		Individual sub-cycle values					Average by initial TCE[c]	
Experiment	Cycle	Aqueous concentration (µg liter^{-1})	Amount (µmol)	T_y	$k_{obs\text{-}CH4}$	r^2	$k_{1\text{-}CH4}$	Initial TCE (µmol)	T_y	$k_{1\text{-}CH4}$
1	1a	30	0.030	0.000092	0.91	0.96	0.073	0.030	0.000088 ± 0.00002	0.073 ± ---
	2a	30	0.030	0.00010	2.1	0.95		0.060	0.00010 ± 0.00003	0.10 ± 0.00
	3a	30	0.030	0.000068	2.1	0.98		0.090	0.00026 ± 0.00004	0.063 ± 0.01
2	1a	60	0.060	0.000099	1.6	1.0		0.10	0.00017 ± 0.00004	0.13 ± 0.10
	2a	60	0.060	0.00012	2.5	1.0	0.11	0.11	0.00022 ± 0.00003	0.11 ± 0.06
	3a	60	0.060	0.000067	0.71	1.0	0.10	0.14	0.00029 ± 0.00003	0.061 ± 0.01
	4a	60	0.060	0.00014	2.2	1.0	0.10	0.15	0.00011 ± 0.00007	0.10 ± 0.05
	4b	45	0.040	0.000063	1.3	0.95	0.079	0.18	0.00028 ± 0.00007	0.14 ± 0.03
3	1a	125	0.11	0.000201	1.8	0.97	0.18	0.22	0.00043 ± ---	0.16 ± ---
	1b	90	0.080	0.00039	1.1	0.98	0.063			
	2a	125	0.11	0.00026	1.9	1.0	0.084			
	2b	100	0.090	0.00029	1.1	0.93	0.069			
	3a	125	0.11	0.00020	1.7	0.98	0.075			
	3b	100	0.090	0.00023	1.0	0.98	0.058			
4	1a	155	0.14	0.00027	0.87	1.0	0.050			
	1b	110	0.10	0.00020	0.86	0.98	0.059			
	2a	155	0.14	0.00032	1.8	0.93	0.071			
	2b	110	0.10	0.00014	3.6	0.93	0.20			
5	1a	200	0.18	0.00030	2.7	0.99	0.12			
	1b	170	0.15	0.00011	1.0	0.99	0.069			
	2a	200	0.18	0.00032	3.3	0.94	0.17			
	2b	170	0.15	0.00012	2.9	0.94	0.13			
6	1a	250	0.22	0.00043	3.0	0.99	0.16			
	1b	200	0.18	0.00020	2.3	0.95	0.13			
	2a	250	0.22		3.4	0.97				

[a] – Initial aqueous methane (CH_4) for sub-cycles was 1.1 mg liter^{-1} (0.12 mmol).

[b] – Initial trichloroethene (TCE) additions for "a" sub-cycles represent calculated values; amounts for "b" sub-cycles represent observed values.

[c] – Mean ± standard deviation.

[d] – Due to discrepancies in gas chromatography not all sub-cycles yielded viable values.

Table S1.3 Transformation Yield (T_y, net mol TCE net mol^{-1} CH_4); initial TCE degradation rate constant ($k_{obs\text{-}TCE}$, d^{-1}) and corresponding coefficient of determination (r^2); and biomass normalized rate constants ($k_{1\text{-}TCE}$, liter mg^{-1} cell d^{-1}) in Phase II for experiments one through six and their respective five-day whole cycles

	Initial TCE level[ab]		Individual whole cycle values				Average by initial TCE level[c]	
Experiment	Aqueous concentration (µg liter^{-1})	Amount (µmol)	T_y	$k_{obs\text{-}TCE}$	r^2	$k_{1\text{-}TCE}$	T_y	$k_{1\text{-}TCE}$
1	30	0.030	0.000094	0.216	1.0	0.017	0.000091 ± 0.00001	0.018 ± 0.000
			0.00010	0.228	1.0	0.018		
			0.000081	0.164	0.86			
2	60	0.060	0.00012	0.164	0.99	0.014	0.00013 ± ----	0.011 ± 0.003
			0.00011	0.135	0.99	0.0078		
			0.00010	0.237	0.95	0.010		
			0.00013	0.224	0.98	0.012		
3	125	0.11	0.00027	0.172	0.99	0.0094	0.00025 ± 0.00003	0.0082 ± 0.001
			0.00027	0.136	0.99	0.0071		
			0.00022	0.139	0.99	0.0081		
4	155	0.14	0.00026	0.156	1.0	0.0094	0.00025 ± 0.00001	0.0087 ± 0.001
			0.00024	0.175	0.97	0.0080		
5	200	0.18	0.00021	0.0914	0.92	0.0048	0.00021 ± 0.00000	0.0047 ± 0.000
			0.00021	0.096	0.93	0.0046		
6	250	0.22	0.00030	0.103	0.70	0.0050	0.00023 ± 0.0001	0.0036 ± 0.002
			0.00016	0.049	0.41	0.0023		

[a] – Initial trichloroethene (TCE) additions represent calculated values.

[b] – Total aqueous methane (CH_4) for whole cycles was 2.2 mg liter^{-1} (0.25 mmol).

[c] – Mean ± standard deviation.

[d] – Not included in average due to changes in total CH_4 added.

Table S1.4 Transformation Yield (T_y, net mol *cis* 1,2-DCE net mol^{-1} CH_4); initial CH_4 degradation rate constant ($k_{obs\text{-}CH4}$, d^{-1}) and corresponding coefficient of determination (r^2); and biomass normalized rate constant ($k_{1\text{-}CH4}$, liter mg^{-1} cell d^{-1}) in Phase III for experiments one through five and their respective three-day sub-cycles

		Initial *cis* 1,2-DCE level[ab]		Individual sub-cycle values				Initial	Average by initial *cis* 1,2-DCE[c]	
Experiment	Cycle	Aqueous concentration (µg liter^{-1})	Amount (µmol)	T_y	$k_{obs\text{-}CH4}$	r^2	$k_{1\text{-}CH4}$	*cis* 1,2-DCE (µmol)	T_y	$k_{1\text{-}CH4}$
1	1a	364	0.40	0.0016	1.08	0.96	0.10	0.30	0.0026 ± 0.001	0.041 ± ---
	2a	364	0.40	0.0016	1.22	0.99	0.16	0.40	0.0015 ± 0.000	0.12 ± 0.03
	3a	364	0.40	0.0016	0.658	0.99	0.10	0.60	0.0021 ± 0.001	0.092 ± 0.04
2	1a	545	0.60	0.0014	1.56	0.98	0.058	0.70	0.0018 ± ---	0.11 ± ---
	1b	280	0.30	0.0018	0.499	1.0	0.041	0.80	0.0026 ± 0.001	0.052 ± 0.02
	2a	545	0.60	0.0024	1.81	0.96	0.13	1.0	0.0024 ± 0.001	0.084 ± 0.04
	2b	290	0.30	0.0035	0.443	0.97		1.2	0.0032 ± 0.001	0.056 ± 0.01
	3a	545	0.60	0.0025	1.11	0.99	0.090			
	3b	315	0.40	0.0012	0.595	1.0				
3	1a	1100	1.20	0.0026	0.803	0.99	0.049			
	1b	830	0.90	0.0021	0.508	0.96	0.034			
	2a	1100	1.20	0.0036	0.863	0.98	0.047			
	2b	720	0.80	0.0019	0.536	0.94	0.036			
	3a	1100	1.20	0.0035	0.887	0.96	0.071			
	3b	680	0.80	0.0027	0.525	0.99	0.044			
4	1a	900	1.00	0.0020	0.789	0.98	0.056			
	1b	740	0.80	0.0023	0.758	1.0	0.043			
	2a	900	1.00	0.0028	1.36	1.0	0.11			
	2b	630	0.70	0.00043	1.16	1.0	0.059			
5	1a	720	0.80	0.00060	1.73	0.95	0.12			
	1b	670	0.80	0.0045	1.81	0.93				
	2a	720	0.80	0.0016	1.36	1.0	0.083			
	2b	600	0.70	0.0018	2.22	0.98	0.11			

[a] – Initial aqueous methane (CH_4) for sub-cycles was 1.1 mg liter^{-1} (0.12 mmol).

[b] – Initial *cis* 1,2-dichloroethene (*cis* 1,2-DCE) additions for "a" sub-cycles represent calculated values; "b" sub-cycles represent observed values.

[c] – Mean ± standard deviation.

Table S1.5 Transformation Yield (T_y, net mol *cis* 1,2-DCE net mol^{-1} CH_4); initial *cis* 1,2-DCE degradation rate constant ($k_{obs\text{-}cDCE}$, d^{-1}) and corresponding coefficient of determination (r^2); and biomass normalized rate constant ($k_{1\text{-}cDCE}$, liter mg^{-1} cell d^{-1}) in Phase III for experiments one through five and their respective five-day whole cycles

		Initial *cis* 1,2-DCE level[ab]		Individual whole cycle values				Average by initial *cis* 1,2-DCE level[c]	
Experiment	Cycle	Aqueous concentration (μg liter^{-1})	Amount (μmol)	T_y	$k_{obs\text{-}cDCE}$	r^2	$k_{1\text{-}cDCE}$	T_y	$k_{1\text{-}cDCE}$
1	1	360	0.40	0.0016	0.30	1.0	0.034	0.0020 ± 0.0000	0.027 ± 0.007
	2			0.0020	0.34	0.99	0.025		
	3			0.0019	0.29	0.92	0.022		
2	2	545	0.60	0.0019	0.29	0.73	0.019	0.0021 ± 0.0002	0.018 ± 0.002
	3			0.0022	0.25	0.66	0.017		
3	1	1090	1.2	0.0025	0.12	1.0	0.0075	0.0029 ± 0.0003	0.013 ± 0.005
	2			0.0030	0.21	1.0	0.013		
	3			0.0031	0.22	1.0	0.018		
4	1	910	1.0	0.0022	0.10	1.0	0.0064	0.0020 ± 0.0003	0.0084 ± 0.003
	2			0.0017	0.18	0.99	0.010		
5	1	730	0.80	0.0016	0.045	0.15	0.0022	0.0017 ± 0.0001	0.0035 ± 0.002
	2			0.0018	0.10	0.74	0.0049		

[a] – Initial *cis* 1,2-dichloroethene (*cis* 1,2-DCE) additions represent calculated values.

[b] – Total aqueous methane (CH_4) for whole cycles was 2.2 mg liter^{-1} (0.25 mmol).

[c] – Mean ± standard deviation.

Table S2.1 Reported Transformation Yield (T_y, mol HAH mol^{-1} growth substrate); Transformation Capacity (T_c, mg HAH mg^{-1} cell); maximum degradation rate (k, mg substrate mg^{-1} cell d^{-1}); and initial pseudo first-order degradation rate constant ($k_{1\text{-CAH}}$, liter mg^{-1} cell d^{-1})

			[Aqueous] (mg liter^{-1})					k		
HAH[1]	Source[2]	Bacteria and growth substrate	HAH	Growth substrate	Enzyme	T_y	T_c	HAH	CH_4	$k_{1\text{-CAH}}$
1,1-DCE	B	Mixed culture CH_4 fed	0.054	0.80	---	0.00022	---	---	---	---
	B, C	Mixed culture CH_4 fed resting cells	0.79	0	sMMO	0.00044	---	---	0.039	---
	B, C	Secondary growth substrate: formate	0.77	450	sMMO	0.00074	0.013	---	0.055	---
	B, D	Pure CAC1 batch culture fed secondary growth substrate: formate	NR	900	sMMO	0.0020	0.038[3]	---	---	---
	E	Pure *M. trichosporium* OB3b culture fed secondary growth substrate: formate	NR	900	sMMO	---	---	---	---	1.4
	H, I	Pure *M. trichosporium* OB3b culture fed secondary growth substrate: formate	0.4-12	NR	pMMO	---	---	---	---	<0.04
	J	Pure *M. album* BG8 culture fed secondary growth substrate: formate	0-0.40	900	pMMO	---	---	---	---	0.13
CF	A	Mixed CH_4 fed chemostat-culture resting cells	17	0	---	---	0.0065	0.35	0.006	---
	A, F	Mixed chemostat-culture fed secondary growth substrate: formate	17	900	---	---	0.015	1.5	0.024	1.0
	A, F	Mixed CH_4 fed chemostat-culture resting cells	29	0	---	---	0.0083	0.34	---	0.085–0.26
	D	Mixed-chemostate culture fed secondary growth substrate: formate	NR	900	sMMO	---	0.062[3]	---	---	---
	E, F	Pure *M. trichosporium* OB3b culture fed secondary growth substrate: formate	0.8-20	900	sMMO	---	---	---	---	23
	F	Pure *M. trichosporium* OB3b culture resting cells	0.1	0	sMMO	---	---	---	---	0.2–0.41
	F	Pure *M. trichosporium* OB3b culture CH_4 fed	0.1	4.3, 0.76, 0.35	sMMO	---	---	---	---	0.029, 0.10,

										0.19
	G	Mixed culture CH_4 fed resting cells	NR	0	sMMO	---	~0.022[4]	---	---	---
	G	Mixed culture fed secondary growth substrate: formate	NR	900	sMMO	---	~0.054[4]	---	---	---
	H, I	Pure *M. trichosporium* OB3b culture fed secondary growth substrate: formate	0.5-14	NR	pMMO	---	---	---	---	<0.04
1,2-DCA	D	Mixed-chemostat culture fed secondary growth substrate: formate	NR	900	sMMO	---	1.5[3]	---	---	---
	E	Pure *M. trichosporium* OB3b culture fed secondary growth substrate: formate	NR	900	sMMO	---	---	---	---	1.4
	G	Mixed culture CH_4 fed resting cells	NR	0	sMMO	---	~0.10[4]	---	---	---
	G	Mixed culture fed secondary growth substrate: formate	NR	900	sMMO	---	~0.21[4]	---	---	---
	H, I	Pure *M. trichosporium* OB3b culture fed secondary growth substrate: formate	0.4-12	NR	pMMO	---	---	---	---	<0.04

[1] – HAH – halogenated aliphatic hydrocarbon; 1,1-DCE – 1,1-dichloroethene; CF – chloroform; 1,2-DCA – 1,2-dichloroethane.

[2] – A. Alvarez-Cohen and McCarty 1991; B. Anderson and McCarty 1997; C. Dolan and McCarty 1997; D. Chang and Alvarez-Cohen 1996; E. Oldenhuis *et al.* 1991; F. Speitel *et al.* 1993; G. Chang and Alvarez-Cohen 1995; H. van Hylckama Vlieg *et al.* 1996; I. Alvarez- Cohen and Speitel 2001; J. Han *et al.* 1999.

[3] – Largest value given.

[4] – Approximated from figure 3 in original text.

Table S3.1 Properties and purity of CAHs evaluated in this work

			Values computed at 20 ^{o}C		
CAH[a]	Chemical name	Provider	Density (g/cm^3)	Henry's constant [D][b]	Purity (%)
CF	Chloroform	Fisher Scientific	1.472	0.122	--
CT	Carbon tetrachloride	Fisher Scientific	1.584	1.01	--
TCE	Trichloroethene	Acros Organics	1.470	0.335	99.6
cis 1,2-DCE	*cis* 1,2-Dichloroethene	Acros Organics	1.280	0.135	97.0
1,1-DCE	1,1,-Dichloroethene	Aldrich Chemical Co.	1.213	0.904	99.0
trans 1,2-DCE	*trans* 1,2-Dichloroethene	Aldrich Chemical Co.	1.260	0.138	--
1,2-DCA	1,2-Dichloroethane	Aldrich Chemical Co.	1.256	0.0318	99.0

[a]- CAH – chlorinated aliphatic hydrocarbon.
[b]- Dimensionless Henry's constants taken from USEPA (2012); $C_{Air}\ C_{Liquid}^{-1}$.